Physics

Cole Memorial Library

MONTHLY NOTICES

OF THE

ROYAL ASTRONOMICAL SOCIETY

Volume 118 No. 2 1958

OHIO STATE UNIVERSITY
DEC 4 1958
LIBRARY

Published and Sold by the

ROYAL ASTRONOMICAL SOCIETY
BURLINGTON HOUSE
LONDON, W.1

Price £1 0s. 0d.; *in U.S.A.* $3

Annual Subscription for volume of six numbers: £5 5s. 0d. ; *in U.S.A.* $16

XUM

The Geophysical Journal

OF THE

ROYAL ASTRONOMICAL SOCIETY

Editors

A. H. Cook
M.A., Ph.D., F.R.A.S., F.G.S.
National Physical Laboratory
Teddington

T. F. Gaskell
M.A., Ph.D., F.R.A.S.
British Petroleum Company
London

Price £1 per number; in U.S.A. $3. Annual Subscription £3; in U.S.A. $9

No. 2 of Volume I, containing original contributions from Australia, India, Israel, and the U.S.S.R., as well as from the United Kingdom, is now available.

CONTENTS

H. A. Lubimova, Thermal history of the Earth with consideration of the variable thermal conductivity of its mantle

B. A. Bolt, H. A. Doyle and D. J. Sutton, Seismic observations from the 1956 atomic explosions in Australia

C. L. Pekeris and I. M. Longman, The motion of the surface of a uniform half-space produced by a buried torque-pulse

Harold Jeffreys, The times of *P* up to 30° (second paper)

Harold Jeffreys, Rock creep and thermal instability

S. D. Chopra, On the equivalence of saddle point approximations and ray theory in elastic wave problems

This number also contains a note on progress in Geophysics entitled " Some recent developments in the study of microseisms in Great Britain and the United States ", by J. Darbyshire and H. M. Iyer ; and a report on the Geophysical Discussion, held at the Society's Rooms in January 1958, on " Chemical and radiometric methods of surveying ".

Orders should be addressed to :

The Assistant Secretary
Royal Astronomical Society, Burlington House, London, W.1

MONTHLY NOTICES

OF THE

ROYAL ASTRONOMICAL SOCIETY

Vol. 118 No. 2

INTERFEROMETRIC MEASUREMENTS OF WAVE-LENGTHS

IV. The accuracy of measured wave-lengths

M. G. Adam and S. Nichols

(Communicated by the Director of the University Observatory, Oxford)

(Received 1957 December 5)

Summary

Solar absorption lines are very different in character from the corresponding laboratory lines, and the wave-length accuracy obtainable for them is considerably less. It is moreover possible that some part of the red shift and change in red shift with line strength originates in the micrometer measurement of the broad absorption and narrow emission lines. An investigation is made of the accuracy and consistency obtainable in measuring arc and solar wave-lengths by the method of circular channels. It appears from this investigation that red shifts can be obtained which are significant to better than 0·001 A.

Introduction.—The recent interest in the interpretation of solar wave-lengths (**9, 10, 12**) makes it more than ever important to consider the reliability of the observations against which the various theories must be tested. For a number of years we have been developing and using a new method of wave-length measurement and have been especially concerned with the reduction of systematic errors such as revealed themselves in earlier accepted wave-lengths. We now test our method, both for its potential accuracy with narrow-line spectroscopic sources, and also for the actual dependence we may place on our measurements for vacuum-arc and solar lines.

A wave-length accuracy of one or two ten-thousandths of an angström can be achieved, in the visible region, for narrow-line laboratory sources (**5**), but in the measurement of solar wave-lengths there are several factors which set a limit of uncertainty considerably greater than this. The limitations are inherent in the nature of the solar spectrum, not only because we are concerned with continuous spectrum interferometry, but also because of the considerable intrinsic breadth of the absorption lines.

In continuous spectrum measurements we are restricted to the use of only very short spacers in the interferometer (**14**), perhaps less than one-tenth of those used for the emission line sources. This reduces the resolution obtainable; it means that the chromatic variation of phase change upon reflection at the silvered surfaces of the plates is important, and it magnifies the effect of any errors due to irregularities in the interferometer plates. The accuracy obtainable, by the method of circular channels, as far as this restriction and general instrumental limitations are concerned, we have investigated by measurements on the very

XUM

narrow lines emitted by a mercury isotope lamp. These measurements extend over the whole visible spectrum and moreover provide us with the phase change corrections and chromatic variation in camera focal length, which are required in increasing the wave-length range of our solar and arc determinations (Section 1).

The Fraunhofer lines are so different in character from the laboratory arc lines with which they are compared that the question arises to what extent the observed solar wave-lengths, and so the red shifts and systematic variations in red shifts, are due to the observer's personal judgment in the micrometer measurement of emission and absorption lines of very different widths. Williams and Middleton (**15**) consider that it is not possible to make micrometer measurements to an accuracy greater than 1/40th of the half-width of the line. But a solar absorption line of moderate strength (say Rowland number 8) has a half-width of some 0·200 A and on this criterion a wave-length uncertainty of 0·005 A. In the green this is already half the Relativity shift. We have tried to answer this question in the first place by independent measurements on the same arc and solar plates by two observers, in fact using different machines, and secondly by measuring the same arc and solar lines with three different spacers in the interferometer. For the arc line changing the spacers chiefly changes the resolution, but for the solar spectrum it also alters the appearance of the plates quite considerably, both in the breadth of the channels in which the lines are measured, and in changing the amount of inter-order scattered light. These measurements are described in Section 2 and used to form an estimate of the reliability of the measured red shifts.

1. *Measurements of mercury lines from an isotope lamp*

1.1. *Wave-lengths obtained with short spacers and the correction for the dispersion of phase change.*—The source in this instance was a G.E.C. water-cooled cold-cathode lamp containing approximately 0·1 mg of Hg 198 with pure argon at 10 mm pressure. The flow of water was maintained continuously in order to avoid self-reversal and line broadening, and the currents were kept below 25 milliamps. The wave-lengths from this type of lamp are slightly longer than those from the electrodeless lamps, but values for both types of lamp have been very carefully determined by Barrell (**5**).

The procedure in measuring wave-lengths by the method of circular channels has already been fully described in Papers I and III (**1, 3**). The Oxford spectroscope was used undiaphragmed in its one prism form (**11**) and carefully focused for each of the strongest mercury lines, from 5790 A to 4046 A, in turn. The luminous column of the mercury lamp was imaged to fill the spectroscope collimator while giving full illumination over the height of the slit, as for the arc spectra (**1**). A 33 cm field lens in the spectroscope focal plane together with the interferometer collimating lens imaged the spectroscope collimator as a circle 3·8 mm diameter between the interferometer plates (**3**). Similarly in the cadmium side arm a circular diaphragm before the lamp was imaged to give an identical and coincident light patch in the same plane. The cadmium pattern was photographed on the plate in the image of the usual cross-shaped diaphragm, with two side arms as described in Paper III (**3**), to take care of the different spreading of the beams from lines at different positions in the spectroscope focal plane. Following the investigations described in Paper III a new interferometer

stand has been constructed with a different method of supporting and adjusting the plates to reduce as far as possible any distortion of the plates in setting up the interferometer.

Fused quartz plates with a wedge angle of $2\frac{1}{2}'$ were used in the etalon. The smaller angle (cf. 15′ in the earlier work) reduces the shift of the pattern centre with wave-length, as does also the smaller dispersion of fused quartz compared with crystalline quartz. With these plates the pattern centre shift at 4046 A leads to a wave-length change of only 0·0009 A for the outermost rings of an outlying line, the effect on the final measured wave-length is practically negligible, and definitely so if a line is measured first on one side and then on the other of the cadmium pattern centre. Three spacers were used in the interferometer, 10 mm, 2·5 mm and 1·5 mm fused quartz rings, which covers the range of spacers which would normally be used for solar wave-lengths. The five strongest mercury lines λλ 5790·7, 5769·6, 5460·8, 4358·3, 4046·6 A were measured with each spacer. Except for the pair of yellow lines which were photographed together always with one on either side of the pattern centre, the minimum deviation of the spectroscope was changed slightly between exposures so that each line was measured in four positions close in and far out on the red side of the pattern centre and close in and far out on the violet side.

Four plates were measured for each line for the 2·5 mm and the 10 mm spacers and eight plates for the 1·5 mm spacer. This was done in the usual way (**1, 2**) on a rotating stage micrometer. From the measured diameters fractional orders of interference ϵ were deduced for the line by the method of least squares; this gives incidentally a least squares value $\Delta D^{*2} = 4f^2\lambda/t$, as in Paper I (**1**), where f is the camera focal length, t is the plate separation and λ the wave-length. In the cadmium pattern the cross was used to give a least squares value of ΔD^{*2} from which fractional orders were deduced for the three pseudo-cadmium "lines", i.e. the vertical arm of the cross and the two side arms. In deducing wave-lengths from the line-ϵ we assume that t varies linearly with line position on the plate from the centre cadmium "line" to the appropriate side "line": all measured lines lie between the centre cadmium line and one side arm. Because our exposures of standard (cadmium) and unknown (mercury) are simultaneous we need only consider the chromatic variation of the refractive index of air with atmospheric conditions. Pressures and temperatures were recorded for each exposure, and we can estimate the effect on our wave-lengths from Babcock's Tables (**4**). The correction begins to be important at 4046 A, but under our conditions even here the effect is only of the order of 0·0003 A, and this has been ignored.

We have calculated wave-lengths, eliminating phase change correction, from our results for three spacers in the following way: suppose that for any one spacer the order of interference for the cadmium red line (wave-length λ_{Cd} is p_1 (integral) and ϵ_1 (fractional) and correspondingly p_2 and ϵ_2 for the mercury line (wave-length λ). If Δ is the phase change correction to ϵ_2 corresponding to zero correction for the cadmium red line at 6438·4696 A then

$$(p_2+\epsilon_2-\Delta)\lambda = (p_1+\epsilon_1)\lambda_{Cd},$$

i.e.

$$(p_2+\epsilon_2)\lambda = (p_1+\epsilon_1)\lambda_{Cd} + \lambda.\Delta.$$

If we write $k = \lambda.\Delta$, k is so small compared with the first term on the right-hand side ($2t$), that the uncertainty of λ in k is quite negligible. Our unknown wave-length λ

XUM

is then given by

$$\lambda = \frac{(p_1+\epsilon_1)\lambda_{Cd}}{p_2+\epsilon_2} + \frac{k}{p_2+\epsilon_2}.$$

The first term on the right-hand side we will call the apparent λ (i.e. neglecting the phase change correction). Now for the plates taken with any one spacer $(p_2+\epsilon_2)$ changes very little and $k/(p_2+\epsilon_2)$ is constant to the accuracy with which it is required in this equation. Thus from any number of plates we can take, for the spacer, a mean value of the apparent wave-length (λ app.) and a mean equation

$$\lambda - \frac{k}{p_2+\epsilon_2} = [\lambda \text{ app.}]_{\text{mean value}}.$$

Our three spacers then provide three such mean equations at each wave-length, in the two unknowns λ and k, for which we may make a least squares solution.

Table I shows in column 2 the fractional part of the absolute wave-length so obtained and in column 3 the value of Δ given by this solution. Column 1 shows Barrell's wave-length (**5**) for the similar lamp. When we remember that Barrell's wave-lengths have been obtained with six spacers from 2·5 cm–12·5 cm compared with 1·5 mm–10·1 mm in the present instance, these results may be regarded as very satisfactory in that they differ from Barrell's by well under 0·001 A over the whole visible range.

TABLE I

Measured wavelengths and phase change corrections

Barrell λ(A)	Observed λ	Δ	δ
4046·5716	·5722	0·0496	0·0485
4358·3377	·3379	·0309	·0317
5460·7536	·7542	·0076	·0069
5769·5992	·5989	·0051	·0054
5790·6635	·6640	0·0058	0·0040

The phase change correction Δ we determine in this way is not the best we can get from our material. The most reliable values of phase change come from the fractional orders measured with short spacers, since $d\epsilon/d\lambda = -2t/\lambda^2$, any wave-length uncertainty has a larger effect on the ϵ values derived from longer spacers. We have therefore taken Barrell's accurate wave-lengths and used them with the ϵ's from the 1·5 mm spacer to establish the best value of the phase change corrections; this procedure gives the corrections δ in column 4 of Table I. These values of δ are higher than Barrell and Teasdale-Buckell's phase-change corrections (**6**), or the often-quoted values given by Childs (**8**), but not so high as the values deduced from Schultz's experimental results (**13**). The δ, λ curve is, however, undoubtedly peculiar to any particular pair of silver coatings and we could hardly expect any better agreement. Our plates were kindly coated for us (by evaporation) in Dr Kuhn's laboratory. The mean reflectivity at λ 5500 A was 91 per cent, mean transmissivity 6½ per cent. The smooth curve drawn through the plot of δ and λ as given above in Table I is then our definitive curve for work with this pair of silver films; the one in fact used for the arc and solar lines in

Section 2 was deduced, slightly differently, from the first four of the 1·5 mm plates and is negligibly different from the δ, λ curve above.

1.2. *Chromatic variation in camera focal length and its application to wave-length determinations.*—The narrow lines of the mercury 198 lamp permit the determination of the quantity ΔD^{*2} from the few measured arcs of the line interference pattern, but for ordinary vacuum-arc lines and especially for solar lines the values of ΔD^{*2} so obtained would not be sufficiently accurate. We do better to obtain ΔD^{*2} for the line from the cadmium red line pattern, knowing the ratio of the camera focal length at wave-length λ to that at 6438·4696 A. Our measures in Section 1.1 enable us to determine once and for all the chromatic variation of

$$\left(\frac{\Delta D^{*2}}{\lambda}\right)_{\text{Hg}} : \left(\frac{\Delta D^{*2}}{\lambda}\right)_{\text{Cd red}}$$

which is in fact the ratio $(f_\lambda/f_{6438})^2$. All the spacers should give the same value for this quantity; the values used were obtained from the plates taken with the 2·5 mm and the 10 mm spacers, which we should expect to give more reliable values. The two sets agreed at any one wave-length to two parts in 10^4 (see requirement in Paper I), and the mean values at each wave-length, together with the value previously obtained at 5085·8 A (Paper I), were used to draw a smooth curve showing the chromatic variation of the square of the camera focal length. This curve has the same form as the curve supplied for the axial chromatic aberration of the camera lens, both giving minimum values at about 4700 A, where $(f_\lambda/f_{6438})^2$ is 0·99863.

We can now test this curve and the whole procedure we propose to use for our arc and solar lines by re-reducing our measured diameters in 1.1 using the ratio of camera focal lengths to determine ΔD^{*2} for any line from the cadmium red value on the plates and applying the phase change correction from the δ, λ curve in Table I to the resulting fractional order. The wave-lengths then given by the three spacers are shown in Table II, in the form observed wave-length—Barrell's wave-length, Barrell's wave-length being given in column 1. We see that none of the residuals exceeds 0·001 A and the mean for any one spacer is less than half this value. We may then conclude that our method of wave-length measurement even with spacers as narrow as 1·5 mm is capable of giving absolute wave-lengths with an accuracy better than 0·001 A from as few as eight (or even fewer) plates.

TABLE II

Wave-length accuracy using phase change corrections δ *and adopted variations of camera focal length.*

(Observed wave-length—Barrell's wave-length)

Barrell λ (A)	1·5 mm spacer	2·5 mm spacer	10 mm spacer
4046·5716	+0·0008	+0·0001	+0·0008
4358·3377	+ ·0001	− ·0005	+ ·0008
5460·7536	− ·0003	− ·0004	+ ·0004
5769·5992	− ·0008	− ·0006	+ ·0002
5790·6635	±0·0000	−0·0006	−0·0001
Mean	±0·0000	−0·0004	+0·0004

XUM

2. *Measurements on vacuum-arc and solar lines*

The measurements in Section 1 were all made on narrow lines and our results in Table II show no systematic changes with spacer, i.e. with resolution. The 2·5 mm and 10 mm plates were in fact measured by M.G.A. and the 1·5 mm plates by S.N. on the same machine. If there were any differences due to measuring habit we should expect them to be greatest for the 1·5 mm plates and four of these were measured by M.G.A. as well as by S.N., two at 5460·8 A and two at 4046·6 A. The mean difference in the wave-lengths obtained from these plates was 0·0005 A (algebraic) and 0·0006 A (arithmetic). We can therefore conclude that these narrow lines show no systematic effects due to personal equation and changes in resolution. But the broader vacuum-arc and much broader solar lines are more susceptible to such effects and require separate investigation. Arc and solar plates for this purpose were obtained in the green. The experimental arrangements were essentially the same as those described in Section 1, except that the spectroscope was used in its five prism, diaphragmed, form, two 60° prisms, one 30° prism, in a Littrow arrangement. The collimator image between the interferometer plates was now rectangular and this image was made coincident and central with the circular patch from the cadmium lamp.

2.1. *Comparison of measurements by different observers.*—A test for the effect of measuring habit on the wave-lengths derived for arc and solar lines was made on the three iron lines 5266·6, 5269·5 and 5270·4 A. These are moderately strong iron lines in both Sun and arc, but 5270·4 A is blended in the Sun and has been measured now in the arc only. Plates for the Sun and arc were obtained with the 2·5 mm spacer and five plates for each were measured and reduced by both M.G.A. and S.N., S.N. measuring on the original rotating table micrometer and M.G.A. on a new and improved form of this instrument.

TABLE III

Comparison of measurements for arc lines

(Differences $\lambda_N - \lambda_A$)

Mean λ (A)		5266·5534	5269·5346	5270·3538
Arc Int:		30	60	30
Plate	A 882	−0·0009	−0·0006	+0·0001
	A 883	± ·0000	+ ·0003	+ ·0001
	A 884	+ ·0003	− ·0002	+ ·0002
	A 885	± ·0000	+ ·0007	+ ·0006
	A 888	−0·0005	−0·0002	+0·0001
Mean		−0·0002	±0·0000	+0·0002

The agreement between the two independent measures of the arc plates is shown in Table III where the difference between the wave-lengths as measured by S.N. (λ_N) and the wave-length as measured by M.G.A. (λ_A) is shown for each line and plate. The wave-length at the head of each column is the mean value for all the measures corrected to zero pressure in the vacuum-arc; the intensities are those listed by Burns and Walters (**7**). Table IV shows the corresponding results for the solar lines, the mean values are corrected for Earth's motion (for intensities we give the Rowland numbers of the lines). We see that the agreement for the measurements of the arc plates is very good, the

mean values for the five plates differing by only one or two ten-thousandths of an angström. For the solar plates the differences are greater, but the mean measured wave-lengths agree to less than 0·001 A which is a good deal better than might have been expected from Williams' criterion.

TABLE IV

Comparison of measurements for solar lines

(Differences $\lambda_N - \lambda_A$)

Mean λ (A)		5266·5605	5269·5454
Rowland No.		6	8d?
Plate	A 878	+0·0001	−0·0021
	A 879	+ ·0031	− ·0006
	A 881	− ·0008	+ ·0001
	A 889	+ ·0008	− ·0018
	A 890	+0·0002	+0·0005
Mean		+0·0007	−0·0008

2.2. *Wave-length determinations using different spacers.*—In investigating the effect of changing spacers in the interferometer we must be careful to choose solar lines as far as possible free from blends. For this reason we have made the test primarily on the iron line 5324·193 A Rowland number 7 which shows an apparently undistorted profile in the Utrecht Atlas, and Rowlands' Revision shows no line of number greater than −3 likely to affect it. Along with this line we have measured the iron lines at 5328·053 A Rowland number 8d? and 5328·544 A Rowland number 4; these are not as free from possible blending effects, but they were considered measurable at least with the 1·5 mm and 2·5 mm spacers. With a 5 mm spacer the inter-order scatter for the solar spectrum is considerable and must in particular make the measurements of a close group of three lines unreliable (there is a chromium line of Rowland number 2 between the two iron lines at 5328·1 and 5328·5 A).

Wave-lengths have been obtained for these lines using the 1·5 mm, 2·5 mm and 5 mm spacers in the interferometer. The results for the arc lines are shown in Table V; columns 3, 4, 5 show for each spacer the difference between the mean value for all the spacers in column 2, and the measured wave-length, with the standard deviation of the measured wave-length. The measures refer to seven or eight plates for each spacer, except for the weakest line 5328·5 A, for which the number of observations is six in column 3, three in column 4 and five in column 5. The mean values in column 2 are corrected to zero arc pressure.

TABLE V

Arc wave-lengths measured with different spacers

(Mean λ − measured λ)

Arc Int.	Mean λ (A)	1·5 mm spacer	2·5 mm spacer	5 mm spacer
30	5324·1777	−0·0010 ± 0·0003	+0·0011 ± 0·0004	±0·0000 ± 0·0001
50	5328·0372	−0·0018 ± 0·0003	+0·0020 ± 0·0004	−0·0002 ± 0·0001
15	5328·5313	−0·0003 ± 0·0003	+0·0007 ± 0·0004	−0·0003 ± 0·0005
	Mean	−0·0010	+0·0013	−0·0002

XUM

Although the differences between the wave-lengths measured with different spacers are larger than for the mercury lines, the change with spacer length is not of the systematic sort we might fear, for example from a wrong phase change correction, and the average differences from the mean values are only of the order 0·001 A. The lines were moved relative to the pattern centre, but there was not as much variation in line position as for the mercury line plates, and probably not enough to eliminate the accidental errors of the experimental set-up.

The corresponding results for solar lines are shown in Table VI, in this case eight plates were measured for each spacer. The mean values in column 2 are the means (corrected for Earth's motion) from the 1·5 mm and 2·5 mm spacers only, since, as we have pointed out above, the 5 mm spacer values are likely to be uncertain (although we see that the isolated line 5324·2 is not apparently very much affected). The average differences of the 1·5 mm and 2·5 mm spacer wave-lengths from the mean value are again only of the order of 0·001 A.

TABLE VI

Solar wave-lengths measured with different spacers

(Mean λ − measured λ)

Row. No.	Mean λ* (A)	1·5 mm spacer	2·5 mm spacer	5 mm spacer
7	5324·1868	−0·0008 ± 0·0006	+0·0007 ± 0·0004	−0·0013 ± 0·0003
8d?	5328·0463	−0·0016 ± 0·0005	+0·0016 ± 0·0004	−0·0024 ± 0·0005
4	5328·5376	−0·0006 ± 0·0004	+0·0006 ± 0·0005	−0·0022 ± 0·0005
	Mean	−0·0010	+0·0010	−0·0020

* From the 1·5 mm and 2·5 mm spacers.

The fact that they are in the same sense and of the same size as those for the arc lines supports the suggestion that in both cases they arise from the accidental errors of the particular plate orientation and line positions used for these particular arc and solar measures. This means that the red shift as determined by different spacers is even less subject to error than the absolute wave-lengths. Table VII shows the red shifts for the three lines as given by the 1·5 mm and 2·5 mm spacers; the 5 mm spacer red shifts are not included because this spacer appears

TABLE VII

The red shift given by different spacers

El.	Row. No.	Mean λ (A) Solar	1·5 mm spacer	2·5 mm spacer
Fe	7	5324·1868	8·9 mA	9·5 mA
Fe	8d?	5328·0463	8·9	9·5
Fe	4	5328·5376	6·6	6·4

to be already too long for the spectroscopic resolution (**14**). We see that for any one line the difference between the red shifts given by the two spacers is well under 0·001 A.

Conclusion

On the basis of our tests described in Sections 1 and 2 we can conclude first of all, that as far as experimental technique is concerned, our procedure by the method of circular channels eliminates, or reduces below 0·001 A, the "scale error" of any region in the visible spectrum. That is the error arising because the wave-lengths in the region as a whole are not properly related to the primary standard. Moreover a fairly small number of plates suffices to give a wave-length accuracy for individual lines of 0·001 A. In the second place we find that the "personal equation" of different observers in deriving wave-lengths from the peculiar "circular channel" patterns is very small, both for the narrow vacuum-arc lines and also for the broad solar lines. For three arc lines and two solar lines any systematic difference in the wave-lengths determined by different observers is only 0·0002 A for the arc lines, and even for the solar lines the mean values for individual lines do not differ by as much as 0·001 A.

Finally we have some evidence that the micrometer measurement of broad lines is more meaningful than has been suggested (**12**). Thus different observers measuring the same plates arrive at very closely the same wave-lengths, and also changing the interferometer spacer gives differences, (small and non-systematic), which are very closely the same for the broad solar lines as for the narrow arc lines, provided the spacer is not too long for the spectroscopic resolution. The significance of the micrometer measurements is the most difficult and the most fundamental of our problems. There is no doubt that the full story of the solar red shifts is to be found in detailed contour measurements of high resolution spectra on an absolute wave-length scale. Such a programme is, however, impracticable for any but a very few lines, and in any statistical approach we are bound to rely on micrometer measures. Our investigations here described show that, provided the interferometer spacer is properly related to the spectroscopic resolution, red shifts consistent and reliable to under 0·001 A can be obtained for unblended solar lines. This is an accuracy probably more than sufficient to test the various theories with which we try to account for the shifts.

University Observatory,
Oxford:

1957 *November* 21.

References

(1) M. G. Adam, *M.N.*, **112,** 546, 1952; Comm. Univ. Obs. Oxford, No. 36. Paper I.
(2) M. G. Adam, *M.N.*, **115,** 405, 1955; Comm. Univ. Obs. Oxford, No. 49. Paper II.
(3) M. G. Adam, *M.N.*, **115,** 422, 1955; Comm. Univ. Obs. Oxford, No. 50. Paper III.
(4) H. D. Babcock, *Ap. J.*, **111,** 63, 1950.
(5) H. Barrell, *Proc. Roy. Soc.* A, **209,** 132, 1951.
(6) H. Barrell and P. Teasdale-Buckell, *Proc. Phys. Soc.*, B **44,** 413, 1951.
(7) K. Burns and F. M. Walters, *Publ. Alleg. Obs.*, **VI,** 159, 1929.
(8) W. H. J. Childs, *Journal of Scientific Instruments*, **3,** 132, 1925–6.
(9) E. F. Freundlich and E. G. Forbes, *Ann. d'Ap.*, **19,** 183, 1956: **19,** 215, 1956.
(10) L. Herzberg, *Canad. J. of Phys.*, **35,** 766, 1957.
(11) H. H. Plaskett, *M.N.*, **112,** 177, 1952; Comm. Univ. Obs. Oxford, No. 33.
(12) E. H. Schröter, *Zs.f. Ap.*, **41,** 141, 1957.
(13) L. G. Schultz, *J.O.S.A.*, **41,** 261, 1951.
(14) P. J. Treanor, *M.N.*, **109,** 389, 1949. Comm. Univ. Obs. Oxford, No. 28.
(15) W. E. Williams and A. Middleton, *Proc. Roy. Soc.* A., **172,** 159, 1939.

XUM

INTERFEROMETRIC MEASUREMENTS OF WAVE-LENGTHS

V. The radial current interpretation of solar red shifts

M. G. Adam

(Communicated by the Director of the University Observatory, Oxford.)

(Received 1957 December 5)

Summary

The relativity-radial current theory of solar red shifts was thought earlier to imply currents with impossibly high velocities, but with a new model atmosphere, based on 0″·4 granules of high brightness contrast, Schröter finds that the shifts can be explained with streaming velocities of only 2–3 km sec^{-1}. There is quite a good agreement between his theoretical predictions and centre to limb observations of the shift. Our wave-length measures at the solar centre and in the vacuum-arc can also be used to test his theory. They enable us to determine the resultant streaming velocity as a function of line strength; but these velocities do not agree with Schröter's predictions. We then examine the wave-lengths dependence of the shifts using the Allegheny Observatory–Bureau of Standards measures; this test also fails to support the radial current interpretation.

Introduction.—Doppler shifts, due to radial currents in the solar atmosphere, have most generally been considered to account for the failure to find the exact Relativity shift in the Fraunhofer lines. St John originated this explanation in 1928 (**13**) and since that time the theory has been discussed and modified by several writers. McCrea and Mitra (**9, 10**) showed that the change in streaming velocity with depth in the photosphere must be taken into account, and it was pointed out in an earlier paper that the velocities deduced must be mean values for upgoing and downgoing streams (**1**). But when both these factors were taken into account and when the microscopic circulation was associated with granulation, we found that the individual streaming velocities were impossibly high. In a recent important paper Schröter (**12**) develops a more elaborate two-stream model of the photosphere using the latest granulation data, and he overcomes this objection to the radial current theory.

Schröter assumes that the observed mean velocities come from very much smaller granules than was previously supposed; he considers granules 0″·4 diameter with high brightness contrast. The contrast is assumed to vary across the disk from a brightness ratio, granular to intergranular, of 1·45 at the centre rising to a maximum of 1·81 95 per cent of the way across ($\cos\theta = 0{\cdot}3$), and then falling rapidly. In the two-stream model the high contrast is in accordance with high temperature differences between the streams; in Schröter's model the differences vary with depth reaching a maximum of 900° abs. at an optical depth in the continuous spectrum of $\tau = 0{\cdot}5$. The streaming velocities are then calculated for any depth by turbulence theory, from the temperature deviations from the mean value. The velocities in the effective layers are now only of the order 2–3 km sec^{-1} up and down; not at all improbable values. By detailed

calculations of line contours as formed in each stream Schröter shows that the composite line becomes asymmetrical, and finds the associated apparent shift for lines of different strengths and the change in shift from centre to limb. In particular he reproduces fairly closely the centre shifts and centre-to-limb variation in the shifts which were discussed in 1948 (**1**).

Observations of red shifts across the solar disk give the most obvious test of the radial current hypothesis, but our measures of absolute wave-lengths at the centre (coupled with the vacuum-arc measurements) give alternative and no less significant tests of the theory. With the new measures presented in this and the preceding paper we have now determined absolute wave-lengths over the spectral range 4200–6600 A, and within that range the line strengths vary from practically the weakest to the strongest measurable lines of neutral elements. Some description of the new measurements for strong lines is given in Section 1 of the paper, and these red shifts, together with the earlier results, form the observational material upon which Schröter's hypothesis is examined in Section 2.1. In Section 2.2 the radial current interpretation is considered for the very extensive measurements from the Allegeheny Observatory–Bureau of Standards work. The paper concludes with a very brief further discussion of the main features of our measured red shifts, since neither the Oxford nor the A.O.–B.S. measures can yet be reconciled with the radial current interpretation.

1. *The observational material*

We have previously measured absolute wave-lengths in both Sun and arc for 20 lines, ranging from Rowland numbers 1–8, in spectral regions from 5080–6600 A. To these lines we have now added those shown in Table I. The new lines were chosen to extend our measurements to the strongest Fraunhofer lines and, excepting the Balmer lines, we have now included the strongest lines of neutral elements in the visible spectrum. On the logarithmic scale of intensities which we use, the Balmer lines extend the range only very little, and their characteristic rounded contours would make it difficult to measure the wave-lengths by micrometer methods. The next strongest, Mgb lines and the calcium resonance line, have sharp cores, and with heavy photographic densities it is not unduly difficult to measure them. The additional lines in Table I are numbered 21–34 (following the first 20) for convenience in referring to them in the later parts of the paper. The equivalent widths in the last column are in milliangströms as given by Allen (**4, 5**). There are several sources of equivalent widths for the stronger lines, but for the sake of consistency we have used Allen's measures for all 34 lines we shall discuss.

The wave-lengths in both Sun and arc were measured by the method of circular channels with details of the arrangements as in Paper IV. For the green region the spectroscope was used in its 5-prism form; at 4227 A where the spectroscopic dispersion is higher it was used in its 3-prism form. The wave-lengths below for lines 21, 22, 23, 30, 31 all refer to a 2·5 mm spacer in the interferometer. In the Mgb region both solar and arc observations include also some plates taken with a 1·5 mm spacer. The plates were measured and reduced as explained in the earlier papers, the ratio of camera focal lengths and the phase change correction for the different regions were obtained from the work described in Paper IV. Table II shows the absolute wave-lengths now obtained for the

XUM

TABLE I

Additional lines measured

Line No.	El.	Rev. Rowland Table Int.	Wave-length in A	Eq. width (Allen) mA
21	Ca	20d	4226·742	1230
22	Fe	4	4227·442	170
23	Fe	6	4233·613	220
24	Mg	15	5167·330	752
25	Fe	5	5167·510	152
26	Fe	6	5171·612	151
27	Mg	20	5172·700	1200
28	Ti	2	5173·751	75
29	Mg	30	5183·621	1600
30	Fe	6	5266·565	220
31	Fe	8d?	5269·552	388
32	Fe	7	5324·193	254
33	Fe	8d?	5328·053	341
34	Fe	4	5328·544	196

solar and vacuum-arc lines 21–31 with the standard deviation of the mean value and the number of observations. For lines 24–29 the values from the two spacers used have been given equal weight in forming the mean wave-length. The wave-length measurements for lines 30–34 have already been discussed in Paper IV. The results given in Table II for lines 30, 31 are those obtained by M.G.A. alone; the wave-lengths for lines 32–34, measured by S. Nichols alone, have already been given in Paper IV, Tables V and VI.

TABLE II

Measured wave-lengths: solar and vacuum-arc

			Sun			Arc				
(1)	(2)	(3)	(4)	(5)	(6)	(7)	(8)	(9)	(10)	(11)
21	Ca	4226·7	·7385	±0·0006	5	·7268	±0·0003	8	0·0000	·7268
22	Fe	4227·4	·4369	0·0006	5	·4270	0·0002	5	0·0004	·4266
23	Fe	4233·6	;6123	0·0007	5	·6031	0·0003	5	0·0003	·6028
24	Mg	5167·3	·3308	0·0011	7	·3236	0·0008	6	0·0006	·3230
25	Fe	5167·5	·5012	0·0008	7	·4879	0·0007	7	0·0003	·4876
26	Fe	5171·6	·6062	0·0007	12	·5958	0·0005	7	0·0003	·5955
27	Mg	5172·7	·6966	0·0006	12	·6859	0·0006	6	0·0006	·6853
28	Ti	5173·8	·7490	0·0008	12	·7417	0·0004	8	0·0001	·7416
29	Mg	5183·6	·6155	0·0006	8	·6063	0·0009	9	0·0003	·6060
30	Fe	5266·6	·5601	0·0009	5	·5541	0·0003	5	0·0006	·5535
31	Fe	5269·6	·5458	0·0007	5	·5348	0·0003	5	0·0002	·5346

(1) Line number; (2) El.; (3) Wave-length in angströms; (4) Mean obs. solar wave-length; (5) St. dev. of mean; (6) Number of obs.; (7) Mean arc wave-length; (8) St. dev. of mean; (9) Number of obs.; (10) Press: correction in angströms; (11) Vac.-arc wave-length.

The solar wave-lengths in Table II, column 4, are a mean value for a slit height of 18 mm at the centre of the 180 mm image; they are corrected for the Earth's rotation and orbital motion.

With the exceptions noted below, the mean vacuum-arc wave-lengths in column 7 were obtained under our usual arc conditions, pressures not greater than 10 cm of mercury, currents less than 8 amps and pole separations not less than 10 mm. Self-reversal in the calcium resonance line was most easily avoided

TABLE III

Solar red shifts

(1)	(2)	(3)	(4)	(5)	(6)	(7)	(8)	(9)
1	Fe	5068·8	383	2·93	z^7P^0–e^7D	9·6	−1·1	25·6
2	Fe	5074·7	1094	4·20	y^5F^0–e^3G	12·8	+2·0	20·9
3	Fe	5078·97	1092	4·28	y^5F^0–f^5G	8·2	−2·6	17·3
4	Fe	5079·2	66	2·19	a^5P–y^5P^0	9·6	−1·2	20·9
5	Fe	5079·7	16	0·99	a^5F–z^5F^0	9·8	−1·0	20·5
6	Fe	5083·3	16	0·95	a^5F–z^5F^0	10·4	−0·4	21·8
7	Fe	6008·6	982	3·87	z^3D^0–e^3F	8·4	−4·3	14·3
8	Mn	6013·5	27	3·06	z^6P^0–e^6S	7·6	−5·1	12·6
9	Mn	6016·6	27	3·06	z^6P^0–e^6S	7·3	−5·5	15·3
10	Mn	6021·8	27	3·06	z^6P^0–e^6S	6·1	−6·7	15·3
11	Fe	6024·1	1178	4·53	y^3F^0–f^5G	9·9	−2·9	17·6
12	Fe	6027·0	1018	4·06	c^3F–v^3G^0	6·7	−6·1	10·1
13	Ca	6493·8	18	2·51	3^3D–$3d4p^3F^0$	11·3	−2·5	22·8
14	Fe	6494·98	168	2·39	a^3H–z^5G^0	12·9	−0·9	27·1
15	Ca	6499·6	18	2·51	3^3D–$3d4p^3F^0$	10·6	−3·2	14·2
16	Fe	6569·2	1253	4·71	y^3D^0–g^5F	7·0	−6·9	11·9
17	Ca	6572·8	1	0·00	4^1S–4^3P^0	4·6	−9·3	5·0
18	Fe	6575·0	206	2·58	b^3F–z^3G^0	7·0	−6·9	9·1
19	Fe	6592·9	268	2·72	a^3G–y^3F^0	12·9	−1·1	17·0
20	Fe	6593·9	168	2·42	a^3H–z^5G^0	15·7	+1·7	11·2
21	Ca	4226·7	2	0·00	4^1S–4^1P^0	11·7	+2·7	291·0
22	Fe	4227·4	689	3·40	z^5F^0–e^7F	10·3	+1·3	40·2
23	Fe	4233·6	152	2·47	z^7D^0–e^7D	9·5	+0·5	52·0
24	Mg	5167·3	2	2·70	3^3P^0–4^3S	7·8	−3·2	145·5
25	Fe	5167·5	37	1·48	a^3F–z^3D^0	13·6	+2·6	29·4
26	Fe	5171·6	36	1·48	a^3F–z^3F^0	10·7	−0·3	29·2
27	Mg	5172·7	2	2·70	3^3P^0–4^3S	11·3	+0·3	232·0
28	Ti	5173·8	4	0·00	a^3F–z^3F^0	7·4	−3·6	14·5
29	Mg	5183·6	2	2·70	3^3P^0–4^3S	9·5	−1·5	308·7
30	Fe	5266·6	383	2·99	z^7P^0–e^7D	6·6	−4·6	41·8
31	Fe	5269·6	15	0·86	a^5F–z^5D^0	11·2	±0·0	73·6
32	Fe	5324·2	553	3·20	z^5D^0–e^5D	9·2	−2·1	47·7
33	Fe	5328·1	15	0·91	a^5F–z^5D^0	9·2	−2·1	64·0
34	Fe	5328·5	37	1·55	a^3F–z^3D^0	6·5	−4·8	36·8

(1) Line number; (2) El.; (3) Wave-length in angströms; (4) Mult. number; (5) Ex. Pot. in volts (low); (6) Transition; (7) Red shift Δ mA; (8) Resid. shift δ mA; (9) $10^6 W/\lambda$.

XUM

by using lower currents and pressures and close pole-pieces, and two of the calcium observations and one of the five observations for lines 22 and 23 were obtained under these conditions. The close pole-pieces caused no significant change in the wave-lengths obtained. Three of the eight calcium observations were for the unreversed line and these wave-lengths agreed well with those obtained for the sharp absorption core of the self-reversed line. The corrections to zero arc pressures were derived, for all the elements, from Babcock's expressions for the depressions of energy levels in the iron atom (**6**); the corrections are all small, as can be seen from column 10.

Finally in Table III we have collected together all the red shifts which we have so far obtained. The red shifts for lines 1–20 are from Table V of Paper II (**2**); for lines 21–31 they are the differences of columns 4 and 11 in Table II above; for lines 32–34 they are the mean red shifts for the 2·5 mm and the 1·5 mm spacer in Table VII of Paper IV (**3**). I am very grateful to Mr Nichols for permission to include his results for these last three lines. Table III shows also the physical properties of the lines which we shall need for our subsequent discussion. Columns 4, 5, 6 are from Miss Moore's Revised Multiplet Table (**11**) Δ in column 7 is the solar red shift in milliangströms, and δ in column 8 (the residual shift) is the red shift Δ minus the predicted relativity shift ($2{\cdot}12\lambda \times 10^{-6}$). δ is thus the quantity for which we have as yet no agreed physical theory and for which we must account. Column 9 gives a measure of line strength in dimensionless units; it is Allen's equivalent width for the line W, divided by the wave-length λ, both measured in the same units; W/λ is the unit in which Schröter expresses line strengths.

2. *The radial current hypothesis*

2.1. *Observed velocities.*—On the radial current theory the residual shift δ in Table III is a velocity shift and for lines formed at the same geometrical height in the solar atmosphere the velocity has a constant value. In general the higher the level of formation the smaller the outward velocity we should expect, and indeed for very high lines the shift can become red according to Schröter's investigation of resultant line contours. Over medium line strengths it seems reasonable to expect the velocity shift to decrease steadily as the effective level of formation rises, i.e. with increasing line strength. This is only a generalization and ignores questions of abundance, excitation potential and wave-length changes in the continuous absorption coefficient, but these should be of secondary importance. Fig. 1 shows the observed δ/λ as a function of line strength in the form $\log 10^6 W/\lambda$. For convenience in discussion we will indicate by (W/λ) the quantity $10^6 W/\lambda$. Let us assume that there is a linear relation between δ/λ and $\log (W/\lambda)$ which we express by

$$\delta/\lambda = c(\log (W/\lambda) - \log (W/\lambda)_0) \qquad (1)$$

in which c is constant and $(W/\lambda)_0$ is the line strength at which the resultant velocity is zero. Our quantity δ can then be expressed in the form

$$\delta = a\lambda + c\lambda \log (W/\lambda) \qquad (2)$$

where a is $-c \log (W/\lambda)_0$. In making a fit to this expression, it seems fairer to the hypothesis to omit from the solution the strongest lines 21, 24, 27, 29 (open

circles in Fig. 1). They must be formed in the highest layers of the atmosphere and possibly do not continue the steady progression of velocity shift and line strength which we may expect for the less strong lines.

From Table III we have then 30 observational equations of the form (2) and a least-squares solution of these gives

$$\delta = -(1{\cdot}764 \pm 0{\cdot}392) \times 10^{-6}\lambda + (0{\cdot}999 \pm 0{\cdot}299) \times 10^{-6}\lambda \log (W/\lambda) \qquad (3)$$

in which δ and λ are measured in the same units. Or in form (1) we have

$$\delta/\lambda = 0{\cdot}999 \times 10^{-6} (\log (W/\lambda) - 1{\cdot}765) \qquad (4)$$

which is the straight line shown on Fig. 1. Equation (4) gives zero velocity for lines where $\log (W/\lambda) = 1{\cdot}765$, i.e. lines of Rowland number about 8. Our faintest line is Rowland number 1, $\log (W/\lambda) = 0{\cdot}699$; for such a line equation (4) gives $\delta/\lambda = -1{\cdot}07 \times 10^{-6}$ corresponding to an upward velocity of $0{\cdot}32\,\mathrm{km\,sec^{-1}}$, and all stronger lines must have smaller velocities than this.

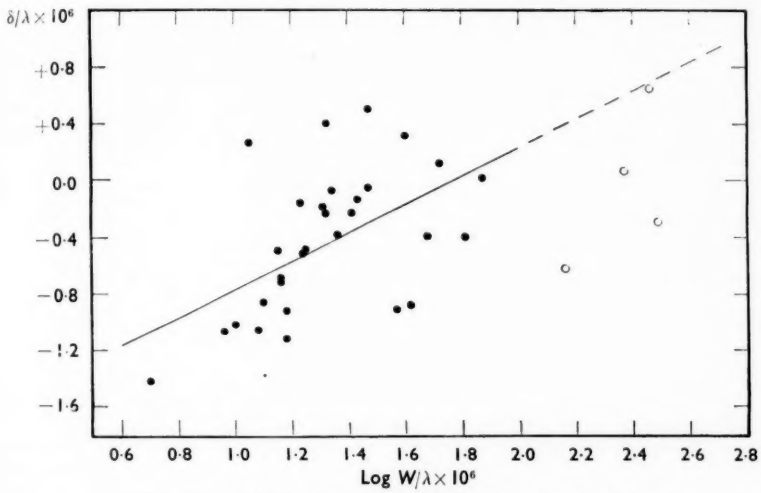

FIG. 1.—*Residual velocity shift* (δ/λ) *as a function of line strength.*

Schröter tested his theory of red shifts against two series of solar observations, the Oxford measures of 14 lines at 6100 A of mean equivalent width 0·088 A (**1**), and the Potsdam observations (**7**) of 9 lines at 4400 A of mean equivalent width 0·113 A. The Oxford measures give absolute wave-lengths from centre to limb, while the Potsdam observations give only the change in wave-length across the disk, and Schröter assumes for them an absolute value of the centre red shift. He then shows that both series of observations can be fitted on the radial current theory with a resultant outward streaming velocity at the centre of the disk (v) of $0{\cdot}42\,\mathrm{km\,sec^{-1}}$. Fig. 2 shows the Oxford observed Δ's, expressed in $\mathrm{km\,sec^{-1}}$, as a function of $\cos\theta$, θ being the angle between the line of sight and the normal to the solar surface; the range in $\cos\theta$ and the estimated uncertainty of the velocity is shown with each observed point. The theoretical relation is given by Schröter's equation (37)

$$\Delta_\theta \text{ (in km sec}^{-1}) = 0{\cdot}636 - v \,.\, \beta_\theta \,.\, \cos\theta$$

XUM

in which 0·636 is the Relativity shift in km sec^{-1} and β_θ, which depends mainly on the granulation contrast, is given in his Fig. 8. Curve (*a*) on Fig. 2 is Schröter's predicted curve with $v = 0{\cdot}42$ km sec^{-1}. But our equation (4) above gives for the Oxford lines ($\log(W/\lambda) = 1{\cdot}16$) a resultant velocity at the centre of the disk of 0·184 km sec^{-1}, and for the Potsdam lines ($\log(W/\lambda) = 1{\cdot}41$) a velocity of 0·107 km sec^{-1}. If we substitute these velocities in Schröter's theoretical expression we obtain the upper curves (*b*) and (*c*) respectively in Fig. 2, which no longer agree with the observations. The curve (*b*) would be still higher if we had included the four strongest lines in our solution for equation (4).

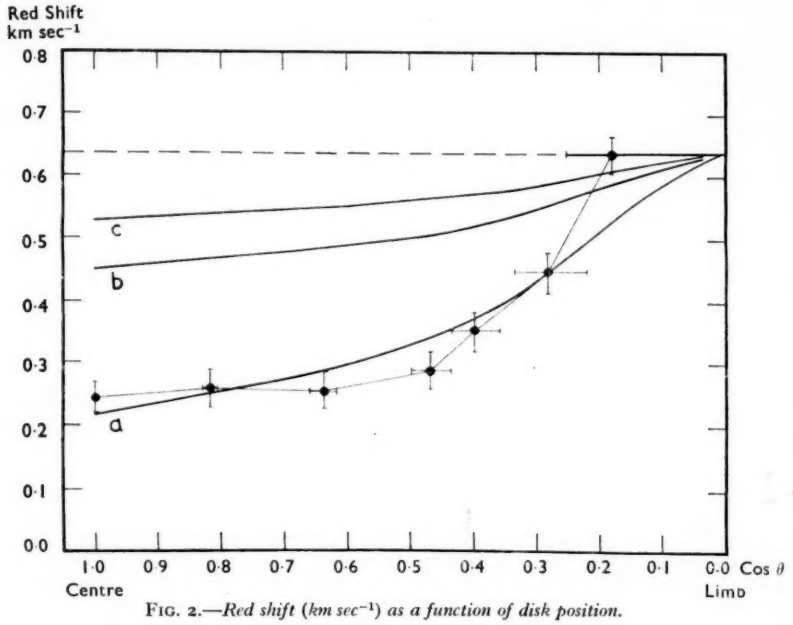

FIG. 2.—*Red shift (km sec^{-1}) as a function of disk position.*

Our velocities now deduced are based on absolute measures of both solar and arc wave-lengths, which are used to give the general form of the velocity–line strength relation. In the 1948 results the wave-lengths were measured by the older method of parabolic channels using atmospheric oxygen lines as standards, and the vacuum-arc wave-lengths were from a variety of sources in the literature. The first five of the 1948 lines have re-appeared in our later measures by the method of circular channels (lines 8–12 in Table III, from Paper II), and the new centre red shifts are corrected in the direction which the collected observations now indicate. The uncertainty in the absolute values of the red shifts in 1948 means that the observed curve in Fig. 2 may be shifted bodily parallel to the velocity axis, but the shape of the curve should not be affected. Such a displacement would give limb red shifts well in excess of the Relativity value which is shown by the dotted line on Fig. 2. We must note, however, as was pointed out in 1948, that the observations in Fig. 2 correspond to low resolution on the solar disk and Miss Hart's results (**8**) indicate that the rapid increase in red

shift must be closer to the limb. The exact form of the centre-limb change in red shift is clearly a matter of first importance and we hope soon to have a better determination of it, from observations made with the large image given by the new solar telescope at Oxford; but these plates have not yet been measured.

Schröter points out that, while line strength is the most important factor, the red shift depends also on excitation potential. It is possible that some of the very considerable scatter of the observed points in Fig. 1 may be due to this effect. We have therefore examined the residuals of our 30 observational equations for δ as a function of excitation potential. The correlation coefficient between the residuals and the lower state excitation potentials is, however, quite meaningless, being only +0·0080 for the 30 observations.

2.2. *Wave-length dependence of red shifts.*—In the last section we assumed that our residual shifts were velocity shifts, but we find that the velocities they indicate do not account for the observed centre-limb behaviour of the red shifts.

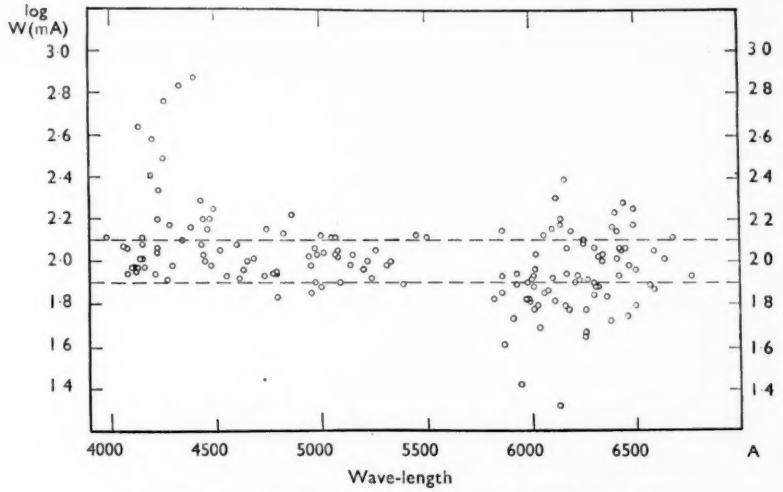

FIG. 3.—*Line strength–wave-length distribution of the A.O.–B.S. red shifts.*

We will now go further and enquire whether the solar red shifts show the essential feature of velocity shifts in their dependence upon wave-length. For a given level of formation in the solar atmosphere, say a given line strength, the resultant streaming velocity should be constant and the residual shifts δ should be proportional to the line wave-length. Our results in Table III, which were designed to cover a large range in line strength, do not give enough observations at any one line strength to make this test in its simplest form, but we can use again the very large collection of red shifts in the Allegeheny Observatory–Bureau of Standards investigations. Fig. 3 shows the line strength–wave-length distribution of the 158 observations already discussed in Paper II*. We see that if we restrict ourselves to line strengths between 80 mA and 125 mA (between

* The A.O.–B.S. wave-lengths are for the integrated solar disk, and these must be slightly longer than centre wave-lengths. Estimating the difference between the two from the observed centre-limb change in Fig. 2 and limb darkening observations we find that it is less than 0·001 A.

XUM

the dotted lines in Fig. 3) we can include a large number of red shifts with a wave-length range from 4100–6800 A, and for this analysis we will take log (W/λ) as constant; the maximum range in log (W/λ) is 1·09–1·47.

For the 76 lines included within these limits Fig. 4 shows the residual shift δ, (observed red shift–Relativity shift), as a function of wave-length. We see that the scatter of the points is considerable and the general distribution gives little indication of the strictly linear dependence of δ on λ demanded by the radial current hypothesis. On this hypothesis the relation between the two is of the form $\delta = m\lambda$ where m is constant. The mean value of δ/λ for the 76 points is $-0{\cdot}55 \times 10^{-6}$, and the line (a) on the figure shows the relation between δ and λ we should expect from this value. The line is obviously a very inadequate representation of the distribution; the scatter of the observed points about it is clearly not random, but varies systematically with wave-length. Over the first half of the wave-length range there is a marked increase of δ with λ instead of a decrease, so much so, that at 5000 A the residual shifts are positive, indicating an ingoing resultant velocity instead of an outgoing one. In the red the residual shifts have systematically larger negative values than the relation indicates.

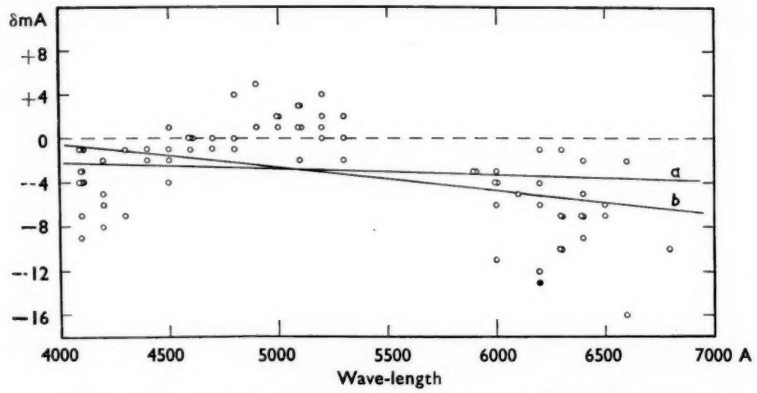

FIG. 4.—*Residual shifts as a function of wave-length.* (*A.O.–B.S. observations*).

The observed δ, λ relation obviously requires representation by some form more complicated than a linear one. But since a linear relation is predicted by the radial current theory we have made a least squares solution for the line of closest fit. This is the line (b) on Fig. 4. The equation is

$$\delta = 8{\cdot}01 \pm 2{\cdot}73 - (2{\cdot}11 \pm 0{\cdot}51) \times 10^{-6}\lambda \qquad (5)$$

in which both δ and λ are in milliangströms. If in this expression the second term is regarded as corresponding to the resultant velocity demanded by the radial current hypothesis, how are we to account for the large and quite well determined constant term? On the radial current theory δ is directly proportional to λ, and the first term in (5) should not be significantly different from zero. We must conclude then that radial currents and the Relativity shift are not, by themselves, sufficient to account for the observed red shifts and their variation with wave-length; some additional hypothesis must be included.

Conclusion

The radial current hypothesis is the only physical theory put forward to account for solar red shifts, and Schröter's very careful investigation on the basis of very small, high contrast, granules is made in accordance with all the latest theories of the solar atmosphere. Moreover his model atmosphere is able to account for other observational phenomena. But when we examine the theory for red shifts over a wider range of observational material than Schröter considered, both that presented here and the very numerous measures given by the Allegheny Observatory–Bureau of Standards, we find that we are not yet justified in accepting his explanation. We lack, at present, the observational evidence that the shifts are, in fact, velocity shifts, but if nevertheless we interpret them as such, we find that the velocities deduced from the centre of disk values do not accord with the change in red shift to the limb.

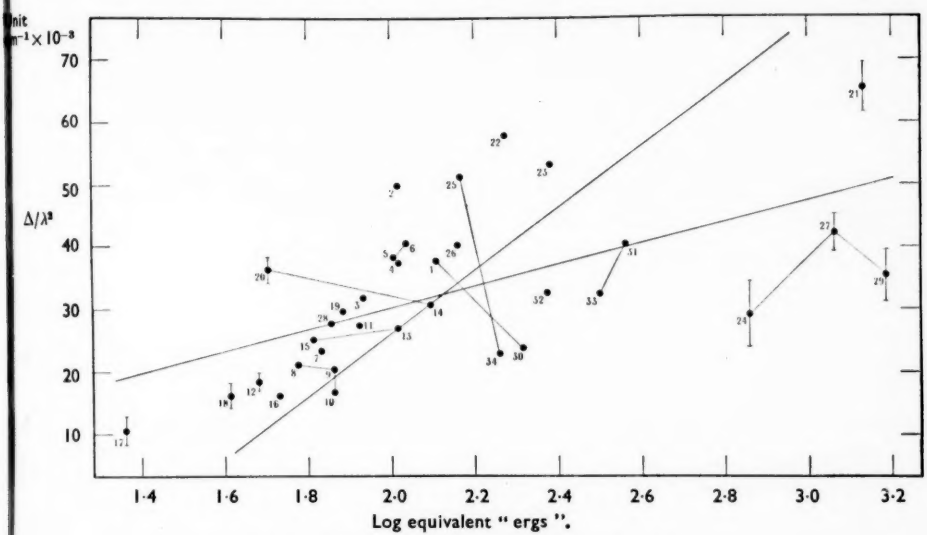

FIG. 5.—Δ/λ^2 *as a function of log equivalent "ergs".*

Observationally our only certain information about the centre shifts is that they increase with line strength. In Paper II we found a high statistical correlation between the shift expressed in cm^{-1} and the logarithm of the line strength expressed in equivalent "ergs". Our range in log equivalent "ergs" is now more than doubled and Fig. 5 shows the plot of these two quantities for the 34 points of Table III; the factors for obtaining equivalent "ergs" are 1·101 for the new lines 21–23 and 0·964–0·929 for the new lines 24–34. Although the scatter of the points in Fig. 5 is considerable, the correlation coefficient is +0·587 and for the 34 observations this indicates a significance level better than 0·001: the computed regression lines are shown on the figure.

We may use our observations, as set out in Fig. 5, to point out some features of the shifts. The outstanding and somewhat disappointing feature is the very large scatter of the points. The preceding Paper IV shows that we may hope to get red shifts accurate to better than 0·001 A. As far as accidental errors now are

XUM

concerned the standard deviations in Table II show that the maximum uncertainty in Δ for our strongest and most difficult lines is only 0·0014 A, the vertical lines through some of the points in Fig. 5 show the corresponding estimated uncertainty in Δ/λ^2 for these lines, and similarly for some of the weakest lines. It appears then that the scatter of the points in Fig. 5 is outside the range of observational uncertainty. If it were produced by the peculiar perturbations of atomic energy levels we should expect to find members of the same multiplet showing the same deviations. We have joined together such lines in Fig. 5 and we see, that among the medium to strong lines, there is no evidence for such an effect. Our measures include now three resonance lines, 17, 21, 28 in Table III, but these show no special peculiarities in their red shifts. It is of course possible that the scatter is due to unsuspected blends in the solar spectrum, but it is greater, rather than smaller, for the stronger lines and these lines should be much less affected by any faint blends. We cannot but conclude that there remains some substantial physical effect in the solar atmosphere, influencing the red shifts, which we have not yet taken into consideration. So far as the observations go, we have seen that it is certainly of such a magnitude as to obscure the presence of shifts due to radial currents.

I gratefully acknowledge the constant help and advice I have received from Professor Plaskett; I should also like to thank Miss J. A. Bailey for her valuable computational assistance.

University Observatory,
Oxford:
1957 *November* 21.

References

(1) M. G. Adam, *M.N.*, **108**, 446, 1948; Comm. Univ. Obs. Oxford, No. 26.
(2) M. G. Adam, *M.N.*, **115**, 367, 1955; Comm. Univ. Obs. Oxford, No. 49. Paper II.
(3) M. G. Adam and S. Nichols, *M.N.*, **118**, 97, 1958. Comm. Univ. Obs. Oxford, No. 65. Paper IV.
(4) C. W. Allen, *Mem. Comm. Solar Obs.*, **5**, 1934.
(5) C. W. Allen, *Mem. Comm. Solar Obs.*, **6**, 1938.
(6) H. D. Babcock, *Ap. J.*, **67**, 240, 1928.
(7) E. F. Freundlich, A. v. Brunn and H. Brück, *Z.f. Ap.*, **1**, 43, 1930.
(8) A. B. Hart, *M.N.*, **114**, 17, 1954; Comm. Univ. Obs. Oxford, No. 43.
(9) W. H. McCrea and K. K. Mitra, *Obs.*, **57**, 379, 1934.
(10) K. K. Mitra, *Obs.*, **59**, 160, 1936.
(11) C. E. Moore, *A Multiplet Table of Astrophysical Interest*, rev. ed., Princeton, 1945.
(12) E. H. Schröter, *Z.f. Ap.*, **41**, 141, 1957.
(13) C. E. St. John, *Ap. J.*, **57**, 195, 1928.

PERIODS AND LIGHT-CURVES OF VARIABLE STARS IN NGC 121

A. D. Thackeray

(Received 1957 September 9)

Summary

82 photographs of the globular cluster NGC 121 on the outskirts of the Small Magellanic Cloud, covering a total range of 9 years but mostly concentrated in three consecutive seasons, are used to derive periods and light-curves of 5 variables within 1′ of the cluster. Of these, three are short-period variables (periods between 0·50 and 0·64 days) of Bailey *a* and *b* type with the usual relations between period, amplitude and shape of light-curve. The other two, among the reddest and brightest of the cluster-stars, have periods of 140·2 and 112·4 : days. The light-variations are presented in the form of step-estimates on a " basic " sequence.

Four other short-period variables have been found on the plates which are too far from the cluster to be members. They are sufficiently faint to be regarded as possibly the first instance of RR Lyr variables in the general field of the Small Magellanic Cloud.

NGC 121 ($0^h\,24{\cdot}4$, $-71°\,48'$; 1950) was discovered by John Herschel but was first resolved as a cluster on Harvard photographs (**1**) and recognized as a globular cluster by Mohr (**2**). The Harvard workers accepted the cluster as a member of the Small Magellanic Cloud. This view was also adopted by Gascoigne and Kron (**3**) in their observations of colours and magnitudes of Cloud clusters; for NGC 121 they found $P = 11{\cdot}44$, $P - V = +0{\cdot}70$. The cluster lies 35′ *nf* the globular cluster 47 Tuc.

When the faint (19th mag) variables were discovered in the cluster at the Radcliffe Observatory (**4**) it was at first suspected that the cluster might lie beyond the Small Cloud. However, Baade's revision of the distance scale, and the discovery of other clusters in the Large Cloud with equally faint variable stars, led Thackeray and Wesselink (**5**) to deduce increased distances of both Clouds in good agreement with Baade's revised scale. At the time of writing, no radial velocity of NGC 121 is available, but there seems to be no reason to doubt that it is in fact a member of the Small Cloud, especially since the 21 cm radio observations have shown that the boundary of the Cloud extends beyond the position of the cluster.

The discovery of these short-period variables was also important in that it indicated the presence of Population II objects in both Clouds. In this paper periods and light-curves of these variable stars are presented. Special interest attaches to such data since the discovery that the RR Lyr variables in the galactic nucleus (**6**) differ from those in many globular clusters as studied by Bailey. It is therefore considered worthwhile to publish results for NGC 121 based on step-estimates of magnitude, prior to the final establishment of a sufficiently faint magnitude sequence.

XUM

Observations.—A total of 82 blue photographs of NGC 121, all taken with the Radcliffe 74-inch reflector, have been used for estimating the variables. Of these 29 were taken by Dr A. J. Wesselink, 9 by Dr M. W. Feast and the remainder by the writer. Exposures were on Kodak 103aO emulsion, mostly of 30 min, but a few were of 10 or 15 min. A few red exposures are also available, one being shown in Plate I (*b*) for comparison with a blue exposure. Owing to the great need for series of plates on closely adjacent nights and at large hour angles, many plates were taken in conditions far from perfect. The faintness of the variables implied that good estimates could only be made on plates of first quality. Consequently, some of the original plates could not be used at all for estimates and in many cases all that could be said of some variables was that they were fainter than some limit brighter than minimum.

Blink discovery of the variables.—Pairs of plates were examined in the blink comparator belonging to the Royal Observatory, Cape, which has very kindly been made available on loan to the Radcliffe Observatory by H.M. Astronomer. In all a total of nine variables has been discovered (five in the cluster). A few others, recorded as possibly variable on blink comparisons, were rejected on further examination. Variables 1 to 4 were discovered by the writer at a very early stage while concentrating on the cluster itself. V5 was discovered by Dr Wesselink while examining the plates for another purpose, and V6 to V9 were discovered by the writer while carrying out further blinks of the whole area (30′ × 40′) covered by the plates.

TABLE I

Positions of variables and comparison stars in field of NGC 121 (seconds of arc)

Variable	ΔX	ΔY	r
1	+ 38.	+ 3	38
2	+ 57	+ 12	58
3	− 2	+ 40	40
4	+ 51	− 6	51
5	− 129:	− 288:	316
6	− 68	− 147:	162
7	− 510:	+ 581:	773
8	+ 2	− 40	40
9	− 19:	− 421:	421
Comparison			
A	− 22	+ 108	
B	+ 138	− 37	
a	+ 43	+ 2	
b	+ 44	+ 37	
c	+ 7	+ 53	
d	+ 67	+ 22	
e	+ 59	− 2	

The blink-search for variables has been carried out in such a way that no accurate estimate of the completeness of discovery can be made—as was possible in the discovery of the numerous variables in the Sculptor system (7). The chance of discovery of each variable in NGC 121 appears to be smaller than in the Sculptor system, for which a considerable number of very high quality plates were available. Nevertheless it is believed that during the course of blink-comparison of 15 pairs of plates the discovery is complete within 4′ of NGC 121 in so far as the resolution of these plates allow. Further out, where seven pairs of plates have been searched and where the chance of discovery is smaller, it

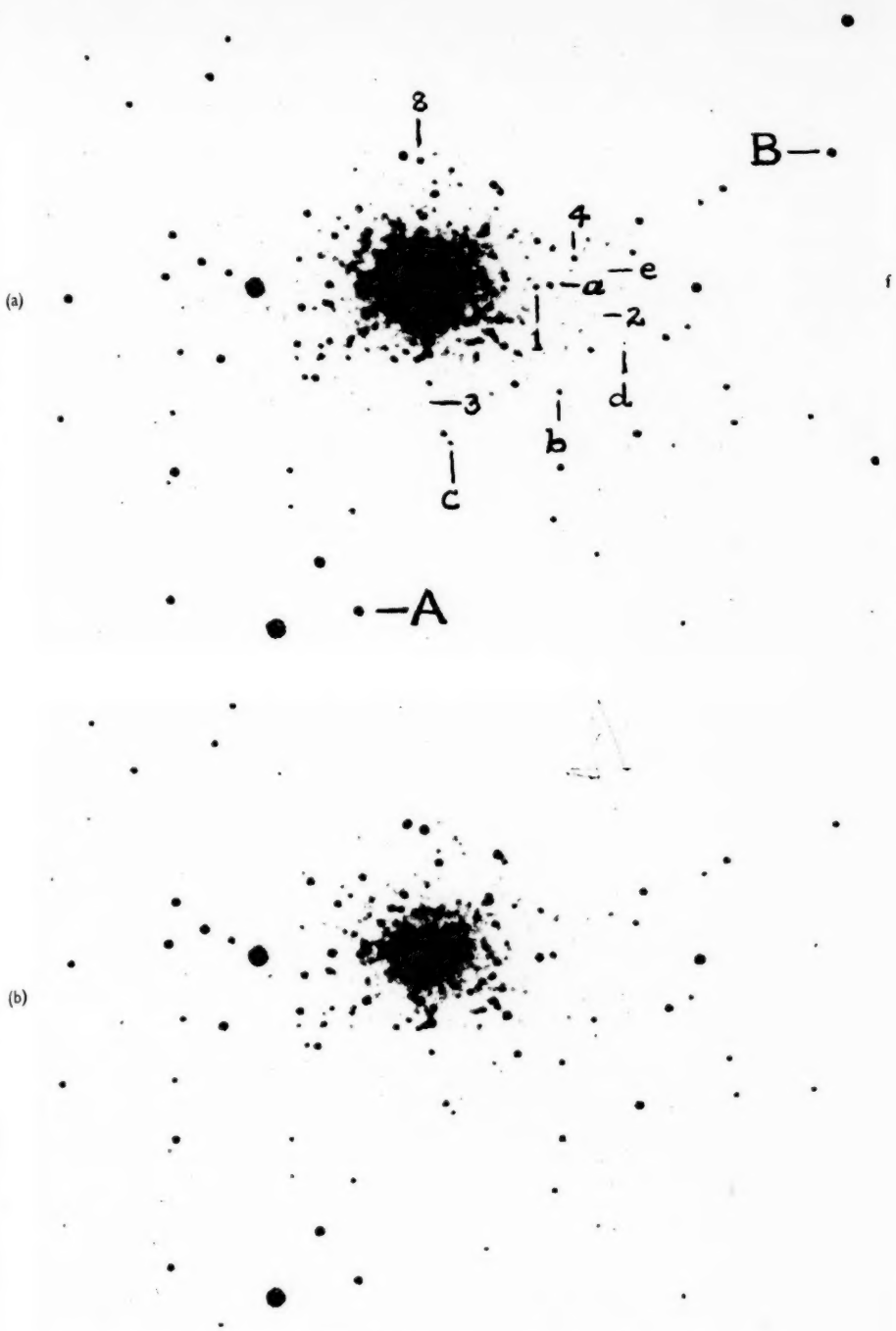

NGC 121 in blue (a) *and red* (b) *light with variable and comparison stars marked.*
Scale: 1 *mm* = 2″·2.

A. D. Thackeray, Periods and light-curves of variable stars in NGC 121

cannot be claimed that the four variables found are the only ones above the limit of the plates.

Identification of variables.—The positions of the nine variables relative to the cluster were measured on a Toepfer micrometer (also kindly loaned by the Royal Observatory, Cape). The measures are listed in Table I, together with the distances of each variable from the cluster centre. This table also lists positions of seven comparison stars on the same system of coordinates. Variables 1–4 and 8, together with the comparison stars, are marked on Plate I (*a*). The fields of variables 5, 6, 7 and 9 are illustrated in Fig. 1.

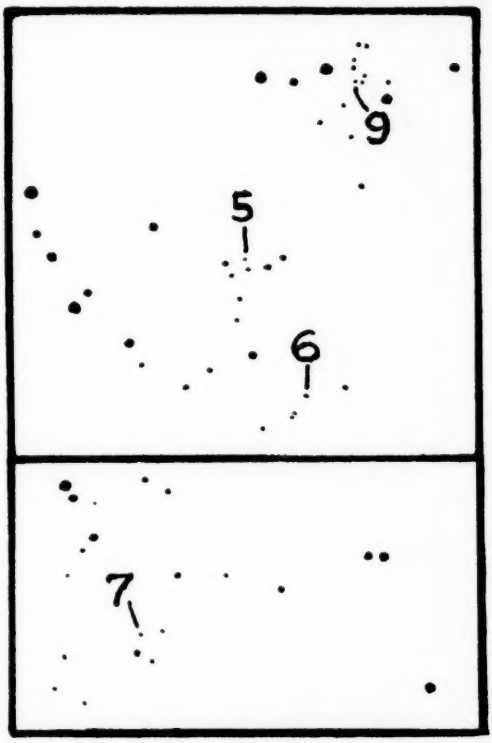

FIG. 1.—*Fields of outlying variables near NGC 121.*
Scale: 1 mm=6″·7. South is at top, following to right.

Owing to the limited field of the Toepfer micrometer only one CPD star could be included in the measures; consequently there is some doubt concerning the orientation and scale of the measures in Table I. Nevertheless, the combined use of measures and charts should amply suffice for identification of all the variables.

Estimates.—The basic sequence of comparison stars A, B, a to e, was used for all the variables nearest to the cluster, viz. Nos. 1–4, 6 and 8. Each variable was estimated as so many steps brighter or fainter than a given comparison star, the number of estimated steps between each pair of comparison stars being left free to vary from plate to plate. At the conclusion of the estimates it was found

XUM

that the average step differences were as follows: AB 3, Ba 5, ab 4, bc 2, cd 4, de 2, and hence we have the following sequence:—

Star	A	B	a	b	c	d	e
Step	0	3	8	12	14	18	20

If on a particular plate a variable were estimated as c1v2d (instead of c2v2d) the resultant estimate was 15+ (instead of 16).

Estimates of eight out of the nine variables have been set out in a table deposited with the Society.

Derivation of periods.—For a variety of reasons it proved to be far more difficult to secure satisfactory long series of plates of NGC 121 on the same or

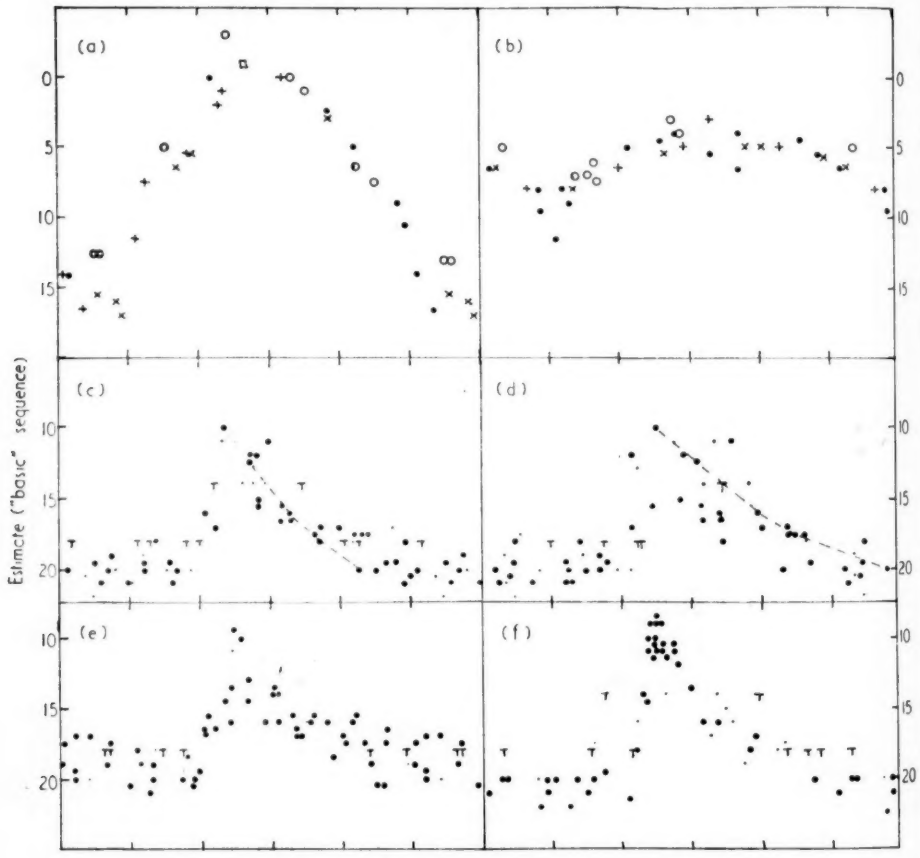

FIG. 2.—*Light-curves of variables in NGC 121.*

Ordinates : individual estimates on the " basic " sequence.
Abscissae : phase, with arbitrary zero. Observations covering 0·2 P are repeated right and left

(a) V1; $P^{-1}=0{\cdot}007132$.
(b) V8; $P^{-1}=0{\cdot}00890$.
(c) V2; $P^{-1}=1{\cdot}8783$.
(d) V2; $P^{-1}=2{\cdot}8782$ (incorrect).
(e) V3; $P^{-1}=1{\cdot}56284$.
(f) V4; $P^{-1}=1{\cdot}96651$.

consecutive nights than of the Sculptor system. One reason was that NGC 121 never attains a zenith distance less than 46° at Pretoria. Consequently the derivation of periods for these variables presented considerable difficulty in some cases. The period of V4, which has a very sharp rise to maximum, could be found easily, especially as the series of plates included a fortuitously large number of maxima.

The individual observations of the five variables considered as cluster-members are plotted against phase in Fig. 2, according to the periods found. V2 is plotted twice, for $P^{-1} = 1{\cdot}8783$ considered to be the true value, and also for $P^{-1} = 2{\cdot}8782$, which is considered incorrect. For the two long-period variables, closely adjacent observations are grouped together.

TABLE II

Mean light-estimates of NGC 121 variables.
(Estimates on basic sequence)

V1			V2			V3			V4			V8		
Ph	Est	n	Ph	Est	n	Ph	Est	n	Ph	Est	n	Ph	Est	n
0·65	14·2	4	0·80	20·2	9	0·77	17·7	10	0·11	20·7	7	0·05	6·0	3
0·75	15·2	4	0·98	19·8	10	0·01	19·5	13	0·29	20·2	7	0·16	8·5	3
0·83	9·5	2	0·13	16·5	2	0·15	15·5	6	0·44	16·9	5	0·22	11·5:	1
0·95	5·5	4	0·17	10·3:	2	0·22	12·5	6	0·50	10·2	12	0·26	8·0	3
0·06	0·0	4	0·26	13·2	9	0·34	15·5	9	0·56	11·9	6	0·37	6·7	4
0·13	−1·0	1	0·34	16·0	4	0·44	16·2	5	0·66	15·7	5	0·54	4·5	7
0·25	0·0	2	0·45	17·5	4	0·55	17·0	6	0·76	17·5	4	0·71	4·6	5
0·35	2·2	3	0·53	18·1	5	0·65	18·8	5	0·90	19·0:	3	0·91	5·1	5
0·44	5·8	2	0·66	19·5	7									
0·55	9·0	3												

	V1	V2	V3	V4	V8
P	140·2	0·53240	0·63986	0·50852	112·4:
JD 2430000+	4219	4277·36	4277·59	4331·28	3619*
m_{max}	−1·0	10·3	12·5:	10·2	4·5
m_{min}	+15·2	20·2	19·5	20·7	11·5:
$\overline{m}$	7·1	15·2	16·0:	15·4	8·0:
$(m-M)/P$	0·28	0·10	0·23	0·10	0·4:

* Epoch of *minimum* for V8.

Mean estimates of these five variables at different phases are tabulated in Table II, together with the mean estimate at maximum and minimum. It follows that the median estimate of the three short-period variables is

$$\overline{m}\ (\text{est.}) = 15{\cdot}44$$

in the "basic" sequence, i.e. almost precisely midway between comparison stars c and d.

For the two long-period variables we have, with double weight to V1,

$$\overline{m}\ (\text{est.}) = 7{\cdot}4.$$

Notes on individual variables: cluster members.

V1. Period $140^{d}{\cdot}2$, light-curve Fig. 2(*a*). This star appears to be a regular long-period variable and is considerably redder than any other cluster member with the exception of V8. Its minimum photographic light is almost precisely equal to the median magnitude of the short-period variables. In the diagram of the light-curve, different cycles are denoted by different symbols and the

small scatter may be real. The rise to maximum is steeper than the decline and contains a suggestion of a still-stand. In considering the shape of this and the other light-curves it must be borne in mind that if the step-differences vary in magnitude along the sequence, as may well be the case, then distortions of the curves will occur.

V2. Period $0^d{\cdot}53240$, Fig. 2(*c*). The derivation of this period proved to be more difficult than for any of the other cluster members. However, it is believed that the reciprocal period $P^{-1}=1{\cdot}8783$ as used in Fig. 2(*c*) is correct. The observations are replotted in Fig. 2(*d*) for a reciprocal period $P^{-1}=2{\cdot}8782$ and the scatter is appreciably greater (the value 2·8783 gives an equally bad plot). The dashed curve shows the decline from maximum as recorded on a long series on one night (JD 2434277).

V3. Period $0^d{\cdot}63986$, Fig. 2(*e*). This variable, with period longer than V2 and V4, has a slower rise to maximum, and apart from two well-established bright maxima has a considerably smaller amplitude. Thus the star is of Bailey type *b*, as compared with V2 and V4 of type *a*.

V4. Period $0^d{\cdot}50852$, Fig. 2(*f*). A typical *a* variable with steep rise to maximum and relatively large amplitude.

V8. Period $112^d{\cdot}4$?, Fig. 2(*b*). A very red star with an apparently regular period, but there is more evidence of fluctuations about the mean curve than for V1. The light-curve is rather peculiar in that more time is spent near maximum than minimum. There is some resemblance to the rounded light-curve of T Cen ($P=90^d{\cdot}7$). It is considered more likely to belong to the red long-period variable class than to be an eclipsing variable, although Dr Wesselink has reminded me of the similar light-curve of the eclipsing variable W Cru ($P=198^d{\cdot}5$).

A possibility remains that there is a double cycle with period 225 days, with uneven maxima and minima. Unfortunately one set of minima is very poorly represented on this period. If there is a double cycle in a period of 225 days, the star bears some resemblance to the RV Tau class, but no galactic RV Tau star is known with a period greater than 90 days.

Non-members of NGC 121

V5. Although no series of observations on the same night covers the full rise from minimum, the initial rise is shown on JD 2433977 and a rapid decline is shown on several occasions. The observations are well represented by $P^{-1}=1{\cdot}89037$; this indicates a Bailey *a*-type variable with $m-M=0{\cdot}12P$. Although a "local" sequence was used for the estimates, the median magnitude is found to be about the same as that for V2 to V4. However, the star is too far from NGC 121 to be a member.

V6. The nearest to NGC 121 of the variables considered as a non-member. At an angular distance of 162″ from the centre of the cluster, a minimum linear distance of 40 pc is implied, and is it very doubtful that a globular cluster would extend this far. According to Kron (**8**), NGC 121, which appears as No. 2 on his list, has a radius of 10 pc.

Only three maxima were observed, JD 2433654 (two plates), 2434217 and 2434304. On the latter occasion a rapid decline occurs, while three days later the star appears to have been caught on the rise. No period has been found to fit all the observations satisfactorily, but a reciprocal period $P^{-1}=1{\cdot}660$ is

considered possible if one allows considerable scatter in the brightness at maximum.

V7. The distance from the centre of the plates is so great that the images are seriously affected by coma and the estimates are extremely difficult. The behaviour on JD 2434277 marks it as a short-period variable but no derivation of period has been attempted.

V9. This variable is subject to rapid fluctuations but no certain period has been found. As for V7, the individual estimates were rather difficult. The amplitude is probably smaller than for the other variables and may vary with time. There is no indication of a steep rise to maximum. The behaviour suggests that of a *c*-type variable and a reciprocal period $P^{-1} = 2{\cdot}6209$ appears to be the most probable value. However, $P^{-1} = 1{\cdot}623$ also fits the observations moderately well. The mean magnitude is about the same size as that of the other short-period variables or if anything slightly brighter.

This star is the nearest of the nine variables to the globular cluster 47 Tuc whose centre lies 26′ away. It is not considered likely that this or any of the other variables is connected with 47 Tuc.

Conclusions.—The five variables 1, 2, 3, 4 and 8 are all within 1′ of the centre of NGC 121 and are to be considered as certain cluster-members. The three short-period variables (2, 3 and 4) follow the familiar relationship between period, amplitude and shape of light-curve as found in globular clusters in the Galaxy, notably as found by Martin (**9**) in ω Cen. Their properties are not those of the short-period variables found by Gaposchkin (**6**) in the galactic nucleus.

As compared with a density of one variable per 0·63 square minutes in the area centred on NGC 121, we have found only one variable per 300 square minutes in the surrounding neighbourhood. Allowing for incompleteness of discovery, this latter density is certainly under-estimated, possibly by a factor two. V6 is the nearest of these outliers to NGC 121 but it is too far to be considered a member. We therefore consider V5, 6, 7 and 9 to be all field variables. Since all four of these variables have short periods and have median magnitudes approximately equal to those within NGC 121, the interesting possibility emerges that they represent the first instances of RR Lyr-type variables in the general field of the Small Magellanic Cloud. The only way to test this hypothesis is to examine other fields in the region of the Cloud.

By contrast with the above minimum figure of one variable per 300 square minutes, Shapley (**10**) in his study of RR Lyr variables within the Galaxy found an average density of one variable per 6 square degrees (with a magnitude limit of about 16) the greatest concentration being in MWF 209 where he found one per 2·5 square degrees. Baade (**11**) in a search for faint RR Lyr variables in high galactic latitude found five of about 17 mag. in 8·5 square degrees. These concentrations are so much less than that found in the neighbourhood of NGC 121 that even allowing for the fact that the magnitude limit of the present search is some two magnitudes fainter than Baade's, we find considerable support to the hypothesis that variables 5, 6, 7 and 9 of this paper are actually outlying members of the Small Cloud.

The similarity of NGC 121 to globular clusters within the Galaxy in the behaviour of its variable stars proves the existence of a Population II component to the Small Cloud, and the existence also of a general field of type II now appears to be indicated.

I am greatly indebted to Drs Wesselink and Feast for their valuable assistance in securing additional photographs of NGC 121, so essential to the derivation of periods, and further for reading and commenting on this paper.

Radcliffe Observatory,
Pretoria.
1957 *August* 31.

References

(1) H. Shapley and H. H. Wilson, *H.C.*, **276,** 1925.
(2) J. Mohr, *H.B.*, **899,** 15, 1935.
(3) S. C. B. Gascoigne and G. E. Kron, *P.A.S.P.*, **64,** 196, 1952.
(4) *Obs.*, **71,** 219, 1951.
(5) A. D. Thackeray and A. J. Wesselink, *Nature*, **171,** 693, 1953.
(6) S. Gaposchkin, *Variable Stars* (Acad. Sci. U.S.S.R.), **10,** 337, 1955.
(7) A. D. Thackeray, *Obs.*, **70,** 144, 1950.
(8) G. E. Kron, *P.A.S.P.*, **68,** 233, 1956.
(9) W. Martin, *Ann. Leyden*, **XVII** pt. 2, 1938.
(10) H. Shapley, *P.N.A.S.* **25,** 424, 1939.
(11) W. Baade, *A.N.*, **244,** 153, 1931.

XUM

ANALYSIS OF RADIAL VELOCITIES OF DISTANT B TYPE STARS

M. W. Feast and A. D. Thackeray

(Received 1958 January 1)

Summary

Radial velocities of 314 early B type stars with calculated distances (based on photoelectric colours and MK classifications) greater than 1 kpc are analysed for differential galactic rotation. The incorporation of Radcliffe velocities of southern stars renders the distribution in longitude much more uniform than in earlier analyses. At distances greater than 2 kpc there is even a marked deficiency of northern material.

First-order analyses of stellar and interstellar velocities are carried out for various distance groups (Section 5, Table III). A negative K-term (Section 6) is found in the region 1 to 2 kpc, but more distance groups do not suggest that this is due to a general contraction of the galaxy. The possible connection with the deviation of the vertex is briefly discussed. The K-term in the region 1 to 2 kpc is diminished considerably when a systematic correction, apparently applicable to the Lick velocities of faint B stars (Section 3), is taken into account. The effect of this correction is also to increase the derived values of the Oort A constant. The group of stars at distances greater than 3·0 kpc yields an abnormally low value of A, but this is regarded as chiefly a result of selection leading to a large proportion of overestimated distances in this group.

The velocity dispersion found for the inner part of the galaxy is not found to have an abnormal value (Section 7).

The Camm linear approximation is used (Section 8) to derive a value of the Oort A constant. The final value $A = 17{\cdot}5 \pm 1{\cdot}5$ km/sec/kpc is adopted.

Two partly independent methods are used to derive a value of R, the distance to the galactic centre; the most probable value is 8·9 kpc (Section 10, Table IX). A value of 0·5 for the ratio of the axes of the velocity ellipsoid appears to be appropriate to distant B stars.

The calibration of the MK luminosity scale is tested (Section 11) for stars in the range B5 to O9·5.

A curve of differential rotation $\omega(R)$ is derived (Section 12). The results show no significant deviation from the radio results and suggest that ω'' is positive in the range of R covered by the observations.

---

1. *Introduction.*—In determining the constants of galactic rotation according to the Oort–Lindblad theory the radial velocities of the O and B type stars have always played an important role. A most complete and authoritative discussion of the early observations and analyses was given by Plaskett and Pearce (**1**) in 1936. Since that time several other analyses have been undertaken, some depending partly on new observations, others modifying the method of analysis in various ways. The principal deficiency in all this work has been the lack of velocities for faint B type stars in the southern Milky Way. This deficiency has now been remedied by observations at the Radcliffe Observatory (**2, 3**) and in fact the position has been reached that for the more distant stars there is a greater concentration available for analysis in the southern than in the northern

Milky Way. In view of this substantial increase in observational material it is obviously desirable to carry out a new analysis. This is particularly appropriate at the present moment since some recent investigators have deduced rather widely discrepant values of Oort's rotational constant A.

Besides the new southern radial velocities we have also been able to take advantage in the present work of two other significant improvements in the observational data referring to B type stars. These are the recent determination of photoelectric magnitudes and colours, and of spectral types on the MK system for large numbers of B type stars in both hemispheres.

2. *Data selected for analysis.*—In the present work we have attempted to restrict the observational material to those stars with reliable magnitudes, colours, types and radial velocities. To this end a list was first compiled of all stars in the General Catalogue of Radial Velocities (GCRV) (**4**) with spectral types $B5$ or earlier and from this list stars were selected which satisfied each of the following three criteria:

(1) The quality of the velocity is *a*, *b* or *c*.

(2) The absolute magnitude of the star is known on the basis of the calibration of the MK system (e.g. Of stars were omitted as their absolute magnitudes are rather uncertain).

(3) The photoelectric magnitude and colour of the star are known on the B, V system or can be converted to that system (U magnitudes are also known for many of the stars discussed but we have made no use of them in the present work).

Criteria (2) and (3) effectively reduce the list to stars occurring in the catalogues of Morgan, Whitford and Code (**5**) and Hiltner (**6**).

To this list were added stars from the recent Radcliffe Catalogues (**2, 3**) which satisfy approximately the same conditions. The following points concerning these stars are to be noted:

(*a*) If the velocity was considered constant it is included; otherwise the star was rejected. It is possible that this is a somewhat more stringent condition than (1) above.

(*b*) For stars taken from Table II of (**2**) and (**3**) the MK type given there is adopted. There is some overlap between the Radcliffe MK types and those of other workers (principally (**5**) and (**6**)). Since the overlap is only fragmentary it has seemed best to retain the Radcliffe types throughout for these stars.

(*c*) The magnitudes and colours adopted for stars from (**3**) (Table II) are mainly due to Oosterhoff (**7**). A few values were, however, taken from other sources (e.g. (**5**)). The magnitudes and colours adopted for stars in (**2**) (Table II) are mainly unpublished measurements at the Cape Observatory, kindly supplied by Dr R. H. Stoy. Since photoelectric magnitudes and colours were not available for about 40 stars in Table II (**2**) these stars had to be rejected.

(*d*) For some of the stars in the first list (that selected from the GCRV) new velocities have been published in the Tables I of (**2**) and (**3**). Generally we have adopted the mean of the Radcliffe and GCRV velocities unless one or the other was known for some reason to be uncertain. It should be noted that for these stars the Hiltner (**6**) or Morgan, Whitford and Code (**5**) spectral types were adopted for the sake of consistency in preference to the Radcliffe types.

For the stars in the list prepared as above, it is possible to determine for each star its absolute magnitude, the correction for interstellar absorption, and the

distance. In the case of those stars which are in Hiltner's catalogue (**6**), Hiltner has himself given his deduced distance moduli and these have been adopted in our work. The intrinsic colours used by Hiltner are given in his Table 6 and are essentially the same as those given by Morgan, Harris and Johnson (**8**). The absolute magnitude calibration of the MK system used by Hiltner is given by Johnson and Hiltner (**9**). For stars not in Hiltner's catalogue the magnitudes and colours of Morgan, Whitford and Code (**5**), Oosterhoff (**7**) and Stoy (unpublished) were converted to the B, V system by the following (usually accepted) formulae:

(*a*) Oosterhoff's C_1 $B-V=1{\cdot}107C_1+1{\cdot}371$,

(*b*) Morgan, Whitford and Code's C_1 $B-V=2{\cdot}07C_1+0{\cdot}30$,

(*c*) Stoy's SCI and SPg $B-V=0{\cdot}85$ SCI $+0{\cdot}26$, $V=$ Spg $-0{\cdot}92$ SCI $-0{\cdot}06$.

The same set of intrinsic colours used by Hiltner was then used to deduce the interstellar reddening and absorption. A value of 3·0 for the ratio of total to selective absorption was used. In deducing the absolute magnitudes of the stars from the MK types the calibration of Morgan and Keenan (**10**) was adopted. This calibration is slightly different from the one adopted by Hiltner. The differences have been discussed by Johnson and Hiltner (**9**) and from this discussion it might perhaps be concluded that the Morgan–Keenan calibration is the more suitable of the two for the group of stars studied here and for this reason we have adopted it for stars not found in Hiltner's catalogue. In any case the differences between the two calibrations are small, probably considerably smaller than the uncertainties of the quantities involved; the fact that a slightly different calibration has been used for these stars as compared with those taken from Hiltner's Catalogue will not affect the analysis in any significant way. It may be noted here that for stars classified as luminosity class I at Pretoria we have used a mean of the Ia and Ib luminosities.

Finally from the catalogue prepared in the above manner, those stars with heliocentric distances (r) equal to or greater than 1 kpc were selected for analysis. From the point of view of studies of galactic rotation the motions of the more distant stars are of considerably greater interest, at the present time, than ones near the Sun. Furthermore, whilst a great deal of the previous work has been restricted to regions nearer the Sun than 1 kpc we now have sufficient data to investigate more distant regions. It may also be noted that in restricting ourselves to stars beyond 1 kpc we avoid the difficulties associated with the Sco–Cen cluster.

With all these restrictions we are left with a catalogue of 319 stars. Of these, four stars were rejected because of abnormally high galactic latitude ($b>25°$) and one (HD 151397) was rejected because of its very high velocity (from four plates) in the opposite sense to galactic rotation theory. The interstellar velocity from this star was however retained for analysis. We are thus left with 314 stars of which 268 have measured radial velocities of the interstellar Ca II lines. Of these 314 stars 122 depend on Radcliffe velocities alone. The distribution of the stars is shown in Fig. 1, in which the stars are shown projected on the galactic plane. It should be pointed out that although the original selection was for spectral types earlier than B5 in the GCRV (and a similar restriction on HD types for the southern stars) a few stars in the final list have MK types later than B5.

No attempt has been made to use the present material to deduce the local solar motion. We have adopted the value of +20 km/sec towards R.A. 18^h,

Dec. +34°, and have corrected all the velocities for this motion using the charts prepared by Smart (**11**).

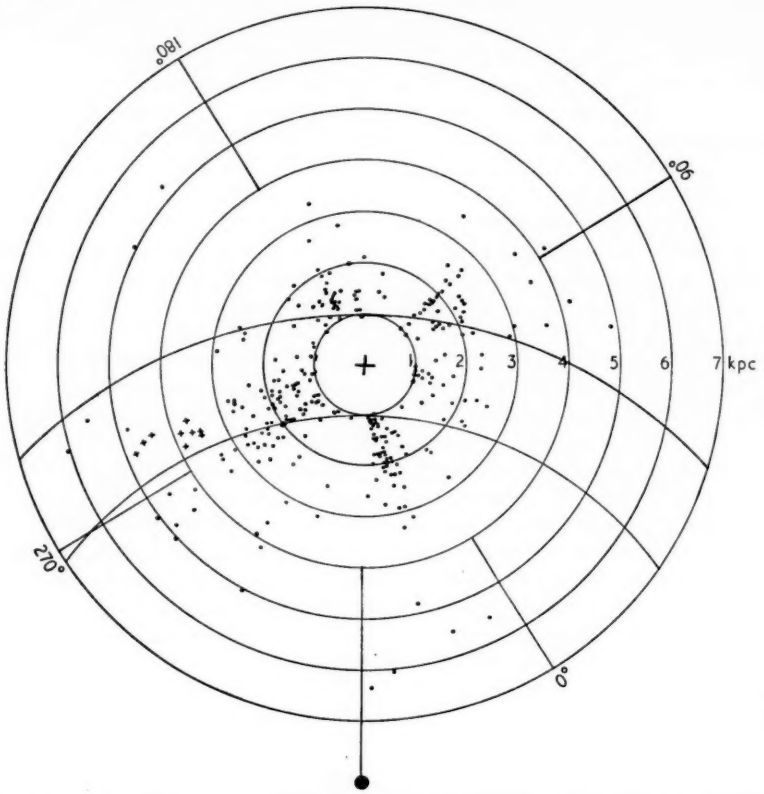

FIG. 1.—*The distribution in the galactic plane of the* B *type stars discussed in the present paper. The position of the Sun is indicated by the large cross at the centre of the figure. The complete circles are drawn at* 1 *kpc intervals. The large filled circle indicates the position of the galactic centre if this is at* $R_0=8{\cdot}2$ *kpc* $l_0=328°$. *The region used in the Camm analysis (Section* 8*),* $|R-R_0| \leqslant 1$ *kpc, is enclosed between the two circular arcs. The* 9 *stars marked by small crosses are those used to determine* R_0 *by the second method of Section* 10. *Some points represent more than one star.*

3. *Comparison of Radcliffe velocities with other Observatories.*—The intercomparison of velocities determined at various Observatories which appears in Table I of the introduction to the GCRV suggests that no serious systematic errors exist for the B stars, and accordingly no systematic corrections were there applied. Examination of the Catalogue shows that, while there is a greater degree of observational overlap for faint B stars than for faint stars of other types, the intercomparisons of velocities rest mainly on stars brighter than $7^{m}{\cdot}0$. Yet it is the material on stars fainter than this limit which is of special interest in modern analyses of galactic rotation; and it is for these fainter stars that the use of different spectrographs and cameras (as mentioned in the GCRV) may invalidate the general derivation of systematic differences between various Observatories.

It is of considerable importance to the present analysis to investigate whether appreciable systematic errors exist for the fainter B stars.

Observations of standard stars with the Radcliffe Cassegrain spectrograph have shown a satisfactory agreement with the GCRV system (**2, 12, 13**), although there is some indication that with the c camera (49 A/mm) the Radcliffe velocities are 1 to 2 km/sec too positive compared with the GCRV. The B stars present a special problem in that Petrie (**14**) has shown that at 49 A/mm the important lines He 4471 and 4026 require large corrections to the wave-lengths usually employed, which vary with luminosity or line-width. The necessity for such corrections has been confirmed at the Radcliffe Observatory when coarse-grained emulsions are used.

Concurrently with the Radcliffe observations of southern O and B stars which are used in this paper, we have observed 97 B stars previously observed elsewhere. These include 23 stars suggested by Petrie for a triple overlap between Victoria, Lick (Neubauer) (**15**) and Radcliffe.

The accompanying Table I shows the comparison of Radcliffe velocities of B stars with the other main contributors—Victoria, Mt Wilson and Lick. Victoria A refers to published velocities from the GCRV, Victoria B to a selection of stars for which revised velocities (based on the new Victoria system of wave-lengths) have been kindly supplied by Dr Petrie. Lick A refers to Lick velocities from the GCRV for stars brighter than $6^{m}\cdot5$; they are mainly the results of the Lick Chile expedition. Lick B refers to stars fainter than $6^{m}\cdot5$; these are mainly determined by Neubauer ((**15**) or only published in GCRV) and two stars brighter than $6^{m}\cdot5$ taken from (**15**) are included in this group rather than Lick A.

TABLE I

Comparison of Radcliffe B star velocities with those of other observatories

Observatory	No. of Stars	Residual (stars) and s.e.	No. of Stars with Ca II	Residual Ca II and s.e.	Mean of Stars and Ca II, and s.e.
Victoria A	23	+2·0 ±0·9	10	+1·1 ±1·7	+1·8 ±0·8
Victoria B	12	+0·3 ±1·4			+0·3 ±1·4
Mt Wilson	22	+3·7 ±1·2	17	+0·6 ±2·0	+2·4 ±1·0
Lick A	32	−0·4 ±1·3			−0·4 ±1·3
Lick B	31	+11·4 ±1·9	24	+6·3 ±2·8	+9·2 ±1·6

Residuals are in the sense Radcliffe minus other observatory.

In all cases except Lick B the agreement between Radcliffe velocities and other determinations is satisfactory. This is particularly so for the new Victoria results. The difference between Mt Wilson and Radcliffe could be fully accounted for if the Victoria wave-lengths for He 4471 and 4026 were applicable to the Mt Wilson material, but whether this is likely to be so cannot be stated from available information. The systematic difference from the fainter Lick velocities is large and is moreover important for the discussions of the present paper. It is not possible at the present time to explain these differences satisfactorily, but in view of the good agreement of the Radcliffe results with the other Observatories and also with the Lick observations of brighter stars, we feel justified in ascribing

XUM

the result to a systematic error affecting the Lick B velocities. The final solutions in the present paper are based on corrections of +10 km/sec applied to the Lick B velocities; but many solutions are also carried out for comparison without applying any correction. It is clearly desirable that further observations of the faint Lick stars should be made, preferably by a number of different Observatories.

4. *The methods of analysis for galactic rotation.*—It will be convenient to collect together in this section some of the equations (mostly well known) on galactic rotation which will be discussed in later sections. The following notations are used:

V = radial velocity corrected for solar motion.
l, b = galactic longitude and latitude (Ohlsson's system).
l_0 = longitude of galactic centre.
$\lambda = l - l_0$.
r = distance of star from Sun.
R = distance of star from galactic centre.
R_0 = distance of Sun from galactic centre.
$\rho = r/R_0$.
ω, ω_0 = angular velocity about galactic centre for any star and at R_0, respectively.
$\epsilon R, \epsilon_0 R_0$ = velocities of expansion of galaxy at distance R and R_0 respectively.
$\kappa = \sqrt{a/b}$ = ratio of axes of the velocity ellipsoid.

Since the system of B stars is highly concentrated to the plane of the galaxy we shall consider only motions in that plane and also neglect variations of the laws of force with distance from the plane. Then in general the state of motion in the galaxy may be represented by a rotation and an expansion or contraction of the system. It may be shown (e.g. Trumpler and Weaver (**16**, p. 581)) that, neglecting a star's peculiar motion, its radial velocity (V) corrected for solar motion may be represented by the equation

$$V = R_0(\omega - \omega_0)\sin\lambda\cos b - R_0(\epsilon - \epsilon_0)\cos\lambda\cos b + \epsilon r\cos^2 b. \qquad (1)$$

In practice it is not possible to employ (1) with the available material to solve for $(\omega - \omega_0)$ and $(\epsilon - \epsilon_0)$ as functions of R and in all work of this kind some approximation to (1) has to be employed. It may be mentioned that the equation deduced by Edmondson (**17**) for spiral motion in the galaxy is a special case of equation (1).

If we assume that there is no general expansion or contraction of the galaxy then (1) reduces to

$$V = R_0(\omega - \omega_0)\sin\lambda\cos b. \qquad (2)$$

This is Bottlinger's well-known equation which has been used extensively in recent years, especially in analysing the results of the 21 cm radio observations. Its application to the present data will be discussed in a later section. The assumption that there is no general expansion or contraction of the galaxy (zero "K-term") is a basic one in most of the 21 cm work and it is very desirable to check it as far as possible with the optical data. For this reason it is important to discuss approximations of (1) which do not assume zero K-term.

If we restrict ourselves to regions where $|R - R_0|$ is small then we may write approximately

$$\omega = \omega_0 + (R - R_0)\omega_0', \qquad (3)$$

$$\epsilon = \epsilon_0 + (R - R_0)\epsilon_0'. \qquad (4)$$

Dashes indicating differentials with respect to R.

If we further follow the normal practice and put

$$A = -\tfrac{1}{2}\omega_0' R_0 = \text{Oort's constant} \tag{5}$$

and

$$C = -\tfrac{1}{2}\epsilon_0' R_0 \tag{6}$$

we find

$$V = \epsilon_0 r \cos^2 b - 2A(R-R_0)\sin\lambda\cos b - 2C(R-R_0)[(r/R_0)\cos^2 b - \cos\lambda\cos b]. \tag{7}$$

This is Camm's linear approximation (**18, 19**) and may be employed in practice to yield values of A, ϵ_0 and C. Now r and R are related by the exact equation

$$R^2 = R_0^2 + r^2\cos^2 b - 2R_0 r\cos\lambda\cos b. \tag{8}$$

If, in addition to the approximations (3) and (4) above, we assume that r/R_0 is small, then we may write approximately

$$R - R_0 = -r\cos\lambda\cos b. \tag{9}$$

The general form (1) then further reduces to

$$V = A_0 r\cos^2 b + A_1 r\sin 2(\lambda - h)\cos^2 b \tag{10}$$

where

$$A_0 = \epsilon_0 + \tfrac{1}{2}\epsilon_0' R_0, \tag{11}$$

$$A_1 = \tfrac{1}{2}R_0\sqrt{(\omega_0')^2 + (\epsilon_0')^2} \tag{12}$$

and

$$\tan h = \epsilon_0'/\omega_0'. \tag{13}$$

Equation (10) may perhaps be called the generalized Oort equation. The well-known Oort equation assuming zero K-term follows immediately from (10). It is

$$V = Ar\sin 2\lambda\cos^2 b. \tag{14}$$

It has frequently been assumed that the K-term arises in some other way than from general expansion or contraction of the galaxy and it is then introduced as a constant term in equations (1), (2), (7), (10) and (14). For instance (14) is then written

$$V = K + Ar\sin 2\lambda\cos^2 b. \tag{15}$$

In an attempt to derive a value of R_0 from the present material (Section 10) we have found it convenient to use a formula due to Titus (**20**):

$$V(\lambda) = \frac{AR_0}{(1-\kappa^2)}\left[\frac{1}{1-(1-\kappa^2)\rho(2\cos\lambda - \rho)} - 1\right]\sin\lambda. \tag{16}$$

Equation (16) is based on the assumption of circular orbits in the galactic plane and general dynamic theory (**21**) which gives a motion at distance R from the galactic centre of the form

$$V(R) = pR/(a_{10} + b_{20}R^2). \tag{17}$$

This approach to the problem may be criticized on the grounds that equation (17) postulates a certain force law. Another possible approach has been suggested by Weaver (**22**) in which the determination of R_0 is likely to rest on a highly restricted number of radial velocities. In this method, the Camm linear approximation to the Bottlinger formula is used without the terms involving non-circular motion. Then, with $|R - R_0|$ small, we may write

$$V = R_0(R-R_0)\omega_0'\sin\lambda\cos b \equiv -2A(R-R_0)\sin\lambda\cos b. \tag{18}$$

XUM

We shall now proceed to apply some of these equations to the observational material.

5. *Generalized Oort analysis.*—The Oort approximation, that is a formula of the form of (10), (14) or (15), depending on how the K-term is treated, has frequently been employed in investigations of galactic rotation. It is strictly applicable only to small values of r. Weaver (**23, 24, 25**) has claimed that very different results may be obtained from this approximation than from equation (2) and he has attributed this to "mathematical bias" in the use of the Oort approximation. It is therefore of considerable interest to analyse the present data according to (10) for comparison with the other methods of analysis dealt with later. Whilst the data will be analysed in this section according to (10) it will become clear that the analysis also applies as it stands if equation (15) should appear more appropriate.

The stars were divided into three groups (A, B and C) according to distance as is shown in Table II, where the distribution amongst the various MK luminosity

TABLE II

Statistics of stars used in Oort-type solutions

Group	A	B	C	AB
Distance range (kpc)	$1{\cdot}0 \leqslant r < 2{\cdot}0$	$2{\cdot}0 \leqslant r < 3{\cdot}0$	$r \geqslant 3{\cdot}0$	$1{\cdot}5 \leqslant r < 2{\cdot}5$
Mean distance (kpc)	1·44	2·34	4·31	1·94
Adopted $\bar{r}$ (kpc)	1·5	2·3	4·0	2·0
Number of				
Stars	172	95	47	137
Ca II velocities	141	86	41	—
Stars luminosity class I	37	43	31	49
Stars luminosity class II & III	48	26	15	35
Stars luminosity class IV & V	67	17	0	39
No luminosity class (early O type)	20	9	1	14

classes is also shown. The group AB for which a solution has also been carried out is of course not independent of groups A and B.

Normal points were formed in each of the seven groups (four groups of stars and three of interstellar gas) for each 10° of longitude. Unit weight was given to all GCRV velocities and to all Radcliffe velocities except those catalogued with a colon, to which half weight was given. In solving equation (10) for a particular group it is very desirable to avoid distortion due to stars in one longitude being at a different mean distance from stars in another longitude. The normal points were therefore corrected linearly (i.e. assume (10) to apply) to distances 1·5, 2·3, 4·0 and 2·0 kpc for the groups A, B, C and AB respectively. The Ca II velocities were also corrected in the same ratio. In groups A, B and AB the changes resulting from this correction are negligibly small. In group C the changes involved are somewhat larger due to the greater range of distances and the smaller number of stars in this group. The normal points for the seven groups are plotted in Figs. 2 to 8. In view of the discussion given earlier of the Lick velocities of faint B stars it has been felt necessary to investigate the effect of the proposed corrections on the galactic rotation constants. Where two points occur, in Figs. 2 to 8, at the same longitude the more positive refers to the

corrected results and the other to the uncorrected results. In view of this duplication we have therefore 14 groups to investigate. Equation (10) was solved by the normal method of least squares for each of the 14 groups. The results and their standard (r.m.s.) errors are given in Table III whilst the curves in Figs. 2 to 8 are drawn according to these solutions. It should be noted that in

TABLE III

Least square solutions of Oort-type analysis

Group	$\bar{r}$	$\overline{A_1 r}$	$\overline{A_0 r}$	l_0+h	A	A_0
			Corrected solutions			
A (stars)	1·5	+27·8±1·8	−4·2±1·3	325°±2°	+18·6±1·2	−2·8±0·9
A (Ca II)	(0·75)	+14·9±1·2	−2·2±0·9	328°±3°	+18·6±1·6	−2·8±1·2
AB (stars)	2·0	+35·2±2·2	−1·4±1·6	328°±2°	+17·6±1·1	−0·7±0·8
B (stars)	2·3	+37·6±4·2	+6·6±2·8	320°±3°	+16·3±1·8	+2·9±1·2
B (Ca II)	(1·15)	+20·4±2·7	+3·0±2·1	319°±4°	+17·7±2·3	+2·6±1·8
C (stars)	4·0	+35·7±7·0	−0·6±5·8	326°±7°	+ 8·9±1·8	−0·2±1·4
C (Ca II)	(2·0)	+27·7±2·2	+0·9±1·8	330°±3°	+13·8±1·1	+0·4±0·9
			Uncorrected solutions			
A (stars)	1·5	+24·1±2·1	−6·8±1·5	326°±3°	+16·1±1·4	−4·5±1·0
A (Ca II)	(0·75)	+13·2±1·2	−4·3±0·7	332°±3°	+16·5±1·6	−5·7±0·9
AB (stars)	2·0	+32·5±2·4	−4·8±1·6	331°±3°	+16·2±1·2	−2·4±0·8
B (stars)	2·3	+34·6±4·4	+3·2±3·0	322°±3°	+15·0±1·9	+1·4±1·3
B (Ca II)	(1·15)	+17·6±2·5	+0·2±2·1	323°±4°	+15·3±2·2	+0·2±1·8
C (stars)	4·0	+32·1±7·4	−3·8±5·9	327°±7°	+ 8·0±1·8	−1·0±1·5
C (Ca II)	(2·0)	+24·2±2·1	−2·3±1·6	332°±3°	+12·1±1·0	−1·2±0·8
	kpc	km/sec	km/sec		km/sec/kpc	km/sec/kpc

Errors are standard errors.

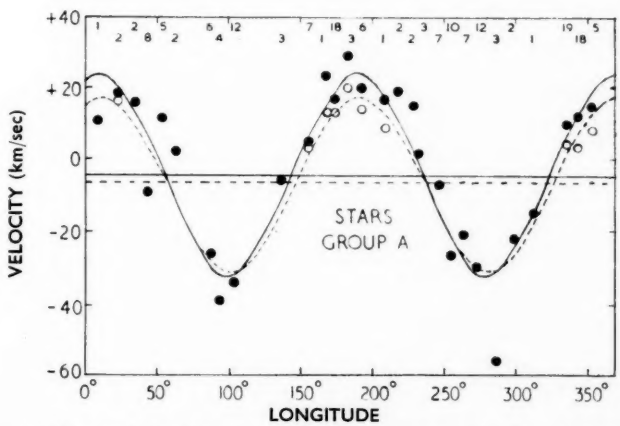

FIG. 2.—*Mean radial velocities, corrected for solar motion, for stars in Group* A *reduced to a mean distance of* 1·5 *kpc and shown as a function of galactic longitude. The first order (Oort) least squares solution and the level of the K-term are shown. In longitudes where Lick B velocities have been employed* (see *Section* 3) *open circles indicate the uncorrected means and the dotted lines the corresponding least squares solution. The number of stars contributing to each point is shown at the top of the figure.*

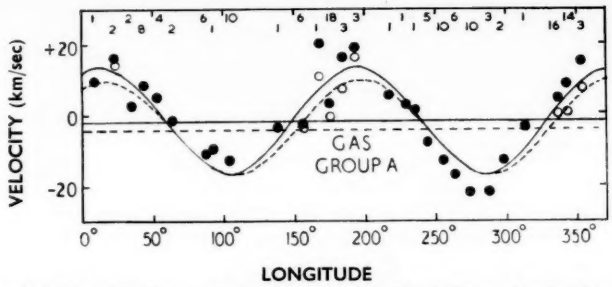

FIG. 3.—*Notation as in Fig. 2. Interstellar* Ca II *velocities in Group* A *reduced to 0·75 kpc.*

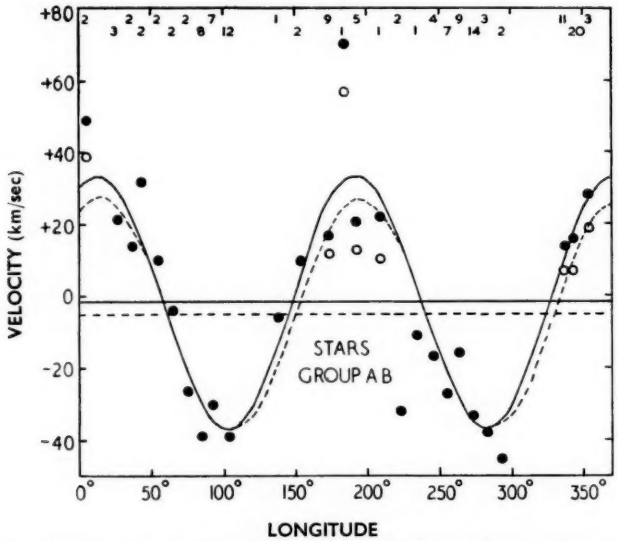

FIG. 4.—*Notation as in Fig. 2. Stellar velocities in Group* AB *reduced to 2·0 kpc.*

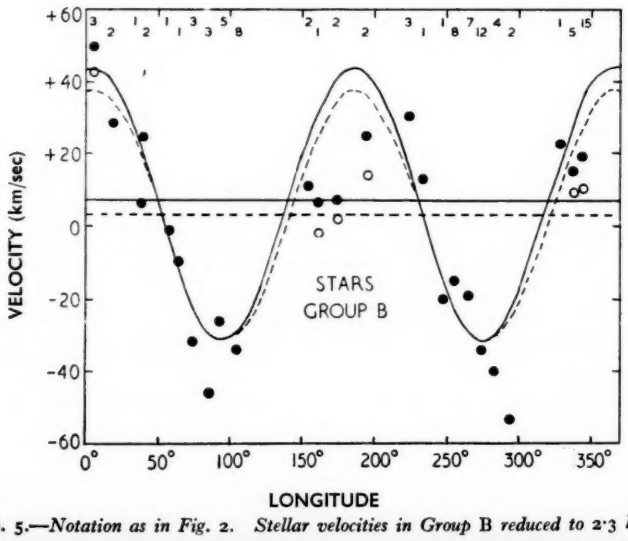

FIG. 5.—*Notation as in Fig. 2. Stellar velocities in Group* B *reduced to 2·3 kpc.*

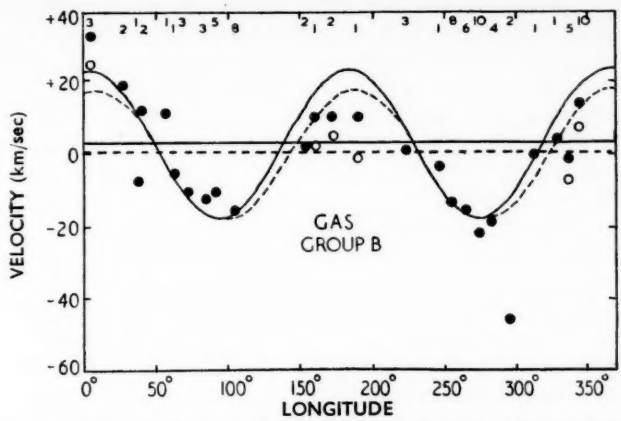

FIG. 6.—*Notation as in Fig. 2. Interstellar* Ca II *velocities in Group* B *reduced to* 1·15 *kpc.*

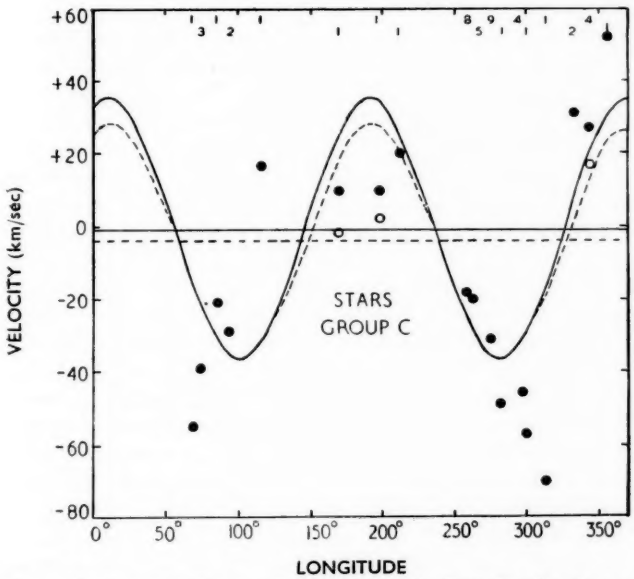

FIG. 7.—*Notation as in Fig. 2. Stellar velocities in Group* C *reduced to* 4·0 *kpc.*

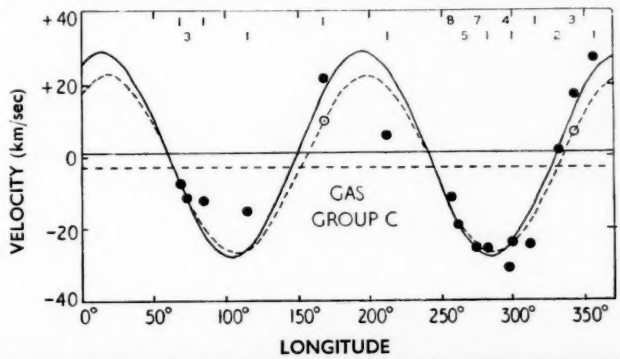

FIG. 8.—*Notation as in Fig. 2. Interstellar* Ca II *velocities in Group* C *reduced to* 2·0 *kpc.*

computing the standard errors of A_1 and A_0 no account has been taken of possible errors in the mean values of r adopted. Thus the errors quoted are likely to be underestimated.

Whilst a discussion of some of these results is best deferred to a later section, when they will be compared with the results derived by other methods, certain points may be discussed at this stage.

The mean value of (l_0+h) for stars and gas is 327° for the uncorrected solutions and 324° for the corrected solutions (group AB not being used in these means). However, both in view of the greater number of stars in group A and doubts as to the validity of the equation (10) for groups as distant as B and C, it may perhaps be best to confine attention to group A. In that case (l_0+h) is 329° for the uncorrected solutions and 326° for the corrected solutions, again taking the mean of gas and stars. It will be clear from the standard errors quoted in Table III that the results do not give any evidence for a significant deviation from 327°·7, the value of the longitude of the centre recently given by van Woerden, Rougoor and Oort (**26**) from 21 cm studies. Within the accuracy of the results therefore we may put $h=0$. It then follows from equations (11), (12) and (13) that $A_0=\epsilon_0$ and $A_1=A$ (the Oort constant) whilst $\epsilon_0'=0$.

It is of interest to note that in groups A and B the value of Ar is very closely half the stellar value for the Ca II velocities and in fact this has been assumed to be the case in calculating A from the Ca II results. The results in group C are of too low an accuracy to tell whether the same result holds good there. Whilst, of course, there is other evidence (optical and radio) for the concentration of the interstellar gas in rather thin ($\sim\frac{1}{2}$ kpc thickness) spiral arms it would appear that this has no noticeable effect on the present analysis, which would be satisfied by a uniform distribution of gas out to at least 2·5 kpc.

The values of A ($\equiv A_1$) given in Table III show a decrease of this constant with increasing distance. The low values given by group C are discussed below. Setting aside group C it does not appear that the differences between groups A and B are large enough to be regarded as significant. From groups A and B, gas and stars, we find mean values of A of +15·6 km/sec/kpc for the uncorrected solutions and +17·8 km/sec/kpc for the corrected solutions. In view of the discussion of the corrections given earlier and also of the results to be given later in this paper the higher value of A is to be preferred. The considerable difference between the two results may perhaps partly explain the anomalously low value of A (13·2) recently derived by Weaver (**24**) from B stars since the Lick velocities requiring correction probably play a considerable part in his analysis.

It is noteworthy that in view of the inclusion of the new southern results the distribution of stars in longitude is much more even than in previous analyses of B star velocities and the results should therefore have greater reliability. The greatest weight of course attaches to group A, which has more stars and a more even longitude distribution than the other groups. We note that, particularly in groups B and C, there is an unfortunate deficiency of stars from northern parts of the Milky Way. Reference to Table II shows that groups A and B contain quite different percentages of dwarfs and supergiants and it is therefore pleasing to note that substantially the same value of A is obtained for the two groups.

We must now discuss the anomalously low value of A found for group C. The result must be regarded as unacceptable unless it is confirmed by much more extensive data.

It can hardly be expected that the Oort approximation will hold for stars beyond 3 kpc. The approximation (9) will fail, and further, as will be shown in Section 12, approximation (3) also fails for many stars of group C. However, failure of these approximations can hardly be the root cause; in Section 10, where second-order effects are considered, a similarly low value of A is still found for group C.

It is probable that the result is due to a statistical effect of selection. Many of the stars in the group were originally selected for observation on account of their large calculated distance moduli; and the group itself represents the tail-end of a frequency distribution of calculated distance moduli $m-a-M$, a being written here for the absorption correction. The group is thus selected for small a and high luminosity; it will contain a relatively high proportion of

(i) stars for which the absorption is abnormally small or has been underestimated,

(ii) stars either truly or erroneously classified as supergiants.

Errors in m can be neglected compared with errors in a or M. But, with a range of some four magnitudes between main sequence stars and supergiants, it seems highly probable that the chief contributory cause to uncertainties in the distances arises from errors in the luminosity classifications, and possibly to failures in the calibration of the MK system. However, it may be noted that the selection effect considered here is particularly sensitive to *systematic* errors in the correction for absorption (e.g. in the ratio total absorption to colour excess). If this ratio has been underestimated, a will be systematically underestimated, especially in group C, and the selection effect will operate to an even greater extent, reinforcing errors of over-estimated luminosities; if on the other hand the ratio has been taken too large, the errors in a will to some extent balance the errors in M.

As previously noted, the standard errors of A in the sixth column of Table III, ignore the effects of errors in $\bar{r}$ and are therefore certainly underestimates, especially for group C, composed of the smallest sample of stars.

As regards the Radcliffe material, revised luminosities are being derived by Petrie's method (**27**) at the Cambridge Observatories through the cooperation of Professor Redman. Such measures will provide a useful test of the suggestion that the low value of A found for group C arises chiefly from errors in the distances.

6. *The K-term.*—The K-term was originally introduced as a constant, as in equation (15). Clearly the values of K appropriate to each group are the same as the values of $\overline{A_0 r}$ in Table III. The work of Plaskett and Pearce (**1**) on the K-term may be summarized as follows:

(*a*) For the nearby B stars K was positive.

(*b*) K decreased with increasing r within the range studied, that is to a maximum value of r of about 1 kpc.

(*c*) The K-term is probably in the main due to systematic motions of groups of stars (especially the Sco–Cen cluster).

(*d*) The small residual left after correction for the effect of (*c*) is probably due to Einstein effect in the B stars.

A recent review of the available data (**28**) by Weaver substantiates the main conclusions of Plaskett and Pearce.

Confining attention for the moment to group A we find a significant and negative K-term. The actual value of $\overline{A_0 r}$ depends of course on whether or not

XUM

the corrected or uncorrected solutions are adopted but in either case the term is significantly different from zero, a value for $\overline{A_0 r}$ $(=K)$ of $-4{\cdot}2 \pm 1{\cdot}3$ km/sec being most likely for these stars. It is therefore interesting to note that the other investigations of galactic rotation for distant objects also yield a negative K-term. The results of Seyfert and Popper (**29**) on faint B stars are:

67 B stars velocities $Ar = +34{\cdot}3 \pm 1{\cdot}5$ km/sec/kpc,
$K = -4{\cdot}0 \pm 1{\cdot}0$ km/sec.

68 Ca II line velocities $Ar = +16{\cdot}6 \pm 2{\cdot}6$ km/sec/kpc,
$K = -3{\cdot}6 \pm 1{\cdot}8$ km/sec.

(Errors are probable errors.)

It is worth pointing out that there are only six stars in common between Seyfert and Popper's work and this paper so that the results are virtually independent.

Trumpler (**30**) has discussed the velocities of 39 galactic clusters in the distance range 0·4 to 4·6 kpc. He finds

$$A = +15{\cdot}0 \pm 1{\cdot}0 \text{ km/sec/kpc and } A_0 = -4{\cdot}3 \text{ km/sec/kpc.}$$

Trumpler noted that this apparently implied a contraction along the galactic plane.

Joy (**31**) found a K-term of $-3{\cdot}8$ km/sec from his cepheid velocities and a value of A_0 of $-2{\cdot}4$ km/sec/kpc was found by Stibbs (**32**) in his more recent work on cepheids (if $l_0 = 328°$ is assumed).

Considering these results alone it might appear possible to interpret them as indicating a real contraction of material (at least of interstellar gas and young stars) in the galactic plane. The linear velocity of contraction at the Sun is then $A_0 R_0$ which for $R_0 = 8{\cdot}2$ kpc is about 25 km/sec using the corrected solution. It is of some interest to enquire into the relationship of the K-term and the well-known deviation of the vertex in star streaming. This is especially so since Tannahill (**33**) has shown that the B stars show the same deviation (about $+15°$) as stars of other spectral types. A formula relating the constants of galactic rotation and contraction (or expansion) to the deviation of the vertex has been derived by Shiveshwarkar (**34**) and when a correction is made for an error in sign (Lindblad (**35**)) it may be used with the present results. In this way, with either the corrected or uncorrected set of constants, a deviation of the vertex of about $+15°$ is obtained in good agreement with observation. Even though Shiveshwarkar's formula may only be valid under certain conditions of mass distribution in the galaxy (see Heckmann (**36**) and Lindblad (**35**)), nevertheless Lindblad's qualitative statement that a deviation of the vertex in the direction of increasing longitude demands a slight contraction of the material in question, would appear to be still applicable.

The failure to detect a large negative K-term in groups B and C must of course greatly weaken the view that the K-term is due to a general contraction of the galaxy. Clearly the solutions for groups B and C are of considerably less weight than solution A, nevertheless groups containing 95 and 47 stars respectively are not negligible. We note furthermore that the results of Seyfert and Popper referred to above are, from the values of Ar quoted, comparable in distance with group B and yet the K-terms obtained from the two investigations are of opposite sign. Moreover, reference to Table III shows that there is no smooth

run of $\overline{A_0 r}$ with $\bar{r}$ in our own solutions. Seyfert and Popper's work is deficient in southern stars, while our solutions B and C are deficient in northern stars. A poor distribution of stars in longitude may have a very marked effect on the deduced value of the K-term as is demonstrated in an actual case by Plaskett and Pearce (**1**).

If we seek to interpret the K-term by Plaskett and Pearce's original idea of the effect of community motions on the galactic rotation curve it might appear that we are now dealing with a sufficiently large volume of space for such community motions to be attributable to larger groupings of stars than individual clusters. In particular we might bear in mind in this connection the possible effect of spiral structure and the possibility of the radial ejection of gas and stars from spiral arms. The recent radio discovery (**26**) of a spiral arm near the centre of the galaxy, expanding outwards with a velocity of 50–100 km/sec, clearly shows that at least in certain regions quite large radial motion in the galaxy may be expected.

7. *Velocity dispersion.*—For stars in the region of 1–2 kpc (group A) and for those 10° longitude intervals containing more than four stars each, the mean dispersion in residual velocity has been calculated. The results which are given in Table IV are uncorrected for observational errors (including undetected binaries and errors in the adopted distances). Whilst there is a considerable scatter in the results it is not felt that this is significant. The particularly large values at 44° and 94° are affected by one or two discrepant velocities.

The mean dispersion of $14{\cdot}8 \pm 2{\cdot}2$ km/sec (using the corrected Lick B velocities) is not far from the value of 12 km/sec previously derived from rather different data (**2**). The figures in Table IV give no support to Weaver's

TABLE IV

Velocity dispersion for stars in Group A

$\bar{l}$	Weight	σ_0(km/sec)
44°	8	34·7
53°	5	15·6
86°	6	7·3
94°	4	44·0
103°	12	11·4
155°	7	5·0
174°	18	13·8
193°	6	23·4
246°	6·5	11·4
255°	9·5	17·0
264°	6·5	19·7
274°	9·5	17·3
336°	19	7·7
343°	18	9·5
352°	5·	17·5
mean σ_0		$14{\cdot}8 \pm 2{\cdot}2$

contention (**37**) that the velocity dispersion is high for stars "in the inner part of the galaxy". Weaver finds for a small group of stars (14 in all) lying between 271° and 338° with one star at 37°, a velocity dispersion of 36 km/sec "a value nearly 5 times as great as that observed in the outer and local arms". From

Weaver's figure it would appear that most of his stars lie between 1 and 2 kpc from the Sun (near 1 kpc). But although our stars cover this same region we have only one star in common.

In another paper (**38**) Weaver obtains a velocity dispersion of 35·9 km/sec from 17 supergiants in this same region (presumably including the 14 stars used in (**37**)). For 87 B stars between 330° and 350° he finds a dispersion of 23·0 km/sec which again is taken as indicating an abnormally high velocity dispersion in this region. The standard error of this value is not given but is probably at least as large as ours, which depends on nearly twice the number of stars (172). In view of this and other possible causes of uncertainty in the data available to Weaver, it would appear necessary to obtain a good deal more data before any variation of velocity dispersion with longitude can be firmly established. Our results are in good agreement with those of Nordström (**39**) who found for 353 stars earlier than B5 and brighter than $6^{m}\cdot0$ a velocity dispersion of 8·8 km/sec and for 379 stars earlier than B5 and fainter than $6^{m}\cdot0$ a dispersion of 14·7 km/sec. His group of fainter stars is obviously more nearly comparable with ours and the dispersion in this group agrees very well with our value of 14·8 km/sec.

In view of the errors in radial velocities and distances associated with fainter stars, we do not consider that the difference between the velocity dispersion of B stars brighter and fainter than 6^{m} should be regarded as significant without a great deal of further investigation.

8. *The application of the Camm linear approximation.*—We now proceed to analyse the data on the basis of the Camm linear approximation—equation (7) above. The most recent use of this equation is the analysis by Stibbs (**32**) of cepheid radial velocities. He assumed $R_0 = 8{\cdot}2$ kpc and solved equation (7) for two different values of l_0: 325° and 328°. The recent radio work (**26**) has shown 328° to be probably the better of the two values so that we did not consider it necessary to carry out the solution for $l_0 = 325°$ for the B stars. However, as the value of R_0 is still subject to considerable uncertainty, it was felt necessary to investigate the effect of a change of R_0 on the solution and for this reason the equations were solved for values of R_0 of 8·2 kpc and 12·0 kpc.

Instead of computing R for each star from equation (8) its value was measured on a diagram showing the stars projected on the galactic plane. In view of the various errors in the determination of r, the values of R thus found are of more than sufficient accuracy. Since equation (7) is only valid for $|R - R_0|$ small we used in the analysis only those stars for which $|R - R_0| \leqslant 1{\cdot}0$ kpc (cf. Fig. 1). This reduces the number of stars to 134 in the case of $R_0 = 8{\cdot}2$ kpc and 131 in the case of $R_0 = 12{\cdot}0$ kpc. Of these stars 127 are common to both solutions.

In the $R = 8{\cdot}2$ kpc solution there are only four stars which depend wholly or partly on the Lick B velocities discussed in Section 3, whilst in the $R_0 = 12{\cdot}0$ kpc solution there are five such stars. The analyses were carried out without applying the corrections to these velocities which are now considered desirable. Since however there are so few stars requiring correction the final results will not have been appreciably affected.

Equation (7) was solved by least squares to give the constants and their standard errors listed in Table V which also contains the corresponding ($l_0 = 328°$) solution by Stibbs (**32**) for the cepheids. In applying the method of least squares the assumption was made both in our work and in that of Stibbs

that the principal source of error is in the velocities (observational error plus velocity dispersion); the errors being considered to be relatively less important in r and $(R-R_0)$. It is not known how far this assumption is justified. Whilst it would, theoretically, be possible to compute regressions of both V on r and r on V it would be difficult in practice to decide how to weight the individual stars in each case and how to determine a weighted mean of the two regressions. Furthermore, in the case of r, systematic errors may well be important and thus a real improvement on the present method of analysis does not appear practical. However the limitation of the least square method used should be clearly recognized since, in any case, it may quite probably have led to an underestimation of the standard errors quoted in Table V. It appears from Table V that the two solutions do not differ significantly. The constants are thus rather insensitive to the adopted value of R_0 in this range.

TABLE V

Results of least square analysis by Camm's linear approximation

	Solution 1	Solution 2	Stibbs (32) (cepheids)
R_0 (adopted) kpc	12·0	8·2	8·2
l_0 (adopted)	328°	328°	328°
ϵ_0 (km/sec/kpc)	− 1·1 ±0·9	− 2·0 ±0·9	− 2·4 ±1·3
A (km/sec/kpc)	+17·6 ±1·5	+17·3 ±1·5	+18·6 ±2·0
C (km/sec/kpc)	+ 4·7 ±2·4	+ 3·4 ±2·5	+ 0·7 ±2·7
Number of stars			
From Group A	88	87	
From Group B	31	35	
From Group C	12	12	
Total	131	134	96

Errors are standard errors.

We see that a K-term is present (non-zero values for ϵ_0 and C). It will be remembered that a negative value of A_0 ($\equiv\epsilon_0$) was found in the Oort analysis for stars in the range 1 kpc $\leqslant r <$ 2 kpc. Since the stars in the present analysis are mainly from this group (cf. Fig. 1), but only of course a selection from this group, the negative value of ϵ_0 is not surprising. It will be recalled that the results of the more distant groups in the Oort analysis did not support the interpretation of the K-effect as due to a dilation of the galaxy. Confirmation of this view may be obtained from a consideration of the residuals in the two Camm type solutions. In both cases the residuals are not randomly distributed with respect to r but are predominantly positive for $r \leqslant 1{\cdot}4$ kpc and predominantly negative for greater values of r. This would appear to confirm that the K-effect cannot be represented in the form used in equation (7) (general galactic expansion or contraction). We may also note that application of formulae (6) and (13) leads to a value of h of about $+15°$ if the values of C in Table V are taken seriously. This would not accord at all well with the Oort analysis given above which indicated $h \doteqdot 0$. This may be taken as another indication that the K-effect is to be interpreted otherwise than by a general galactic dilation.

XUM

9. *The value of Oort's constant A.*—The Camm linear approximation, which we regard as the most reliable approach to the problem of the value of the Oort A constant, yields $A = 17{\cdot}6 \pm 1{\cdot}5$ km/sec/kpc for $R_0 = 12{\cdot}0$ kpc and $A = 17{\cdot}3 \pm 1{\cdot}5$ km/sec/kpc for $R_0 = 8{\cdot}2$ kpc (Table V). With greater weight to $R_0 = 8{\cdot}2$ we adopt $A = 17{\cdot}4 \pm 1{\cdot}5$ km/sec/kpc. In an earlier section it was shown that the Oort approximation gave a value of 15·7 km/sec/kpc for Oort's constant A if uncorrected values of the Lick B velocities discussed in Section 3 were used. On the other hand the corrected velocities give a value of 17·8 km/sec/kpc. As pointed out above, the Camm-type analysis happens to be essentially free of stars requiring this correction. Hence the fact that it gives a value for A close to the value for the "corrected" Oort solutions may be regarded as further evidence for the validity of the applied corrections.

The present work giving greatest weight to the Camm analysis leads us to adopt

$$\mathbf{A = +17{\cdot}5 \pm 1{\cdot}5}\ \text{km/sec/kpc}$$

as the most probable value indicated by the analysis of the present data. We may now compare it with other recent determinations.

Table VI lists several recent determinations of A. Stibbs' value from the cepheids, though slightly higher than ours, cannot be considered as being

TABLE VI

Recent determinations of Oort's constant A

		A (km/sec/kpc) and s.e.
Present paper	Camm analysis, 134 B-stars	$17{\cdot}4 \pm 1{\cdot}5$
	Oort analysis	
	267 B-stars	
	227 Ca II velocities	$17{\cdot}8 \pm (1{\cdot}5)$
	Adopted mean	$17{\cdot}5 \pm 1{\cdot}5$
Stibbs (**32**)	Camm analysis, 96 cepheids	$18{\cdot}6 \pm 2{\cdot}0$
Oosterhoff (**40**)	Re-discussion of (**32**)	$17{\cdot}4 \pm 2{\cdot}1$
Gascoigne and Eggen (**41**)	Camm analysis, 37 cepheids	$17{\cdot}5 \pm 1{\cdot}9$
Petrie *et al.* (**42**)	79 B-stars	
	68 Ca II velocities	$17{\cdot}7 \pm 1{\cdot}6$*
Weaver (**23**)	79 cepheids	$10{\cdot}8 \pm 1{\cdot}8$
Weaver (**24**)	187 B-stars	$13{\cdot}2 \pm 1{\cdot}8$
Weaver (**24**)	Adopted mean	$11{\cdot}5 \pm 1{\cdot}5$
Bahng, Code and Whitford (**43**)	B-stars and cepheids	$11{\cdot}5 \pm 1{\cdot}5$

* s.e. computed from published p.e.

significantly different from it. Furthermore recent rediscussions of some of Stibbs' velocities by Oosterhoff (**40**) and Gascoigne and Eggen (**41**) using more accurate distances for the stars, deduced from photoelectric magnitudes and colours, leads to a value of A practically identical with ours. It is of considerable interest to see that our value of A is in close agreement with that deduced by somewhat different methods by Petrie, Cuttle and Andrews (**42**) from quite independent data on B stars. These values all contrast markedly with the values obtained by Weaver (**23, 24**) and by Bahng, Code and Whitford (**43**) for B stars and cepheids. Both Petrie *et al.* (**42**) and Weaver (**44**) discuss the difference

in their values of A for the B stars and it has been suspected that this difference might partly be due to Weaver depending for absolute magnitudes on MK types and Petrie *et al.* on Petrie's Hγ method (**27**). However since we have based our analysis on MK classifications and yet are in good agreement with Petrie *et al.* it would appear rather unlikely that this is a major cause for Weaver's discrepant value.

We may conclude that, so far as present data on B stars and on cepheids goes, a value of A close to 17·5 km/sec/kpc is preferable both to recent anomalously low values and to the value of 19·5 km/sec/kpc adopted in reducing the 21 cm results (**45**, etc.).

10. *Distance to the galactic centre.*—Referring to Section 4, equations (16) and (18) have been used in two rather different approaches to the problem of determining R_0 from the present material.

(*a*) The symmetry of the function $V(\lambda)$ in equation (16) allows the grouped mean velocities as a function of λ to be formed in the following way. Stars in a particular range λ_1 to λ_2 are grouped together with those between $-\lambda_1$ and $-\lambda_2$ (velocities of the latter being taken with negative sign). It is important to note that this treatment eliminates a general K-term so long as the weights of stars between λ_1 and λ_2 and between $-\lambda_1$ and $-\lambda_2$ are the same.

The form of the function $V(\lambda)$ is not amenable to an analytical treatment by least squares. Instead the sums of the squares $\sum p(\mathrm{O-C})^2$ were directly computed for various values of the parameters A, R_0 and κ. The values of the three parameters giving minimum $\sum$ may be regarded as the most probable, while the significance of the solution may be assessed by finding the range of other values which give

$$\sum < \frac{N-m+1}{N-m} \sum_{\min}$$

where N is the number of observed mean velocities used, and m is the number of degrees of freedom (i.e. number of disposable parameters) (**46**).

In the computations, l_0 was regarded as a known quantity, $l_0 = 327^\circ{\cdot}7$. For the ratio of the axes of the velocity ellipsoid, Hins and Blaauw (**47**) have found the value $0{\cdot}49 \pm 0{\cdot}04$ for faint low-latitude stars. Consequently, for most of the computations we have adopted

$$\kappa = 0{\cdot}5.$$

However, as will appear later, adoption of other values of κ in certain cases did indeed show that no significant diminution of $\sum$ was achieved and therefore that $\kappa = 0{\cdot}5$ is likely to be close to the true value.

An interesting feature of the method is that the product AR_0 which appears as a scale factor in equation (16) can be compared directly with the 21 cm radio observations of the interstellar gas. Schmidt's analysis (**48**) has given a radio value $AR_0 = 156$ km/sec.

Preliminary applications. As a first approach to the problem, the identical material of groups A, B and C already analysed for first-order effects were subjected to the above treatment. It will suffice to describe the results in brief.

Group A. $\sum_{\min}$ was found to diminish steadily from $\rho = 0{\cdot}18$ to $\rho = 0{\cdot}075$. The significance test suggests that $R_0 > 13$ kpc, and a value $A = 18{\cdot}2$ is derived. The method fails, presumably due to:

(i) the smallness of second-order effects,

XUM

(ii) the presence of a large negative K-term which is not completely balanced out in the process of taking means over a 180° range of λ,

(iii) the probable presence of systematic errors in observed velocities at certain λ.

The Lick velocities carry considerable weight in this group, and if they are corrected by + 10 km/s $\sum$ is decreased by a factor 2. We regard this improvement of fit as a further argument in favour of applying this correction to the Lick velocities of faint B stars. The effect of the corrections is to increase A to 20·5, but $\sum$ still diminishes (rather more slowly than before) from $\rho = 0{\cdot}18$ to 0·075.

Finally this group was re-analysed using corrected Lick velocities and a K-term, $K = -4{\cdot}0$ km/sec, as suggested by the first-order analysis. In this instance we find, with $\kappa = 0{\cdot}5$,

$\Sigma_{\min}$	R_0	A	AR_0
3106	8·24	21·1	174
2991	14·0	21·0	294
3058	20·0	20·6	412.

For the first time a minimum is found with $R_0 < 20$, but the flatness of the minimum is such that no statistically significant distinction can be drawn between the three solutions. All three values of AR_0 are larger than that given by the radio observations. We conclude that this group is unsuitable for a determination of R_0, although it does tend to indicate a distance to the galactic centre greater than 8 kpc.

Group B. With $\kappa = 0{\cdot}5$ and uncorrected Lick velocities, $\sum_{\min}$ is found with $\rho = 0{\cdot}20$ and $A = 14{\cdot}6$. Thus, the mean distance of the group being 2·30 kpc, we find $R_0 = 11{\cdot}5$ and $AR_0 = 168$. The significance test suggests that $R_0 > 8{\cdot}5$ kpc.

If the Lick velocities are corrected by + 10 km/sec $\sum$ is diminished by about 30 per cent, the most probable value of A is somewhat increased, and that of R_0 diminished.

Group C. $\sum_{\min}$ is found with $\rho = 0{\cdot}40$ and $A = 9{\cdot}9$. Thus $R_0 = 10{\cdot}0$ is indicated but the significance test shows that $R_0 = 8{\cdot}0$ is not excluded. The low value of A found parallels that found in Section 5.

All three above analyses suggest a value of R_0 greater than 8 kpc. It is clear that the method has to deal with uncertainties due to different causes in the three groups. In group C, where the second-order effects are largest, one has to recognize the greatest errors in calculated distances. In group A the second-order effects are rather too small, despite a comparative wealth of material, to derive much idea about the true value of R_0; besides, as we have seen, the region occupied by group A appears to be influenced by a marked general K-term of about − 4 km/sec.

Final application: group BC′. For a final determination of what may be regarded as the best value of R_0 attainable from this material by the method described, we have formed a new group BC′ of 113 stars with the limits $r = 2{\cdot}0$ to 3·6 kpc. The upper limit of 3·6 kpc will exclude many over-estimated distances. The velocities were corrected by a factor to reduce them all to the mean distance $\bar{r} = 2{\cdot}54$ kpc. In accordance with previous experience of improved fit, the Lick velocities were corrected by + 10 km/sec. Moreover, Lick and McDonald observations were given half-weight. The resulting velocities were grouped into 15 means, tabulated in Table VII where $\lambda' = |l - 327°{\cdot}7|$. In the

third column, p_+ represents the weight of the stars in the range $(l-l_0)=0$ to 180°, and in the fourth p_- represents the weight in the range $(l-l_0)=180$ to 360°. The total weight appears in the fifth column, and the number of stars in the sixth. If a general K-term is to be applied to the material, then we must correct $\bar{V}$ by adding $(p_- - p_+)K/p$.

TABLE VII

Mean velocities for Group BC′

$\bar{\lambda}'$	$\bar{V}$	p_+	p_-	p	n	Δ	
8·4	+17·7	6	0	6	10	+1·8	*
16·7	+24·0	7	1	8	14	+3·2	*
33·6	+51·5	2	4	6	7	+3·2	*
47·8	+30·9	0	6	6	7	+1·0	
55·3	+36·1	0	14½	14½	15	−0·5	
64·2	+18·7	1½	7	8½	10	−2·0	*
72·6	+16·2	1½	9	10½	12	−3·0	*
84·5	+10·5	½	½	1	2	−3·4	*
95·8	−13·0	1	1	2	2	−3·0	*
104·9	−29·1	4½	3	7½	8	−2·4	*
117·6	−40·9	4	0	4	4	−1·1	*
127·0	−28·7	6	0	6	6	−0·2	
135·4	−37·4	7	1	8	9	+0·5	
153·6	− 3·4	½	2	2½	4	+0·9	
172·6	−11·5	0	2½	2½	3	+0·3	

In Table VIII (*a*) appear computed means of $\sum_{\min}$ with $\kappa=0{\cdot}5$ and a series of values of R_0, while in Table VIII (*b*) appear values when $\rho=0{\cdot}30$ is assumed together with various values of κ. From the latter it is clear that $\kappa=1{\cdot}0$ is excluded, although such a value has been suggested as appertaining to main sequence B stars (**16,** Tables 3, 5, p. 332). Nordström (**39**) however gives a value 0·59 for O to B5 stars fainter than $6^m{\cdot}0$. The present material adds support to the value $\kappa=0{\cdot}5$ as appropriate to distant stars of B type, in agreement with Hins and Blaauw's value previously quoted (**47**).

Turning to Table VIII (*a*), with $\kappa=0{\cdot}5$ assumed, we find the best fit with $\rho=0{\cdot}29$, $A=15{\cdot}4$, $R_0=8{\cdot}76$ and $AR_0=135$.

According to the significance test, we find permissible values of ρ from 0·21 to 0·365, or $R_0=12{\cdot}1$ to 7·0 kpc.

TABLE VIII

Determination of minimum $\Sigma p(\mathrm{O-C})^2$ *for group* BC′

(*a*) $\kappa=0{\cdot}5$

ρ	R_0	A	$\Sigma_{\min}$	AR_0
0·20	12·70	15·1	3976	191
0·25	10·16	15·1	3682	153
0·28	9·06	15·3	3607	139
0·29	8·76	15·4	3604	135
0·30	8·47	15·5	3606	131
0·35	7·26	15·5	3790	122

(*b*) $\rho=0{\cdot}3$ $R_0=8{\cdot}47$

κ	A	$\Sigma_{\min}$	AR_0
0·4	15·5	3639	131
0·5	15·5	3606	131
0·6	15·6	3849	132
1·0	14·8	10,722	125

The observations of Table VII are plotted in Fig. 9, where the curve shows the predicted velocities based on equation (16) with the above parameters. Note that the node occurs at $\lambda = 82°$, while the higher amplitude of the curve in the left-hand part compared with the right-hand part forms the basis for the value $\kappa = 0{\cdot}5$. Increasing the value of κ towards unity has the effect of depressing the relative amplitude of the left-hand portion.

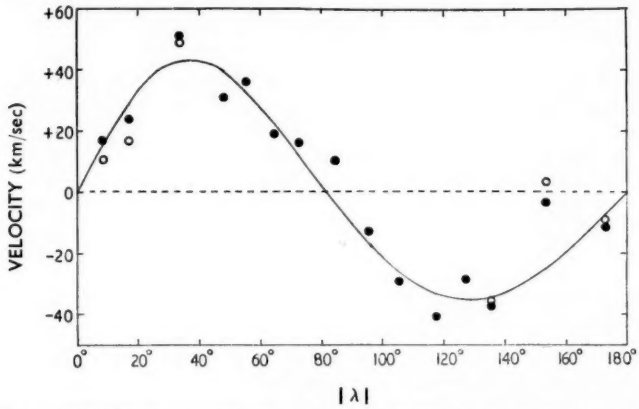

FIG. 9.—*Velocities of 113 stars ($r = 2{\cdot}0$ to $3{\cdot}6$ kpc) fitted to equation (16) with $R_0 = 8{\cdot}8$ kpc and $\kappa = 0{\cdot}5$. Filled circles are based on corrected Lick B velocities (Section 3). Open circles are based on uncorrected velocities. For numbers of stars contributing to each mean see Table VII. Note the greater amplitude of the curve for the region $|\lambda| < 80°$ than for $|\lambda| > 80°$.*

The foregoing analysis depends on fitting all 15 means of Table VII to the theoretical curve, with R_0 as a disposable parameter. As is well known, one of the chief effects of increasing ρ is to shift the node from $\lambda = 90°$ to smaller values. If the node λ_0 can be determined sufficiently accurately, we obtain a direct measure of R_0 from the relationship

$$R_0 = \tfrac{1}{2}\bar{r} \sec \lambda_0$$

which is strictly accurate for circular orbits. Other things being equal, it is the ring of stars at distance R_0 from the galactic centre which can provide the best determination of R_0 from an analysis of radial velocities. It would therefore be legitimate in the present analysis to confine attention to those stars near 90° from the galactic centre. Such a restriction of the material is adopted in method (*b*) below, but here as a compromise we have tried the following alternative.

The last column of Table VII gives the difference in velocities computed for the curves of best fit based on $\rho = 0{\cdot}29$ and $\rho = 0{\cdot}20$. Those entries where the difference exceeds 1·0 km/sec are marked with an asterisk; there are nine such entries which may be regarded as "sensitive directions" for the determination of R_0. If we use only these nine entries we find the following values of $\sum_{\min}$ as a function of ρ:

ρ	$\sum_{\min}$
0·20	1600:
0·28	1314
0·29	1318
0·30	1340
0·35	1590

The most probable value of R_0 is 9·06 kpc. According to the significance test, values of $\sum_{\min}$ up to $1314 \times 7/6$, i.e. 1533 are permissible, whence values of $\rho = 0{\cdot}214$ to $0{\cdot}341$ or $R_0 = 11{\cdot}9$ to $7{\cdot}45$ kpc are permissible. It is interesting to note that the range of values of R_0 in this solution, depending on a smaller weight of observations, has been narrowed by 0·6 kpc.

(*b*) In using equation (18) we have employed a modification of a method due to Weaver (**22**).

Weaver concentrated attention entirely on distant stars for which $|R - R_0|$ is small, and the velocities of such stars are undoubtedly the most sensitive to R_0 independently of ω' and ω''. If for any star or group of stars we know V, l, b, and r and adopt a value of l_0 (327°·7), we may calculate for a set of assumed values of R_0 a corresponding set of values of ω_0'. If then we do this for several stars or groups of stars and plot the results in the R_0, ω_0' plane we obtain a set of curves which should all theoretically intersect at one point which gives the required true values of R_0 and ω_0'. Since it is obvious that only stars with large r can give a value of R_0 of any accuracy, we restrict ourselves to $r \geqslant 3{\cdot}0$ kpc. Also since (18) uses the Camm linear approximation, we have the restriction $|R - R_0| \leqslant 1{\cdot}0$ kpc. Finally since for $(R - R_0) \doteqdot 0$, $V \doteqdot 0$, ω_0' is indeterminate (from (18)), we have the further restriction that $|R - R_0| \geqslant 0{\cdot}5$ kpc. Satisfying these criteria there are only nine stars, all lying between $l = 256°$ and 263°, and with r ranging from 3·5 to 4·8 kpc (cf. Fig. 1). These nine stars define the mean curve shown in Fig. 10. The dotted lines indicate the uncertainty introduced by the standard error of V. The second curve in Fig. 10 is drawn according to

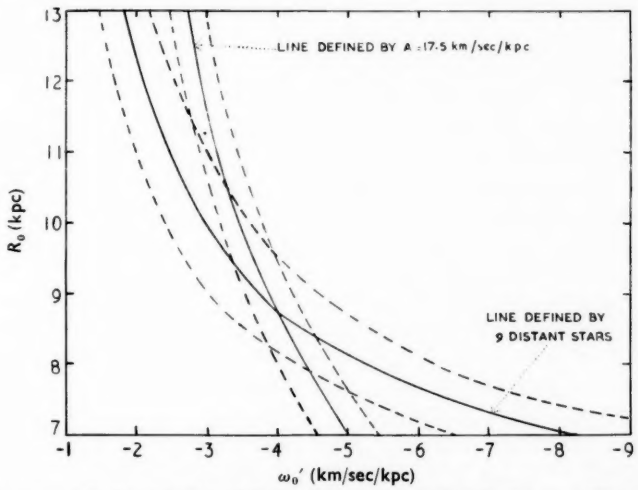

FIG. 10.—*The determination of R_0 by the second method of Section 10. The two solid lines show the R_0, ω_0' relationships defined by 9 distant stars and by a value of Oort's constant of* 17·5 km/sec/kpc. *R_0 is determined by their point of intersection. The dotted lines show the standard errors of the curves.*

the condition $A = -\frac{1}{2}R_0\omega_0' = 17{\cdot}5$ km/sec/kpc. A is well determined, independently of R_0, from many relatively nearby stars (the Camm solution in Section 8 depends essentially on stars with r between 1 and 2 kpc). Again the dotted curves give the uncertainty indicated by the standard error of A.

We find that the most probable value of R_0 is 8·7 kpc, while the permissible range of values is from 7·6 to 11·3 kpc.

This application of the method depends on the comparison of the motions of many relatively close stars with the motions of nine distant stars in the most sensitive direction.

It is of interest to note that of the nine stars used in method (*b*), in conjunction with the value $A = 17{\cdot}5$ km/sec/kpc, only four are common to the group BC′ used in method (*a*). Hence the two methods may be regarded as largely independent.

In Table IX we compare the results for R_0 found by the two methods.

TABLE IX

Determination of R_0 (kpc)

	Most probable value	Range of values
Method (*a*):		
BC′: all stars	8·8	7·0 to 12·1
BC′ restricted	9·1	7·4 to 11·9
Method (*b*):		
$A = 17{\cdot}5$, 9 stars	8·7	7·6 to 11·3
Mean	**8·9**	

To summarize the results of this section:

(i) the most probable value of R_0 is 8·9 kpc, based on the MK scale of distances,

(ii) method (*a*), dependent on an assumed force law for the galaxy, confirms the result found in the Oort analysis that the most distant stars give an abnormally low value of A; this is probably to be attributed to errors in the distances of many stars in group C (Section 5).

(iii) a value of $\kappa = 0{\cdot}5$, for the ratio of the axes of the velocity ellipsoid, appears to be appropriate to distant B stars.

11. *The use of* B *star radial velocities to determine absolute magnitudes.*—If we assume that the radial velocities of the B type stars, corrected for solar motion, follow the simple Oort formula (14) then we may use the velocities to derive the relative absolute magnitudes of the various sub-groups of B stars. This follows since for each star we may determine (rA) from (14) and then reduce these values to some fixed apparent magnitude. If $(rA)_s$ is the value of (rA) reduced in this way then clearly $\log (rA)_s$ is proportional to the absolute magnitude of the star. If a value of A is assumed, the actual absolute magnitude can be deduced. In carrying out this calculation we restrict ourselves to stars with $|\sin 2\lambda| \geqslant 0{\cdot}5$. There are 214 stars between B5 and O5 which satisfy this condition. Adopting $A = 17{\cdot}5$ km/sec/kpc we obtain the results shown in Table X. The fourth column of this table gives the normal calibration of the MK system (**10**).

Whilst the main purpose of the present paper is to use the B stars with an assumed absolute magnitude system for the determination of galactic motions, it is not without interest to reverse the arguments to see that the results obtained

are consistent with those normally adopted. Such an investigation is of especial interest in that Blaauw (**49**) has determined absolute magnitudes of main sequence stars of types B1 to B3 and our material may be used to extend the comparison with the MK calibration to still earlier types. As noted above, the relative values of M in the table are independent of any assumed value of A.

TABLE X

Calibration of B *star absolute magnitudes using the Oort approximation and* $A = 17{\cdot}5$ *km/sec/kpc.*

Spectral Type	No. of Stars	Weight	Normal MK Abs. Mag. (10)	Deduced Abs. Mag.
Main Sequence (Luminosity Classes IV and V)				
			m	m m
B2 to B1·5	15	14	−3·1	−3·6 ± 0·4
B1 to B0·5	30	23·5	−3·6	−4·2 ± 0·3
B0 to O9·5	8	6·5	−4·4	−4·6 ± 0·6
Early O types	29	26·5	−5·1	−4·8 ± 0·2
Giants (Luminosity Classes II and III)				
			m	m m
B5 to B3	6	4·5	−4·0	−4·7 ± 0·6
B2 to B1·5	8	7	−4·6	−3·1 ± 0·6
B1 to B0·5	27	22·5	−4·8	−4·3 ± 0·3
B0 to O9·5	12	10	(−5·4)	−5·4 ± 0·5
O9	5	4·5	(−6·4)	−4·3 ± 0·7
Supergiants (Luminosity Class I)				
			m	m m
B5 to B3	15	14	−6·3	−5·8 ± 0·4
B2 to B1·5	15	15	−6·4	−6·2 ± 0·4
B1 to B0·5	26	24·5	−6·4	−6·4 ± 0·2
B0 to O9·5	15	15	−6·4	−5·7 ± 0·5
O9	3	3	−6·4	−6·3 ± 1·0

Errors are standard errors.

It will be noticed that we have not restricted ourselves to nearby stars as might perhaps have been considered necessary in view of the approximate nature of equation (14). However the results of the Oort type analysis given earlier shows that deviations from (14) for nearby stars, due to K-terms, are likely to be quite as important as deviations from it for distant stars due to "second-order" effects. Thus stars are included irrespective of distance. The corrected Lick B velocities (Section 3) have been used. In general it can be said that the agreement between the last two columns of Table X is remarkably good.

12. *The differential rotation of the* B *stars.*—If we neglect any effects due to a general expansion or contraction of the galaxy then the exact equation for the effect of differential rotation on radial velocities is the Bottlinger equation (2) above. The first attempt to use this formula to obtain $(\omega - \omega_0)$ as a function of R was apparently made by Camm (**18, 19**) using the data available to him on planetary nebulae and cepheids. Recently the method has been applied to

cepheids by Weaver (**23**) and Stibbs (**32**) and by Petrie, Cuttle and Andrews (**42**) to B stars. A determination of $(\omega-\omega_0)$ as a function of R has also been made from 21 cm observations (**45, 50**). These latter observations are the basis of the theoretical model of mass distribution in the galactic system deduced by Schmidt (**48**). It is therefore of interest to analyse the present data in the same way for comparison with these previous investigations, notwithstanding the possibilities of radial motion in the galaxy discussed earlier.

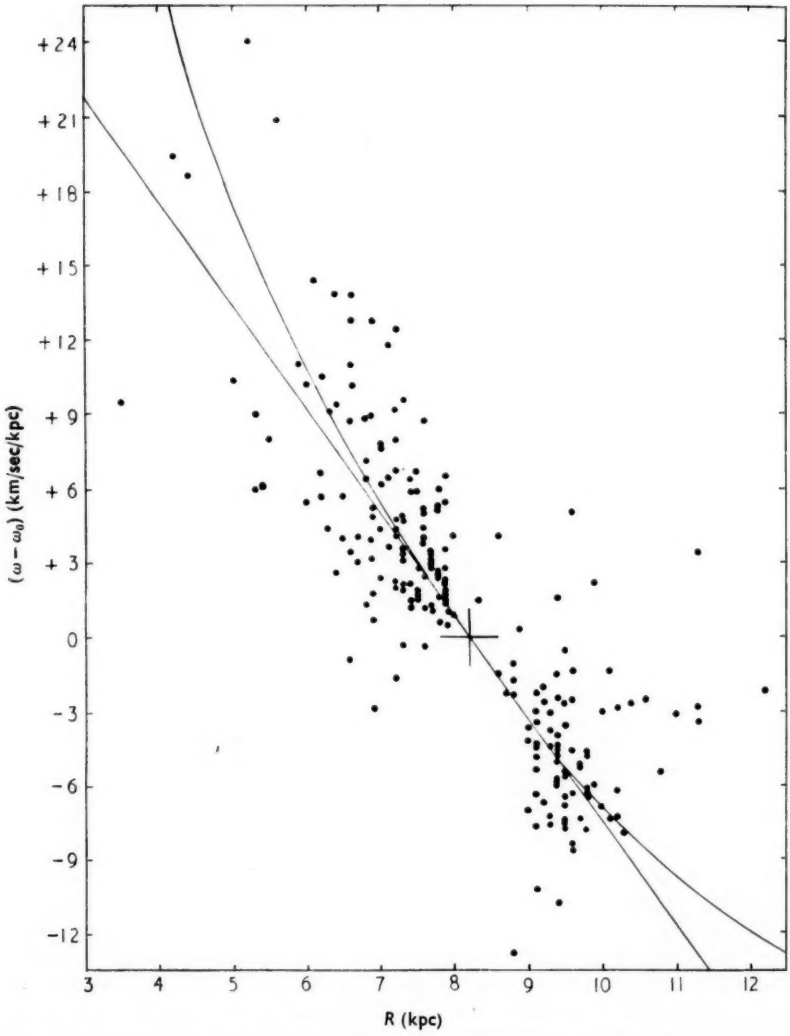

FIG. 11.—*Relationship between R and* $(\omega-\omega_0)$ *for 218 stars. The straight line is drawn for* $A=17{\cdot}5$ *km/sec/kpc* ($\omega'=\omega_0'=$*constant*). *The curve is drawn according to Schmidt's model* (**48**). *A value of* $R_0=8{\cdot}2$ *kpc is assumed. Some points represent more than one star.*

In analysing the data according to equation (2) a longitude of 327°·7 was adopted for the galactic centre and a value of 8·2 kpc for R_0. This value of R_0 was used so that a direct comparison with previous work could be made. All stars with $|\sin\lambda\cos b| \leqslant 0{\cdot}23$ were rejected from the analysis. This left 219 stars of which 186 have measured velocities for interstellar Ca II. Figs. 11 and 12 show the relationship between $(\omega-\omega_0)$ and R in the case of the stars and the

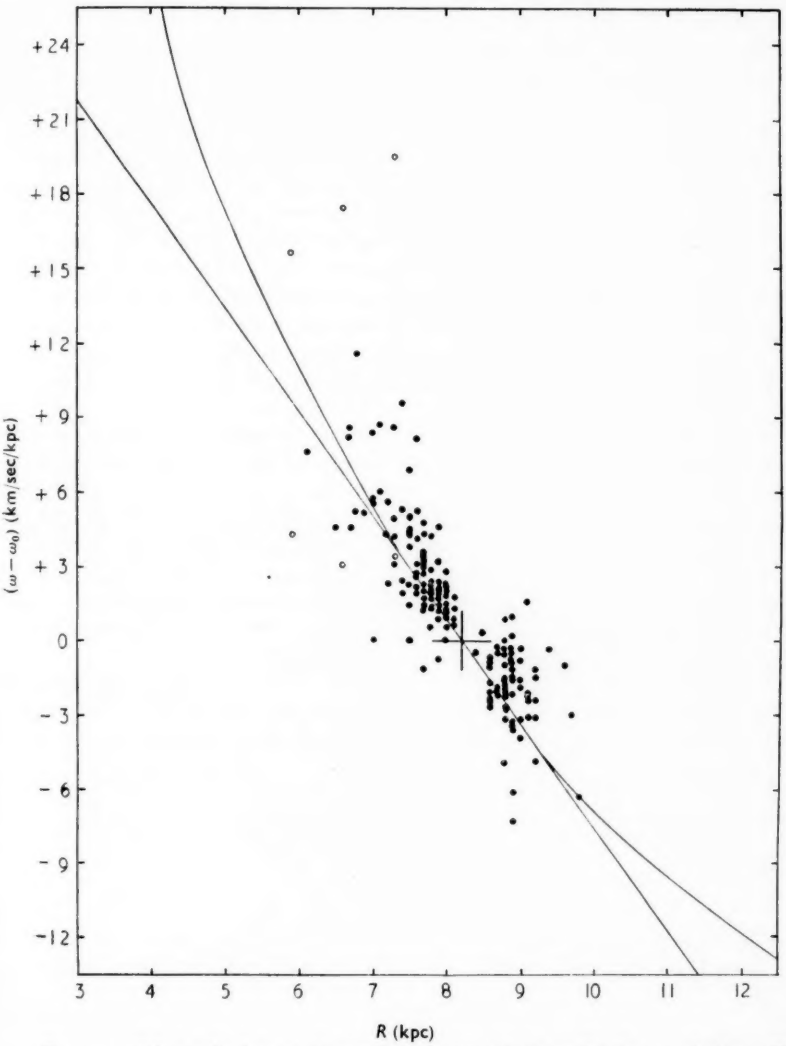

FIG. 12.—*Relationship between R and* $(\omega-\omega_0)$ *for* 186 *interstellar* Ca II *velocities. The straight line is drawn for* $A=17{\cdot}5$ *km/sec/kpc.* $(\omega'=\omega_0'=\text{constant})$. *The curve is drawn according to Schmidt's model* (**48**). *A value of* $R_0=8{\cdot}2$ *kpc is assumed. Some points represent more than one velocity. The six open circles represent* 3 *stars in each of which double interstellar lines have been measured.*

interstellar gas. In the case of the gas the value of R was deduced by assuming $r(\text{Ca II}) = r(\text{star})/2$. The small number of points near $R = R_0$ is due to the selection of the original data for $r \geqslant 1{\cdot}00$ kpc. If the same value of Oort's constant, A, applied throughout the region investigated, the relationship between $(\omega - \omega_0)$ and R would be linear. The straight lines in Figs. 11 and 12 are drawn for $A = 17{\cdot}5$ km/sec/kpc. The curves in the two figures show the expected relationship on Schmidt's model (**48**) of the galaxy and essentially represent the 21 cm observations. The figures give some indication that Schmidt's model is a better fit to the points than a linear relationship. Whilst there is only a slight indication of this, it may at least be claimed that the observations discussed in this paper are not inconsistent with Schmidt's model. This is a point of some interest since the curves obtained by Weaver (**23**) and Stibbs (**32**) for cepheids and by Bahng, Code and Whitford (**43**) for B stars agree neither with each other nor with Schmidt's model. In the case of Weaver's curve ω'' is negative. This point has been discussed by Schmidt (**48**), who concluded that such a state of affairs was very unlikely on theoretical grounds. In the case of Stibbs' results the deviations may be connected with errors in the distances (r) used in the analysis. Lacking photoelectric colours and magnitudes for the majority of his stars, Stibbs had to depend on more approximate methods of determining their distances. This may well have led to fairly large systematic errors for the more distant stars which are the ones that show the deviations from Schmidt's model. In fact a small increase in the average extinction per unit distance in the galaxy over that adopted by Stibbs would probably reduce considerably the discrepancy between his results and the theoretical curve. The results of Bahng, Code and Whitford have so far appeared only in abstract and it is impossible therefore to make a proper comparison between our results and theirs. However our results appear to be based on more extensive data. We cannot therefore regard any differences between the angular velocity curves derived from stars and 21 cm observations as definitely established. The results of Petrie, Cuttle and Andrews (**42**), which cover a somewhat smaller range of R than the present investigation, appear to be in quite satisfactory agreement with our results.

Acknowledgments.—We are indebted to Drs A. J. Wesselink and P. A. Wayman for discussions of various points which arose during the course of this work; also to Mr L. Tilbury for calculations of the corrections for solar motion used for some stars.

Radcliffe Observatory,
Pretoria:
1957 *December.*

References

(1) J. S. Plaskett and J. A. Pearce., *D.A.O. Publ.*, **5**, 1931-1936.
(2) M. W. Feast, A. D. Thackeray and A. J. Wesselink, *Mem.R.A.S.*, **67**, 51, 1955.
(3) M. W. Feast, A. D. Thackeray and A. J. Wesselink, *Mem.R.A.S.*, **68**, 1, 1957.
(4) R. E. Wilson, *General Catalogue of Stellar Radial Velocities* (Carnegie Institution), 1953.
(5) W. W. Morgan, A. D. Code and A. E. Whitford, *Ap.J.* Sup., **2**, 41, 1955.
(6) W. A. Hiltner, *Ap.J.* Sup., **2**, 389, 1956.
(7) P. Th. Oosterhoff, *B.A.N.*, **11**, No. 425, 1951.
(8) W. W. Morgan, D. L. Harris and H. L. Johnson, *Ap.J.*, **118**, 104, 1953.
(9) H. L. Johnson and W. A. Hiltner, *Ap.J.*, **123**, 267, 1956.

XUM

(10) P. C. Keenan and W. W. Morgan (in) *Astrophysics*, ed. J. A. Hynek (McGraw Hill), 1951.
(11) W. M. Smart, Charts issued by the R.A.S. 1923.
(12) D. W. N. Stibbs, *M.N.*, **115,** 363, 1955.
(13) D. S. Evans, A. Menzies and R. H. Stoy, *M.N.*, **117,** 534, 1957.
(14) R. M. Petrie, *D.A.O. Publ.*, **9,** 297, 1953.
(15) F. J. Neubauer, *Ap.J.*, **97,** 300, 1943.
(16) R. J. Trumpler and H. F. Weaver, *Statistical Astronomy* (University of California Press), 1953.
(17) F. K. Edmondson, *P.A.S.P.*, **67,** 10, 1955.
(18) G. L. Camm, *M.N.*, **99,** 71, 1938.
(19) G. L. Camm, *M.N.*, **104,** 163, 1944.
(20) J. Titus, *A.J.*, **49,** 1, 1940.
(21) S. Chandrasekhar, *Ap.J.*, **90,** 131, 1939.
(22) H. F. Weaver, *A.J.*, **59,** 375, 1954.
(23) H. F. Weaver, *A.J.*, **60,** 201, 1955.
(24) H. F. Weaver, *A.J.*, **60,** 208, 1955.
(25) H. F. Weaver, *A.J.*, **60,** 211, 1955.
(26) H. van Woerden, W. Rougoor and J. H. Oort, *C.R. Acad. Sci. Paris*, **244,** 1691, 1957.
(27) R. M. Petrie, *D.A.O. Publ.*, **9,** 251, 1952.
(28) H. F. Weaver (in) *Vistas in Astronomy*, Vol. I, ed. A. Beer (Pergamon Press), 1955.
(29) C. K. Seyfert and D. M. Popper, *Ap.J.*, **93,** 461, 1941.
(30) R. J. Trumpler, *Ap.J.*, **91,** 186, 1940.
(31) A. H. Joy, *Ap.J.*, **89,** 356, 1939.
(32) D. W. N. Stibbs, *M.N.*, **116,** 453, 1956.
(33) T. R. Tannahill, *M.N.*, **114,** 460, 1954.
(34) S. W. Shiveshwarkar, *M.N.*, **95,** 655, 1935.
(35) B. Lindblad, *M.N.*, **96,** 69, 1936.
(36) O. Heckmann, *M.N.*, **96,** 67, 1936.
(37) H. F. Weaver, *A.J.*, **58,** 177, 1953.
(38) H. F. Weaver, *P.A.S.P.*, **65,** 132, 1953.
(39) H. Nordström, *Med. Fr. Lund. Ast. Obs. Ser. II*, No. 79, 1936.
(40) P. Th. Oosterhoff, Reported at the Conference on the Coordination of Galactic Research, Stockholm, 1957. *B.A.N.*, **14,** No. 484, 1958.
(41) S. C. B. Gascoigne and O. J. Eggen, *M.N.*, **117,** 430, 1957.
(42) R. M. Petrie, P. M. Cuttle and D. H. Andrews, *A.J.*, **61,** 289, 1956.
(43) J. D. Bahng, A. D. Code and A. E. Whitford, *Sky and Telescope*, **16,** 529, 1957.
(44) H. F. Weaver, Reported at the Symposium on the Galactic Distance Scale, Cambridge, Mass., 1957.
(45) H. C. v.d. Hulst, C. A. Muller and J. H. Oort, *B.A.N.*, **12,** No. 452, 1954.
(46) A. Pannekoek and E. van Dien, *B.A.N.*, **8,** No. 297, 1937.
(47) C. H. Hins and A. Blaauw, *B.A.N.*, **10,** No. 391, 1948.
(48) M. Schmidt, *B.A.N.*, **13,** No. 468, 1956.
(49) A. Blaauw, *Ap.J.*, **123,** 408, 1956.
(50) K. K. Kwee, C. A. Muller & G. Westerhout, *B.A.N.*, **12,** No. 458, 1954.

XUM

STELLAR GROUPS. II. THE ζ HERCULIS, ε INDI AND 61 CYGNI GROUPS OF HIGH-VELOCITY STARS

Olin J. Eggen

(Communicated by the Astronomer Royal)

(Received 1958 January 1)

Summary

A catalogue of 700 high-velocity stars has been searched for objects that share the well-determined space motions of ζ Herculis (22 stars), ε Indi (14 stars) and 61 Cygni (15 stars). The space motions of these groups can be summarized as follows (the Hyades and Sirius Groups of Paper I have been added for comparison):

Group	A		D	V_t	U	V	W
	h	m	°		km/sec		
Sirius	20	44	−42·7	18·4	−14	0	−12
Hyades	6	18	+ 7·5	44·0	+40	−18	− 2
ζ Her	5	48	−16·5	74·5	+54	−45	−26
ε Ind	6	44	+ 6·7	88·5	+79	−39	+ 6
61 Cyg	6	28	+ 0·3	108·0	+92	−53	− 6

where the values of (A, D) represent the convergent points of the apparent motions and V_t is the total space velocity of each group with respect to the Sun (the vector space velocities are in the direction $l=148°$, $b=0°$; $l=58°$, $b=0°$; and $b=+90°$ for U, V, and W respectively). A search through the same catalogue for stars that might be " members " of synthetic groups with convergent point at $\delta=-90°$ and $V_t=74·5$, 88·5, and 108 km/sec indicated that only 2 or 3 chance members are expected to be included in each group.

The colour–luminosity array for the stars in all three high-velocity groups is very similar to that for the galactic cluster M 67.

In 1911 Benjamin Boss (1912*a*) announced the discovery that a dozen stars or so of large proper motion formed a moving cluster with 61 Cygni. Further investigations by Boss (1912*b*) and by Russell (1912) appeared to establish the reality of the cluster but several years later when Rasmuson (1921) re-examined the evidence with the new material then available, he concluded that "there are great reasons to exclude from the list of moving clusters the 61 Cygni-stream . . .". Still later, Chaudhuri (1940) came to the same conclusion.

The purpose of the present investigation is not to re-hash the available data for the stars originally assigned to the 61 Cygni cluster but rather to search for stars sharing the well-determined space motions of selected high-velocity stars, including 61 Cygni. The stars chosen, for the accuracy of their proper motions, radial velocities and parallaxes, are as follows:

Star	π_t	ρ_0 (km/sec)	μ	U	V	W
	″		″			
β Hyi	0·153	+22·9	2·255	+53	−43	−28
ζ Her	0·101	−69·9	0·608	+54	−47	−24
61 Cyg	0·296	−64·0	5·205	+92	−53	− 6
ε Ind	0·285	−40·4	4·692	+79	−39	+ 6

XUM

where the vector space velocities (galactic), U, V and W, are directed toward $l=148°$, $b=0°$; $l=58°$, $b=0°$; and $b=+90°$, respectively. The catalogue searched consisted of 700 high-velocity stars, mainly from the lists published by Miczaika (1940) and by Roman (1955) but with a few additional stars obtained from recently published lists of radial velocities.

Since most of the trigonometric parallaxes for the high-velocity stars are much less accurately determined than those for the stars listed above, the method used for selecting group members was that described in a previous paper (Eggen 1958; Paper I). Stars were admitted to candidacy for membership in a group if the observed position angle of the proper motion, θ_0, agreed with that computed from the group motion to the extent that $\Delta\theta \sin\lambda < 10°$, where λ is the angular distance of the star from the convergent point (A, D) of the group motion. The candidates were then admitted to group membership only if the difference, $\rho_0 - \rho_c$, between the observed radial velocity, ρ_0, and that computed from the group motion, ρ_c, was less than, or equal to, 5, 6, or 7 km/sec, respectively, for radial velocities of quality a, b or c, as defined by R. E. Wilson (1953).

The first two stars listed above, β Hydi and ζ Herculis, obviously have a common space motion and the convergent point of what will be called the ζ Herculis Group was obtained from the mutual convergent point of the proper motions of these two stars. The values of (A, D) for what will be called the 61 Cygni and ϵ Indi Groups are merely the apices of the motion of the defining stars, computed from the radial velocities, proper motions and parallaxes listed above. The three convergent points and total space velocities with respect to the Sun, V_t, are as follows (those for the Hyades and Sirius Groups, discussed in Paper I, are added for comparison):

Group	A		D	V_t
	h	m	°	km/sec
Sirius	20	44	−42·7	18·4
Hyades	6	18	+ 7·5	44·0
ζ Her	5	48	−16·5	74·5
ϵ Ind	6	44	+ 6·7	88·5
61 Cyg	6	28	+ 0·3	108·0

Eight per cent, or 54, of the 700 stars examined were found to be members of the three high-velocity groups as follows: ζ Herculis, 23 members; ϵ Indi, 15 members; and 61 Cygni, 16 members. The members of the ζ Herculis, ϵ Indi and 61 Cygni Groups are listed in Tables I, II and III, respectively, together with the observed position angle of the proper motion, θ_0, and the normalized residual from the computed value, $\Delta\theta \sin\lambda$; the observed radial velocity, ρ_0, and its residual, $\Delta\rho$, and quality Q; the total annual proper motion μ; the group parallax π_g, computed from $4{\cdot}738\mu/V_t \sin\lambda$; the observed magnitude and colour V_E and $(P-V)_E$; and the spectral type and visual absolute magnitude, M_v. The proper motions are mainly uncorrected values from the *General Catalogue* (Boss 1937) except for a few stars from the Yale zones or unpublished Greenwich determinations. The radial velocities and their quality have been taken from Wilson's (1953) catalogue. The magnitudes and colours were observed on the $(P, V)_E$ system or reduced to that system from observations by Roman (1955) or by Stoy and his collaborators (cf. Evans, Menzies and Stoy 1957). The spectral types are mainly by Roman (1955).

XUM

As a test of the possibility that the group members might be so classified by chance coincidences of θ_0 and ρ_0 with θ_c and ρ_c, the same catalogue of 700 stars was examined for "members" of a synthetic group with convergent point $\delta = -90°$. The galactic coordinates of this convergent, $l = 270°$ and $b = -28°$, place it near the centre of that hemisphere of the sky toward which the velocity vectors of the high-velocity stars show a strong preference (Oort 1926). Eleven per cent, or 76 of the 700 stars examined for membership in the synthetic group gave values of $\Delta\theta \sin\lambda < 10°$. When the criterion that $\Delta\rho \leqslant 5$, 6, or 7 km/sec for stars of quality a, b, and c, respectively, was applied, the following "members" were obtained for three values of V_t:

V_t (km/sec) =	74·5	88·5	108
No. =	3	(1)	3

The one "member" for $V_t = 88{\cdot}5$ km/sec, shown in parentheses, is a star with a small radial velocity of quality c that also satisfies the requirements for the group with $V_t = 74{\cdot}5$ km/sec. Apparently, we might expect two or three accidental members to the groups in Tables I–III but it does not seem possible to dismiss all the members as spurious.

Because of the proximity of the apparent convergent points of the three high-velocity groups, there is some ambiguity in assigning four stars to a particular group. These stars, together with the appropriate values of $\Delta\theta \sin\lambda$, $\Delta\rho$ (in km/sec) and π_g, are as follows:

	ζ Herculis			61 Cygni			ϵ Indi		
	$\Delta\theta \sin\lambda$	$\Delta\rho$	π_g	$\Delta\theta \sin\lambda$	$\Delta\rho$	π_g	$\Delta\theta \sin\lambda$	$\Delta\rho$	π_g
	°		″	°		″	°		″
η Ret	−2	−3	0·016	−8	+5	0·009			
HD 66171				0	+6	0·023	+3	+2	0·030
HD102365				+7	0	0·070	0	+4	0·0855
HD104988				+6	+2	0·023	−1	−1	0·028

The assignment of these stars to the groups in Tables I–III has been guided by the trigonometric values of the parallaxes.

Also, there are two high-velocity white dwarfs that may belong to either the 61 Cygni or ϵ Indi Groups, but because of (1) the uncertainty in the observed radial velocities of these faint stars with poor spectral lines and (2) the possibility that the observed line-shifts do not represent the true radial velocity, it is not possible to assign them definitely to either group. These stars are as follows:

			61 Cygni			ϵ Indi		
	π_t	(p.e.)	$\Delta\theta \sin\lambda$	$\Delta\rho$	π_g	$\Delta\theta \sin\lambda$	$\Delta\rho$	π_g
	″	″			″			″
−32°5613	0·108	0·007	+8	(−18)	0·104	+1	(−1)	0·122
L1534–1	0·059	0·005	+3	(− 6)	0·068	+6	(+4)	0·100

The mean trigonometric parallaxes, π_t, indicate that both stars may belong to the 61 Cygni Group.

Since the observed parallaxes of the stars, except 61 Cygni, ϵ Indi, and the four stars mentioned above, were not used in assigning the members to the groups, a comparison between these and the group parallaxes offers an additional test of the reality of the groups. The parallaxes are listed in Table IV, where the absolute trigonometric values, π_t, were taken from the Yale *Parallax Catalogue*

TABLE I

Members of the ζ Herculis Group

Star	θ_0	$\Delta\theta \sin\lambda$	ρ_0 (km/sec)	$\Delta\rho$	Q	μ	π_g	V_E	$(P-V)_E$	Sp.	M_v
	°	°				″	″	m	m		m
TV Psc	80	+3	+ 6	+1	b	0·115	0·0075	4·6v	+1·6:	M3 III	−1·0:
β Hyi	82	−3	+23	0	a	2·255	0·1510	2·75	+0·52	G1 IV	+3·64
HD9166	117	−2	−14	−6	b	0·115	0·0075	6·76	+1·15	K3 III	+1·14
ρ Per	129	−6	+28	0	b	0·172	0·0120	3·4v	+1·53	M4 III	−1·2
η Ret	26	−2	+45	−3	a	0·189	0·0160	5·26	+0·85	Ko	+1·28
HD30455	153	+3	+55	−3	a	0·435	0·0445	6·97	+0·51	G2 V	+5·22
HD43899	536	+5	+70	+1	d	0·090	0·0155	5·6:	−	Ko	+1·6:
HD68788	212	−6	− ·3	+1	b	0·567	0·0360	8·38	+0·74	K1 V	+6·16
HD71377	257	−1	+65	+6	c	0·094	0·0095	5·54	+1·11	K2 III	+0·42
HD89668	254	+1	+35	+7	c	0·670	0·0465	9·41	+1·02	K3 V	+7·75
HD90250	237	−7	+11	+3	b	0·129	0·0085	6·49	+1·01	K1 III	+1·14
HD98824	259	+7	+ 5	+3	b	0·119	0·0075	7·04	+0·96	K1 III	+1·42
HD100733	262	0	+18	0	a	0·088	0·0055	5·4v	+1·60	M3 III	−0·9:
HD106364	262	+3	−10	+6	b	0·113	0·0075	6·87	+1·05	K2 III	+1·25
								8·77	+0·49	F9 V	+3·15
HD119425	255	+2	−42	−6	b	0·127	0·0085	6·26	+1·22	K3 III	+0·90
φ′ Lup	224	+3	−29	+4	a	0·134	0·0095	3·52	+1·48	gMo	−1·60
HD150275	240	0	−32	+3	b	0·289	0·0210	6·34	+0·91	sg Ko	+2·95
ζ Her	309	0	−70	−1	a	0·608	0·0990	2·80	+0·54	Go IV	+2·78
ε Oct	118	+2	+12	−4	a	0·084	0·0055	4·8:	+1·6:	gM6	−1·5:
HD209134	82	−9	−18	+6	b	2·092	0·1410	5·56	+0·92	K3 V	+6·51
HD219829*	103	−3	−14	−2	b	0·484	0·0310	8·00	+0·72	Ko V	+5·46
HD221354	84	−9	−25	−4	b	1·085	0·0720	6·75	+0·74	Ko V	+6·04

*ADS 16645, $\Delta m = 1^m$, P = 108 yrs: not plotted in Fig. 1. The dynamical parallax is 0″·033.

TABLE II

Members of the ε Indi Group

Star	θ_0	$\Delta\theta \sin\lambda$	ρ_0 (km/sec)	$\Delta\rho$	Q	μ	π_g	V_E	$(P-V)_E$	Sp.	M_v
	°	°				″	″	m	m		m
+66°34	97	0	+10	−6	c	1·76	0·096	10·34	+1·30	dM3	+10·25
λ Aur	141	−1	+66	−3	a	0·845	0·0720	4·68	+0·50	Go V	+ 3·97
HD39853	58	+9	+87	+6	b	0·076	0·0100	5·66	+1·46	K5 III	+ 0·66
HD40409	14	+1	+25	−4	a	0·557	0·0315	4·59	+0·98	sg K3	+ 2·09
HD72324	231	−4	+75	−1	b	0·085	0·0090	6·36	+0·93	G9 III	+ 1·13
HD99196	263	−9	+38	+6	b	0·107	0·0060	5·79	+1·30	K4 III	− 0·32
HD102365	274	0	+15	+4	a	1·585	0·0855	4·87	+0·54	G5 V	+ 4·53
HD104988	276	−1	+14	−1	b	0·521	0·0285	8·19	+0·66	G8 V	+ 5·47
HD112758	283	+7	− 4	+2	b	0·839	0·0450	7·54	+0·70	dK1	+ 5·81
HD115539	272	−7	− 8	−1	b	0·096	0·0050	7·21	+0·87	G8 III–IV	+ 0·70
HD135101	296	+4	−39	+6	b	0·656	0·0410	6·68	+0·58	G5 V	+ 4·74
								7·53	+0·63	dG6	+ 5·59
HD137704	294	−6	−48	−6	b	0·118	0·0070	5·46	+1·33	K4 III	− 0·30
HD142574	295	−2	−61	−4	b	0·091	0·0065	5·44	+1·52	K4 III	− 0·50
HD148704	231	−1	−59	+4	b	0·532	0·0405	7·28	+0·65	G5	+ 5·32
ε Ind	123	0	−40	0	a	4·692	0·2850	4·72	+0·95	K5 V	+ 6·96

XUM

TABLE III

Members of the 61 Cygni Group

Star	θ_0	$\Delta\theta \sin\lambda$	ρ_0 (km/sec)	$\Delta\rho$	Q	μ	π_g	V_E	$(P-V)_E$	Sp.	M_v
	°	°				″	″	m	m		m
HD10145	109	+3	+ 16	+3	b	0·734	0·0325	7·66	+0·58	G5V	+5·22
HD18702	106	+9	+ 66	+1	b	0·677	0·0375	8·12	+0·76	KoV	+6·00
HD23183	115	+3	+ 78	+2	c	0·130	0·0080	6·14	+0·92	Ko III	+0·66
HD32023	76:	+6	+106	+6	c	0·068	0·0080	9·10	+0·47	F8V	+3·62
HD35783	165	0	+ 19	−3	b	0·278	0·0125	7·69	+0·35	F6V	+3·17
HD39091	15	+3	+ 12	−5	b	1·110	0·0495	5·63	+0·46	Go	+4·10
β Col	7	−6	+ 89	+3	a	0·402	0·0290	3·06	+1·10	gK1	+0·37
HD40460	183	+9	+ 96	+1	c	0·078	0·0075	6·59	+0·93	K1 III	+0·97
HD53501	351	0	+ 39	−1	b	0·239	0·0115	4·8:	+1·5:	Mo	+0·1:
HD55526	352	+5	+ 64	−5	a	0·204	0·0115	5·15	+1·14	K4	+0·45
HD66171	204	0	+ 37	+6	b	0·503	0·0230	8·20	+0·51	G2V	+5·01
HD108076	272	+2	− 1	−4	b	0·579	0·0260	8·02	+0·46	Go V	+5·10
HD112943	271	+1	− 12	+2	b	0·768	0·0340	9·79	+1·06	dMo	+7·45
HD120467	254	−8	− 35	−1	b	1·814	0·0840	8·3:	—	dK6	+7·9:
HD182572	49	0	−100	−3	a	0·960	0·0890	5·14	+0·68	G8 IV	+4·89
61 Cyg	52	0	− 64	0	a	5·205	0·2960	5·19	+1·08	K5V	+7·55
								6·02	+1·24	K7V	+8·38

TABLE IV

Comparison of the trigonometric and group parallaxes for the stars in Tables I–III
(Unit = 0″·001)

Star	π_g	π_t	Star	π_g	π
TV Psc	8	13A	HD102365	86	94Y, 89C
β Hyi	151	143Y, 166C	HD104988	28	−10M, 15C
+66° 34	96	102M, 80Yh, 94G	HD108076	26	17M
409166	8	−3G	HD112758	45	79M, 35C
HD10145	32	32M, 45G	HD112943	34	26M, 59Y, 41V, 71C
HD18702	38	38M, 23Y, −10S, 41D	HD119425	22	8A, −5Y, −12W
ρ Per	12	2A, 30M	HD120467	84	83Y, 56C
η Ret	16	7Y	HD129245	8	12G
HD30455	44	7M, 15V	HD135101	41	28A, 7M
λ Aur	72	65A, 65M, 68S	ϕ' Lup	10	6Y
HD35783	12	12G	HD142574	6	27M, 38W
HD39091	50	38C	HD148704	40	54Y, 75C
β Col	29	5Y, 45C	HD150275	21	19A, 9G
HD40409	32	60Y, 8C	ζ Her	99	95A, 108M, 104Yk, 124S
HD53501	12	15Y, 46C	HD182572	89	51A, 75M, 101Yk
HD55526	12	−1Y, 52C	61 Cyg	296	296 mean
HD66171	23	18M, 13G	ϵ Ind	285	285 mean
HD68788	36	10M, 14G, 22D	HD219134	141	140A, 159M, 181S
HD72324	9	23W	HD219829	31	6M, 44Y, −17k, 8S, 52D
HD89668	46	40M, 42Y, −10V, −4C	HD221354	72	22M

(Jenkins 1952) and the group parallaxes, π_g, from Tables I–III; the abbreviations used to designate the source of the individual trigonometric values are those given by Jenkins. Because of the large scatter in the trigonometric values, there is probably no star in Table IV that could be eliminated as a group member on

the basis of this comparison. It is noteworthy that of the 600 stars within 20 parsecs of the Sun for which radial velocities have been determined (Gliese 1957) eight per cent belong to the Hyades, ζ Herculis, ϵ Indi or 61 Cygni Groups.

The colour–luminosity array for the stars in Tables I–III is shown in Fig. 1, where the ζ Herculis, ϵ Indi and 61 Cygni Group members are indicated by crosses, open circles and filled circles, respectively. The standard main sequence (Eggen 1955) is shown with a half-width of $0^{m}\cdot2$. This colour–luminosity array

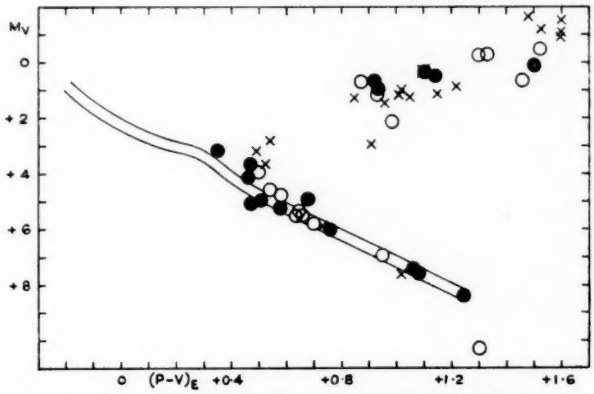

FIG. 1.—*Colour–luminosity array for stars in the ζ Herculis (crosses), ϵ Indi (open circles), and 61 Cygni (filled circles) Groups.*

is almost identical with that obtained from the members of the cluster M 67 (Johnson and Sandage 1955) and, indeed, nearly every group star in Fig. 1 can be matched in colour and in luminosity by a member of the M 67 cluster except for the five bright stars near $M_v \sim -1^{m}$ and $(P-V)_E \sim +1^{m}\cdot5$ to $+1^{m}\cdot6$, which occur in the groups but not in the cluster. These M-type giants, members of the ζ Herculis Group, are mainly known (irregular) or suspected light variables.

In the notation of a previous paper (Woolley and Eggen 1958) the galactic orbits of the members of these high-velocity groups are of class D, that is, the pericentric distances of the stars are between two-thirds and one-half of their present distances from the galactic centre.

I am greatly indebted to Mr J. Alexander, Miss L. Mather and Miss A. F. Heather for much computational assistance.

Royal Greenwich Observatory,
Herstmonceux Castle, Sussex:
1957 *December* 30.

References

Boss, B., 1912 *a*, *A.J.*, **27**, 33.
Boss, B., 1912 *b*, *A.J.*, **27**, 67.
Chaudhuri, P., 1940, *M.N.*, **100**, 574.
Eggen, O. J., 1955, *A.J.*, **60**, 407; *Lick Obs. Bull.* No. 539.
Eggen, O. J., 1958, *M.N.*, **118**, 65.
Evans, D. S., Menzies, A. and Stoy, R. H., 1957, *M.N.*, **117**, 534.
Gliese, W., 1957, *Astr. Rechen-Inst. in Heidelberg*, Mitt. Ser. A, No. 8.

Jenkins, L., 1952, *General Catalogue of Trigonometric Parallaxes*, Yale University Observatory.
Johnson, H. and Sandage, A., 1955, *Ap. J.*, **121**, 616.
Miczaika, G., 1940, *A.N.*, **270**, 249.
Oort, J., 1926, *Groningen Pub.* No. 40.
Rasmuson, N., 1921, *Medd. Lund*, Series II, No. 26.
Roman, N. G., 1955, *Ap.J. Supplement Series* **2**, No. 18.
Russell, H. N., 1912, *A.J.*, **27**, 96.
Wilson, R. E., 1953, *General Catalogue of Stellar Radial Velocities*, Carnegie Institution of Washington, Pub. No. 601.
Woolley, R. v. d. R. and Eggen, O. J., 1958, *M.N.*, **118**, 57.

XUM

THE VELOCITY ELLIPSOID OF Ao STARS

J. B. Alexander

(Communicated by the Astronomer Royal)

(Received 1957 December 28)

Summary

A kinematic average absolute magnitude of $+0^{m}\cdot14$ is derived for stars of spectral type Ao by comparing the line-of-sight velocities near the solar apex with the transverse velocities in a region of the sky 90° away. Assuming that every Ao star has the same absolute magnitude, the approximate distances can be found from the observed apparent magnitudes, and this method applied to 475 stars of this type brighter than $6^{m}\cdot5$ is used to obtain the equatorial linear components of velocity from the proper motions and the radial velocities. The solar motion and the constants of the velocity ellipsoid are evaluated, and the results are compared with those of other investigations. The galactic longitude of the major axis is found to be 354°, and the root-mean-squares of the peculiar velocities in the directions of the principal axes are 18·9 km/sec, 11·1 km/sec and 8·4 km/sec respectively.

---

1. ***Introduction.***—In any study of stellar motions it is always desirable to know the actual linear velocities of the stars concerned, and this requires a knowledge of the distances involved. This is only possible, in general, for nearby stars with well-determined trigonometric parallaxes. Reasonably accurate distances can be found from the apparent magnitudes if we are dealing with a sample of stars which has a small dispersion in absolute magnitude about a known mean value. The stars of type A would seem to satisfy this condition. Most previous investigations on the motions of this spectral class have been made using either proper motions alone or radial velocities alone since there are too few A stars with accurate trigonometric parallaxes to form a significant sample.

In making any statistical study of the movements of a group of stars, it is advantageous to use as homogeneous a set of observational material as possible. In Wilson's *General Catalogue of Stellar Radial Velocities* (1), from which the stars in this treatment are selected, we now have available a comprehensive collection of data reduced to a common system which is probably free from serious systematic error. Only Ao stars brighter than $6^{m}\cdot5$ are included in the present investigation. Types cAo and Aop are excluded as there is evidence to show that these have absolute magnitudes systematically brighter than those of the normal Ao class. Known visual binaries are also not considered. In the interests of homogeneity, the radial velocities and spectral classification are taken exclusively from Wilson.

The proper motions and apparent visual magnitudes used are those given in the Boss *G.C.* There may exist systematic errors in these proper motions which have a marked effect on the derived distributions of the linear components of velocity, but there is no simple way of allowing for these. On the other hand, corrections for accidental errors in the proper motions can easily be made.

There are some Ao stars brighter than $6^{m}\cdot5$ in the Southern Hemisphere which do not appear in Wilson, but this bias in the sampling probably has no serious effect on the final results.

2. *Previous investigations.*—In the various sections, reference is made to the papers listed below. In making any comparisons, due attention must be paid to differences in the spectral ranges of the samples.

Author	*Material used*
Nordström (**2**)	Radial velocities of 697 A-type stars brighter than $6^{m}\cdot0$.
Smart (**3**)	Radial speeds of 643 A stars in Schlesinger's *Catalogue of Bright Stars.*
MacRae and Nevin (**4**)	Radial velocities of 457 B8–A3 stars of average photovisual magnitude $6^{m}\cdot9$.
Wilson and Raymond (**5**)	Proper motions of 4457 *G.C.* stars of spectral type B7–A4 and brighter than $7^{m}\cdot05$.
Delhaye (**6**)	Proper motions of 5089 stars of spectral type B8–A5 and magnitudes between $6^{m}\cdot0$ and $7^{m}\cdot5$.

3. *Absolute magnitude.*—With the usual notation, the equatorial linear components of velocity of a star with coordinates (α, δ) are given by the relations below

$$\left.\begin{aligned} u &= -(\kappa\mu_\alpha/p)\sin\alpha\cos\delta - (\kappa\mu_\delta/p)\cos\alpha\sin\delta + R\cos\alpha\cos\delta \\ v &= (\kappa\mu_\alpha/p)\cos\alpha\cos\delta - (\kappa\mu_\delta/p)\sin\alpha\sin\delta + R\sin\alpha\cos\delta \\ w &= (\kappa\mu_\delta/p)\cos\delta + R\sin\delta \end{aligned}\right\} . \qquad (1)$$

If p is the parallax in seconds, R the radial velocity in km/sec and μ_α and μ_δ are measured in seconds of arc per annum, then the value of κ is about $4\cdot74$.

The parallaxes can be found from the apparent magnitudes only if the absolute magnitudes are known. It is assumed that there exists some average absolute magnitude M_0 which when assigned to every Ao star yields reasonable parallaxes for statistical purposes.

To determine M_0, a trial value of $+0^{m}\cdot5$ is taken. With this figure, the values of u, v and w can be calculated from equations (1) for any star. Two regions are considered.

For 54 stars in an area surrounding the solar apex (the exact direction of the solar motion is not critical for this purpose), the arithmetic means of the equatorial linear components are as follows

$$\bar{u} = -2\cdot6 \text{ km/sec}; \qquad \bar{v} = +15\cdot7 \text{ km/sec}; \qquad \bar{w} = -8\cdot2 \text{ km/sec}.$$

These systematic velocities caused by the solar motion are in this case dependent mostly on the radial velocity data with little weight attached to the proper motions. Hence an exact choice of M_0 is not important in obtaining $\bar{u}$, $\bar{v}$ and $\bar{w}$ for this group of stars.

A similar procedure is performed for 54 stars lying in a belt 90° away from the apex. The corresponding values are

$$\bar{u} = 0\cdot0 \text{ km/sec}; \qquad \bar{v} = +15\cdot1 \text{ km/sec}; \qquad \bar{w} = -5\cdot3 \text{ km/sec}.$$

Here, the means of the velocities depend critically on the choice of M_0. By adjusting M_0 such that $\bar{u}^2+\bar{v}^2+\bar{w}^2$ is the same for both regions, the average

absolute magnitude of the Ao stars in Wilson is obtained. After allowance is made for the small effects of galactic rotation on the systematic motions of stars in a given region, it is found that

$$M_0 = +0^m{\cdot}14 \pm 0^m{\cdot}25.$$

The above value of M_0 is used throughout this paper. The following estimates of absolute magnitude as a function of spectral type and luminosity class are taken from a table obtained by Keenan and Morgan (7). The results are derived from a study of cluster motions and trigonometric parallaxes. Considering that

TABLE I

Type	Main Seq.	Subgiants	Giants		Supergiants	
	V	IV	III	II	Ib	Ia
B8	−0·5	−1·7	−3·0	−4·3	−5·5	−7·0
B9	0·0	−1·0	−2·0	−3·8	−5·5	−7·0
Ao	+0·3	−0·4	−1·1	−3·0	−4·8	−7·0
A2	+1·2	+0·2	−0·7	−2·7	−4·7	−7·0
A3	+1·8	+1·0	−0·3	−2·5	−4·6	−7·0

the majority of Ao stars are placed in luminosity class V, there is no contradiction with the value of M_0 found kinematically.

4. *Solar motion.*—With M_0 taken to be $+0^m{\cdot}14$, the values of u, v and w are evaluated from equations (1) for each of the 475 stars. The components U_0, V_0 and W_0 of the solar motion with respect to a group of N stars are determined from the relations

$$NU_0 = -[u]; \qquad NV_0 = -[v]; \qquad NW_0 = -[w].$$

(Throughout this paper, square brackets denote summation with respect to the appropriate group of stars.) The values of U_0, V_0 and W_0 for the 475 stars are given in row A of Table II below. If 117 stars with velocities greater than 35 km/sec with respect to the standard of rest defined by A are excluded, then we obtain the results B for the remaining 358 stars. Finally, if instead of using arithmetic means to find U_0, V_0 and W_0 we take median counts of the 475 stars, then we derive the values C. The solar motion is taken to be that defined by B.

TABLE II

	U_0 (km/sec)	V_0 (km/sec)	W_0 (km/sec)
A	+0·8	−16·2	+9·2
B	+1·1	−16·5	+8·3
C	+0·6	−17·5	+8·1

These components correspond to a velocity of $18{\cdot}5 \pm 1{\cdot}6$ km/sec towards the following apex (1950):

$$\alpha_0 = 273^\circ{\cdot}8 \pm 2^\circ{\cdot}2; \qquad \delta_0 = +26^\circ{\cdot}6 \pm 2^\circ{\cdot}0.$$

With respect to galactic coordinates the corresponding values are

$$l = 21^\circ{\cdot}4; \qquad b = +17^\circ{\cdot}5 \text{ (Lund pole).}$$

The galactic linear components of the solar motion are

$$X_0 = +16{\cdot}4 \text{ km/sec}; \qquad Y_0 = +6{\cdot}4 \text{ km/sec}; \qquad Z_0 = +5{\cdot}6 \text{ km/sec}.$$

The zero of galactic longitude is defined in terms of essentially local characteristics. For general purposes, it is more convenient to take axes determined by the position of the centre of the galaxy in galactic longitude 328°. Consider two axes ξ and η in the directions ($l=148°$, $b=0°$) and ($l=58°$, $b=0°$) respectively. Then the components of the solar motion in these directions are

$$\dot{\xi}_0 = -10{\cdot}5 \text{ km/sec}; \qquad \dot{\eta}_0 = +14{\cdot}2 \text{ km/sec}.$$

For a group of stars randomly distributed over the celestial sphere, the first-order terms of galactic rotation have no effect on the derived constants of the solar motion. The sample of Ao stars, besides exhibiting a marked concentration towards the plane of the galaxy, tends to show a deficiency of stars for an area in the Southern Hemisphere compared with the diametrically opposite northern region. This latter irregularity has some effect on the systematic means of the velocities, but as a rough estimate puts the resultant errors in X_0 and Y_0 at less than 0·2 km/sec, no attempt is made to allow for this in obtaining the components of the solar motion. As with previous authors, galactic rotation is again ignored when the constants of the velocity ellipsoid are obtained.

From the radial velocities of 874 stars of which about 54 per cent are of type A, MacRae and Nevin obtain an apex at (270°, +36°). With this direction assumed, the magnitude of the solar motion with respect to the A stars alone is found to be 18·37 ± 1·11 km/sec. Nordström obtains a value of 16·3 ± 0·9 km/sec towards (263°·8, +22°·2) for his A stars, although the corresponding velocity for the B8–B9 group is as high as 21·2 km/sec.

From proper motions alone, Wilson and Raymond place the apex at (270°·2 ± 1°·3, +26°·0 ± 1°·2).

5. *Axes of velocity ellipsoid.*—The existence of such groups as the Taurus and Ursa Major clusters shows that the distribution of the peculiar velocities of the Ao stars in the neighbourhood of the Sun cannot be represented by any simple mathematical expression. Suppose, however, adopting Schwarzschild's ellipsoidal hypothesis, that the velocities of our sample can be represented reasonably well by a frequency function of the form

$$\exp\{-(aU^2+bV^2+cW^2+2fVW+2gUW+2hUV)\}.$$

This is later seen to be a plausible assumption when it is found in Section 7 that the histograms of the velocities in the three directions do not depart appreciably from the corresponding Gaussian forms. With an ellipsoidal distribution, steady-state theory applied to the rotating galaxy demands that the axis of greatest mobility for components in the galactic plane is directed towards the galactic centre. Previous work indicates a significant deviation of the observed axes of the velocity ellipsoid of A stars from their "equilibrium" position.

In this section, let (U, V, W) be the peculiar components of equatorial linear velocity of a star found by adding the values (U_0, V_0, W_0) derived in Section 4 to the corresponding components (u, v, w) relative to the Sun evaluated from equations (1). Consider the direction whose direction-cosines with respect to equatorial axes are (l, m, n). The the sum S of the squares of the components of peculiar velocity in this direction is $[(lU+mV+nW)^2]$, where as before the square brackets denote summation. Using Lagrange's Method of Undetermined Multipliers, we obtain the following equations for the directions in which S has

stationary values.

$$\left.\begin{aligned}([U^2]-\lambda)l+[UV]m+[UW]n&=0\\ [UV]l+([V^2]-\lambda)m+[VW]n&=0\\ [UW]l+[VW]m+([W^2]-\lambda)n&=0\\ l^2+m^2+n^2&=1\end{aligned}\right\} \qquad (2)$$

(λ is the undetermined multiplier).

Denote by Δ the determinant

$$\begin{vmatrix}([U^2]-\lambda) & [UV] & [UW]\\ [UV] & ([V^2]-\lambda) & [VW]\\ [UW] & [VW] & ([W^2]-\lambda)\end{vmatrix}.$$

Then each of the three roots of the cubic in λ, $\Delta=0$, when in turn substituted in equations (2), gives a set of values (l, m, n) corresponding to a direction in which S has a stationary value. The situation is analogous to that of the inertia tensor in rigid-body dynamics. Corresponding to the inertia quadric we have in this case the quadric

$$[U^2]x^2+[V^2]y^2+[W^2]z^2+2[VW]yz+2[UW]xz+2[UV]xy=1,$$

and by the above method we are in fact locating the principal axes of this. The process therefore yields three mutually perpendicular directions whatever the distribution of the peculiar velocities may in fact be. In particular, if we are considering the ellipsoidal form

$$\exp\{-(aU^2+bV^2+cW^2+2fVW+2gUW+2hUV)\}$$

then the stationary values of S occur in the directions of the principal axes of the velocity ellipsoid.

The equatorial (1950) and galactic coordinates of the directions found by the above method applied to the 475 stars are given in the first three rows of Table III below. If 131 stars with peculiar speeds greater than 30 km/sec are ignored, the axis of greatest mobility is moved about 12° further away from the direction of the galactic centre. The results for the remaining 344 stars are given in the last three rows. No attempt is made to identify individual stars as members of clusters, but the above restriction should remove, for instance, all likely Taurus members and about half of the Ursa Major group present in the original sample.

TABLE III

	α (1950)	δ (1950)	l	b
	°	°	°	°
x	279·8	− 6·7	353·6	− 2·4
y	358·3	+59·5	83·8	− 2·2
z	193·6	+29·6	36·0	+86·8
x'	286·5	+ 3·3	5·7	− 3·6
y'	22·4	+61·0	95·7	− 0·7
z'	194·6	+28·7	17·1	+86·3

The galactic longitudes of the major axis of the velocity ellipsoid according to other authors are as follows:

Nordström	357°·9 ± 7°·3
Smart	14°
MacRae and Nevin (First Method)	342°·3 ± 10°·7
MacRae and Nevin (Second Method)	353° ± 15°
Delhaye	351°·2 ± 2°·3

6. *Magnitude dispersion.*—In Section 5, it is assumed that the absolute magnitude of an A0 star is $+0^{m}\cdot14$. Errors in the directions of the axes of the ellipsoid found by this analysis result from the fact that the true average absolute magnitude may differ considerably from the above figure and that the individual stellar luminosities have a spread about their mean. Interstellar absorption in the visual wave-lengths will cause further discrepancies, although the error in the derived value of M_0 due to this tends to reduce the effect on a given star. It will be assumed that the frequency function $f(M)$ of the true absolute magnitudes is independent of the position and motion of a star. Firstly, consider motion in the U-component. Suppose we have a group of stars so situated that U is derived from proper motions alone (i.e. the stars are in a belt 90° away from the U-axis). Let the true distance of a star assumed to be at distance d' be d, where $d'=dt$. Then t has a certain frequency function $g(t)$ which is independent of the position and motion of a star, since $g(t)$ is dependent solely on the form of $f(M)$. For a star with velocity U, the motion relative to the Sun is $U-U_0$, where U_0 is the component of the solar motion. We interpret this motion to be $t(U-U_0)$ relative to the Sun. If we use $U_0+\delta U_0$ for the value of the component of the solar motion, we write down $t(U-U_0)+U_0+\delta U_0$ for the star's component of peculiar velocity.

Now the directions of the axes of the ellipsoid found in Section 5 are a function of the quantities $[U^2]$, $[V^2]$, $[W^2]$, $[VW]$, $[UW]$ and $[UV]$. In fact, only the ratios of these six numbers are significant for our purpose. Consider the term $[U^2]$. We form $[U^2]'$ given by the equation

$$[U^2]'=[\{t(U-U_0)+U_0+\delta U_0\}^2]=[\{tU+(1-t)U_0+\delta U_0\}^2].$$

From the definition of the solar motion, we have

$$[U]=0.$$

There is good evidence from comparison with other results that δU_0 is small, and this term is neglected. We thus have the relation

$$[U^2]'=[t^2U^2]+[(1-t)^2U_0^2]$$

i.e.
$$[U^2]'=\frac{1}{N}\int_0^\infty g(t)t^2\,dt[U^2]+\int_0^\infty g(t)(1-t)^2\,dtU_0^2. \qquad (3)$$

We are, in practice, concerned with stars distributed over the whole sky. We shall suppose that equation (3) still holds if $g(t)$ is replaced by $g'(t)$, a function which allows for the fact that the part of the U-component derived from radial velocities is unaffected by magnitude dispersion. The function $g'(t)$ depends on the distribution of the sample of stars relative to the U-axis. We shall assume that equations similar to (3) apply to the V and W components with the same function $g'(t)$ inserted in place of $g(t)$. Define k and l by the two relations

$$k=\int_0^\infty g'(t)(1-t)^2\,dt \Big/ \int_0^\infty g'(t)t^2\,dt$$

$$l=N\Big/\int_0^\infty g'(t)t^2\,dt.$$

We then have the following equations for a group of N stars:

$$\left.\begin{aligned}[U^2]&=l[U^2]'-kNU_0^2\\ [V^2]&=l[V^2]'-kNV_0^2\\ [W^2]&=l[W^2]'-kNW_0^2.\end{aligned}\right\}$$

Similarly, we obtain

$$\left.\begin{aligned}[VW]&=l[VW]'-kNV_0W_0\\ [UW]&=l[UW]'-kNU_0W_0\\ [UV]&=l[UV]'-kNU_0V_0.\end{aligned}\right\} \qquad (4)$$

Hence, for a given set of $[U^2]'$, $[V^2]'$, $[W^2]'$, $[VW]'$, $[UW]'$ and $[UV]'$, we can correct for the effects of magnitude dispersion on the directions of the axes if we know the value of k/l, where

$$k/l = \frac{1}{N}\int_0^\infty g'(t)(1-t)^2\,dt.$$

If the absolute magnitudes follow a distribution of the form $\exp\{-h|M-M_1|\}$ about some value M_1, where $M_1 - M_0 = 5\log_{10}\beta$, then we have

$$g(t) = \tfrac{1}{2}N\alpha t^{\alpha-1}\beta^{-\alpha} \qquad (t \leqslant \beta)$$

$$g(t) = \tfrac{1}{2}N\alpha t^{-\alpha-1}\beta^{\alpha} \qquad (t > \beta)$$

(where $\alpha = 5h\log_{10} e = 2{\cdot}1715h$). The values of

$$\frac{1}{N}\int_0^\infty g(t)(1-t)^2\,dt$$

for various α are given in Table IV. The last two columns correspond to the two values of M_1 for which $|M_1 - M_0| = 0^m{\cdot}25$.

TABLE IV

α	$\beta = 1$	$\beta = 1{\cdot}122$	$\beta = 0{\cdot}891$
10·0	0·02	0·04	0·03
7·0	·05	·08	·05
5·0	·11	·16	·09
4·0	·20	·29	·16
3·0	·55	0·74	·42
2·7	0·90	1·19	0·69
2·5	1·40	1·83	1·08
2·3	2·63	3·40	2·06

The corresponding values of

$$\frac{1}{N}\int_0^\infty g'(t)(1-t)^2\,dt$$

will be somewhat less, the exact values depending on the distribution of the stars concerned. If the value of k/l is $\frac{1}{6}$, we find from equations (2) and (4) that the galactic coordinates of the axes of the ellipsoid for the 475 stars are

l	b
348°·1	− 5°·3
79°·1	− 10°·2
50°·7	+ 78°·5

If k/l is $\frac{1}{3}$, the corresponding longitude of the major axis is 343°. The minor axis is tilted as much as $22\frac{1}{2}$° away from the Galactic Pole, but it is unlikely that this is really the case. If we stipulate that the galactic latitude of the true minor axis is greater than 75° and that $|M_1 - M_0|$ is less than $0^m{\cdot}25$, we must have that α is greater than 3. This value of α corresponds to a standard deviation in the absolute magnitudes about M_1 of about $1^m{\cdot}0$.

The above analysis is rough, but it is expected that it simulates the effects of magnitude dispersion to a large extent.

7. *Velocity distributions.*—We shall take axes *Oxyz* defined by the principal directions found in Section 5, viz.

	α (1950)	δ (1950)
x	279°·8	− 6°·7
y	358°·3	+59°·5
z	193°·6	+29°·6

The peculiar components of velocity in these directions are computed for each star. The velocity distributions taken without regard to sign are given in Tables V, VI and VII. In each case, the Gaussian distribution with the same median velocity is quoted for comparison.

TABLE V

X velocity (km/sec)	Number of Ao stars	Gaussian distribution
0–5	114½	97
5–10	87	91
10–15	61½	79½
15–20	57	65
20–25	40	50
25–30	50½	35½
30–35	24½	24
35–40	16½	15
40–45	11½	9
45–50	5	5
50–55	3	2½
55–60	1	1
60–65	2	½
65+	1	½

The median velocity is 13·0 km/sec.

TABLE VI

Y velocity (km/sec)	Number of Ao stars	Gaussian distribution
0–5	160	157
5–10	128	131
10–15	87	91½
15–20	41	53½
20–25	33½	26
25–30	14½	10½
30–35	4	3½
35–40	2	1
40–45	½	0
45+	4½	0

The median velocity is 7·9 km/sec.

TABLE VII

Z velocity (km/sec)	Number of Ao stars	Gaussian distribution
0–5	199½	196½
5–10	149½	147
10–15	68	83
15–20	31½	34½
20–25	16	11
25–30	3½	2½
30–35	4	½
35–40	2½	
40–45	½	
45+	0	

The median velocity is 6·2 km/sec.

In order to derive the constants of the velocity distributions, the median is to be preferred to other mean values since it is less affected by the presence of an excess of high-velocity stars. The medians and actual root-mean-squares of the velocities in the directions of the principal axes are given below. In the third row, the root-mean-square of a Gaussian distribution with the same median velocity as the actual distribution is in each case quoted.

	X	*Y*	*Z*
Median (km/sec)	13·0	7·9	6·2
Actual r.m.s. (km/sec)	20·3	13·4	10·1
Gaussian r.m.s. (km/sec)	19·3	11·7	9·2

Allowance can be made for accidental errors in the radial velocity and proper-motion data. The probable error of a radial velocity determination is taken to be 2·5 km/sec (**8**). The probable errors of the transverse velocities due to inaccuracies in the proper motions can be evaluated from the corresponding angular errors given in Boss. An average value of 2·5 km/sec is obtained for the sample of Ao stars taken. Correcting for these observational errors, we obtain the following median velocities:

	X	*Y*	*Z*
Median (km/sec)	12·8	7·5	5·7

The corresponding root-mean-squares δ_x, δ_y and δ_z are derived on the assumption that the distributions are strictly Gaussian. In Table VIII these values are compared with previous determinations. Smart assumes that the two minor axes are equal.

TABLE VIII

Author	δ_x km/sec	δ_y km/sec	δ_z km/sec	δ_y/δ_x	δ_z/δ_x
Present	18·9	11·1	8·4	0·59	0·44
MacRae and Nevin	14·8	9·1	9·4	·61	·64
Smart	19·9	11·8	–	·61	–
Nordström	17·1	12·4	8·5	·73	·50
Delhaye	–	–	–	0·63	0·51

The values of δ_x, δ_y and δ_z found by the present method depend on the choice of M_0. Since the solar motion and the components of velocity of the stars relative to the Sun are derived from both proper motions and radial velocities, the effect of an error in M_0 on the distribution of the peculiar velocities is not straightforward. The individual variations in absolute magnitude will also alter the derived components relative to the Sun, and the errors in the peculiar velocities will tend to be greater for directions in which the component of the solar motion is large.

The root-mean-squares of the components in the directions ξ and η (defined in Section 4) are found to be 17·7 km/sec and 12·9 km/sec respectively.

8. In Fig. 1, the projections of the peculiar velocities on the galactic plane are shown. The horizontal axis corresponds to the direction of greatest mobility (in galactic longitude 354°) found in Section 5. Ten of the Ao stars have velocities which fall outside the limits of the figure.

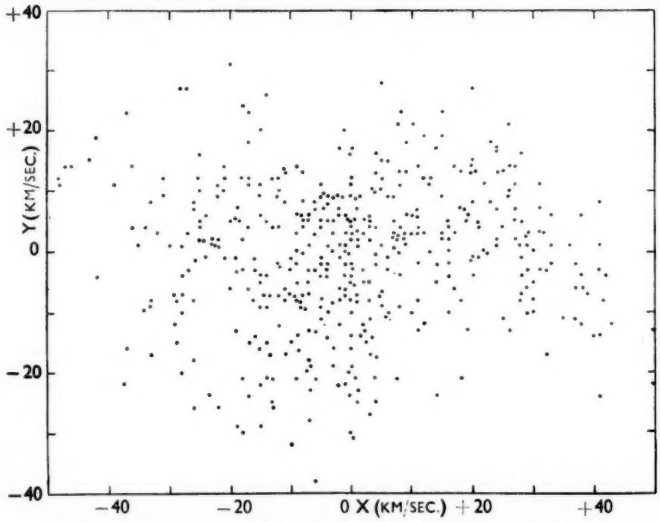

FIG. 1.—*The projections of the peculiar velocities on the galactic plane.*

9. *Conclusion.*—The results for the solar motion are in reasonable agreement with previous work,[1] and this is additional confirmation that the value of M_0 used is near the true figure. The vertex deviation of the velocity ellipsoid found by previous authors is confirmed, and there is evidence to show that this is increased rather than decreased by the removal of the high-velocity members. The ratio of δ_z to δ_x is low compared with other determinations. This may be due to the fact that magnitude dispersion has less effect in the z-direction, for which the component of the solar motion is small, than in the x-direction.

This work was carried out under the supervision of Dr R. v. d. R. Woolley, to whom the writer is greatly indebted for continual advice and discussion. Thanks are also due to Mrs V. A. J. Mitchell, who performed some of the calculations.

Royal Greenwich Observatory,
Herstmonceux Castle, Sussex:
1957 *October.*

References

(1) R. E. Wilson, *General Catalogue of Stellar Radial Velocities*, Carnegie Institute of Washington, Publication 601, 1953.
(2) H. Nordström, *A Study of Stellar Motions Based on Radial Velocities*, *Meddel. Lund Astron. Obs.*, Ser II, No. 79, 1936.
(3) W. M. Smart, *M.N.*, **99**, 61, 1938.
(4) D. A. MacRae and S. Nevin, *A.J.*, **53**, 120, 1948.
(5) R. E. Wilson and H. Raymond, *A.J.*, **47**, 49, 1938.
See also E. T. R. Williams, *A.J.*, **48**, 84, 1939.
(6) A. Delhaye, *Bull. Ast.*, **16**, 1–84, 1951. A summary of this appears in *C.R. Acad. Sci. Paris*, **233**, 1422–4, 1951. See also A. Delhaye, *Bull. Ast.*, **16**, 221–261, 1952.
(7) P. C. Keenan and W. W. Morgan; from J. A. Hynek (ed.), *Astrophysics*, 1st. edn., p. 23, McGraw-Hill, 1951.
(8) See R. v. d. R. Woolley, *M.N.*, **117**, 210, 1957.

XUM

THE CLUSTER SYSTEM OF THE SMALL MAGELLANIC CLOUD

E. M. Lindsay

(Received 1958 January 3)

Summary

A cluster survey of the Small Magellanic Cloud has been completed using the ADH telescope and 30^m exposure 103a.O plates. Altogether 116 objects are regarded as Cloud clusters. These extend to the wing of the Cloud. Apparent magnitudes have been estimated on 10-inch Metcalf plates. The cluster system gives dimensions of 8000 parsecs for the longest diagonal (including the wing) and 5400 parsecs for the smallest diagonal. There seems no evidence of spiral structure in the cluster distribution.

Material for the Catalogue.—A previous paper (**1**), to be referred to as Paper I, contains a list of ninety-four objects which were considered to be clusters in the Small Magellanic Cloud. A further thirty-two objects, contained in Table II of this paper, were regarded as possibly clusters. The material was obtained from ADH plates of long exposure centred on the Cloud at R.A. 0^h35^m, Dec. $-72°{\cdot}8$ and one short exposure plate of 10^m centred at 0^h51^m, $-73°{\cdot}0$. Further material is now available for the outlying regions of the Cloud. This consists of ADH plates, types 103a.O and 103a.E, of 30^m exposures. The plates overlap so as to provide checks on doubtful objects. They cover an area around the Cloud such that clusters outside of this could not with certainty be regarded as Cloud members. On the eastern side the programme ties up with a similar one, now nearly completed, on the Large Cloud.

It is considered that Nos. 1, 3, 14, 28, 30, 31 and 32 of Table II, Paper I, should, in the light of the new material, be accepted as certainly clusters. All of these had been listed by the writer as probably clusters. The last three were on the 10^m exposure plate referred to above. The last one is No. 5 of Table II of Jenka Mohr's list (**2**) of outlying clusters of the Small Cloud found on long-exposure Bruce plates. Seven objects are contained in this Table. Six of these have been verified as clusters on the new ADH plates. No. 4 has not been verified; in its position is an object which is almost certainly a galaxy. Miss Mohr had described this as "hazy; somewhat doubtful as cluster" and it has been omitted from the present list.

In addition to this total of twelve verified objects, ten new clusters have been found, most of which are distant from the main body of the Cloud. Table I *a* gives their number, approximate positions (1900), diameters to the nearest five parsecs and remarks. Table I *b* gives the same data for Jenka Mohr's outlying clusters, her No. 4 being excluded. The diameters were derived from estimated angular diameters on ADH plates, using de Vaucouleurs' distance (**3**) of 46 kiloparsecs.

A note by de Vaucouleurs (**4**) on No. 7 (NGC 643), suggesting it was probably a Cloud member, appeared after the writer had included it in the above list but had not associated it with NGC 643. On a 30^m exposure ADH 103a.O plate

it is a conspicuous object, clearly recognizable as a cluster with 20–30 faint resolved stars. The texture and distribution of the outlying stars suggest it is globular; otherwise it would have been classified as certainly open.

TABLE I *a*

New clusters in the Small Magellanic Cloud

No.	R.A. (1900) h m	Dec. (1900) ° ′	d (parsecs)	Remarks
1	00 18·4	−75 37·4	5	Open.
2	00 43·4	69 28·3	5	Open; faint, poor; the most northerly cluster found.
3	00 45·0	70 26·1	10	Open; faint, poor.
4	01 23·2	73 53·9	75	Open; nebulosity; stellar association with Nos. 101 and 103.
5	01 28·8	76 34·7	5	Open; faint, poor.
6	01 31·5	74 40·4	5	Open.
7	01 33·5	76 04·4	25	Possibly globular, bright; stars resolved; NGC 643
8	01 34·5	75 58·5	5	Open; very faint, poor.
9	01 48·9	74 50·9	5	Open; very compact.
10	01 55·5	78 08·6	5	Open; the most southerly and with No. 7, Table I *b*, the most easterly cluster found.

TABLE I *b*

Miss Mohr's outlying clusters in the Small Cloud (No. 4 omitted)

No.	R.A. (1900) h m	Dec. (1900) ° ′	d (parsecs)	Remarks
1	23 58·9	−74 01·9	45	Circular, possibly globular. Many stars resolved. The most westerly known cluster of the Cloud.
2	01 01·1	70 52·9	5	Open; poor.
3	01 29·5	72 28·0	10	Open.
5	01 32·2	73 22·7	10	Open.
6	01 47·9	74 13·3	30	Circular, possibly globular. Stars resolved.
7	01 55·5	74 42·1	5	Open; very compact.

Table II of Paper I contained thirty-two objects which were considered to be possible clusters; as mentioned above, seven of these have now been included as certain, leaving twenty-five. On the new material there are an additional fourteen objects which resemble clusters, most of which are near the limit of the plates. Their positions are listed in Table II of the present paper. None of these possible clusters has been included in the Catalogue of Table III.

TABLE II

Additional possible clusters in the Small Magellanic Cloud

No.	R.A. (1900) h m	Dec. (1900) ° ′	No.	R.A. (1900) h m	Dec. (1900) ° ′
1	00 09·2	−70 36·0	8	01 09·5	−75 42·9
2	00 14·8	75 07·1	9	01 09·9	71 29·6
3	00 29·7	74 11·3	10	01 20·5	75 31·6
4	00 33·5	71 17·1	11	01 32·3	72 53·6
5	00 43·6	76 21·7	12	01 39·3	71 39·9
6	01 04·3	72 23·8	13	01 40·2	71 46·9
7	01 04·4	71 08·1	14	01 40·9	73 51·1

The Catalogue.—With the clusters of Table I of Paper I, those of Table II of the same paper regarded as certain, and the above objects of Table I *a* and I *b*, 116 objects are now considered to be clusters of the Small Cloud. To avoid confusion these have been collected in Table III and renumbered in order of right ascension (1900). The right ascensions and declinations are approximate, being obtained with reference to stars of known positions plotted on squared paper. The fourth column gives the apparent photographic magnitudes as determined on MF (10-inch Metcalf refractor) plates. In some cases it was impossible to make any estimate of magnitude. The fifth column gives the diameters in minutes of arc. The last column gives a reference to published lists: I and II refer to Tables I and II of Paper I; I *a* and I *b* to Tables I *a* and I *b* above; K to Kron's list (**5**); the Shapley–Miss Wilson numbers (**6**) are those of HC 275 and 276; NGC or IC numbers are in brackets.

TABLE III

Catalogue of clusters in the Small Magellanic Cloud

No.	R.A. (1900) h m	Dec. (1900) ° ′	m_{pg}	d'	Reference
1	23 58·9	−74 01·9	11·7	4·1	Ib1
2	00 08·2	74 02·7	16·0	4·5	II1
3	00 13·8	74 52·4	15·5	5·7	I1
4	00 18·2	74 18·3	13·9	13·6	I2; K1; 276/80
5	00 18·4	75 37·4	15·7	4·5	Ia1
6	00 18·5	74 13·4	15·3	6·8	I4; K4
7	00 20·1	74 18·7	13·2	11·3	I6; K5; 276/82
8	00 20·3	73 21·1	11·6	20·4	I5; K3; 276/81
9	00 21·1	74 37·8	14·7	4·5	I7; K6; 276/84
10	00 22·4	72 05·5	11·1	6·8	I3; K2; (121)
11	00 23·3	73 20·7	14·0	10·2	I8; K7; 276/85
12	00 23·7	73 51·8	15·0	6·8	I9; K8; 276/86
13	00 25·8	73 56·6	15·3	7·9	I10; K9
14	00 28·4	73 09·5	15·3	5·7	I12
15	00 28·8	73 41·8	11·9	13·6	I11; K10; (152)
16	00 31·8	73 43·6	11·9	11·3	I14; K12; (176)
17	00 31·8	74 09·6	—	13·6	I15; K13; 276/95
18	00 33·1	73 33·3	—	26·1	I16; K14
19	00 33·9	74 27·7	—	11·3	II3
20	00 34·2	73 02·1	14·8	5·7	I13; K11; 276/94
21	00 35·3	73 16·1	13·5	5·7	I17; K15; 275/2
22	00 36·6	73 56·3	11·7	11·3	I20; K18; (220)
23	00 36·7	73 18·4	15·4	3·4	I18; K16; 276/98
24	00 36·7	73 56·6	11·7	5·7	I21; K19; (222)
25	00 37·1	73 54·7	11·8	9·1	I23; K20; (231)
26	00 37·4	73 08·2	12·7	6·8	I19; K17; 275/3
27	00 38·3	73 27·1	11·9	13·6	I22; K21; 276/100
28	00 39·5	73 08·5	13·6	4·5	I24; 275/4
29	00 39·9	73 59·1	12·1	9·1	I25; K22; (242)
30	00 42·3	74 02·7	12·0	4·5	I26; K23; (256)
31	00 43·2	73 15·8	13·9	3·4	I27; 275/11
32	00 43·4	69 28·3	—	3·4	Ia2
33	00 44·0	73 21·6	14·3	3·4	I28; 275/14
34	00 44·0	74 01·0	11·9	7·9	I29; K24; (265)
35	00 44·1	74 01·3	13·5	3·4	I30; K25; 276/117
36	00 44·6	74 26·6	13·3	4·5	I32; K27; 276/119

TABLE III (*continued*)

No.	R.A. (1900) h	m	Dec. (1900) °	′	m_{pg}	d'	Reference
37	00	44·9	−74	04·0	12·2	4·5	I31; K26 (269)
38	00	45·0	70	26·1	16·2	9·1	Ia3
39	00	45·5	73	54·1	11·8	17·0	I33; 275/18
40	00	47·1	73	29·1	12·3	12·5	I34; 276/133
41	00	47·6	73	15·0	13·1	4·5	I35; 275/27
42	00	47·7	73	41·0	11·9	5·7	I36; (290)
43	00	48·3	72	32·5	11·9	10·2	I37; K28; 275/30
44	00	48·4	73	28·9	12·8	9·1	I38; K29; 275/32
45	00	49·1	72	43·2	12·7	11·3	I39; K30; 276/139
46	00	49·5	73	24·9	—	11·3	I40; K31; 276/141
47	00	49·6	73	53·3	12·7	9·1	I41
48	00	49·8	71	56·7	11·9	7·9	I42; 275/42
49	00	50·4	72	42·4	11·7	5·7	I43; K32; (299)
50	00	51·3	72	44·9	12·5	4·5	I44; K33; (306)
51	00	51·5	72	39·2	11·8	13·6	I45
52	00	52·0	74	01·7	13·7	3·4	I46; (156)
53	00	52·1	73	23·2	12·7	7·9	I47; K34; 275/51
54	00	52·8	73	01·0	7·4	20·4	I48; K35; (330)
55	00	53·4	74	26·7	14·9	7·9	II14; 275/53
56	00	54·1	72	49·0	11·5	4·5	I49; 275/55
57	00	54·4	73	57·2	—	23·8	I52; K38; 276/165
58	00	54·6	74	52·2	14·1	5·7	I51; K37; 276/164
59	00	54·6	75	01·0	12·0	17·0	I50; K36; (339)
60	00	55·7	72	43·5	—	28·3	I53; K39; (346)
61	00	56·4	72	52·6	12·1	9·1	I54; K40; (1611)
62	00	56·6	72	54·9	12·1	10·2	I55; K41; (1612)
63	00	57·2	72	54·3	12·3	4·5	I56; K42; 275/63
64	00	57·7	73	52·7	13·5	4·5	I57; K43; 276/175
65	00	57·8	73	17·0	13·4	9·1	I58; 276/180
66	00	58·6	73	05·7	11·9	5·7	I60; 275/65
67	00	58·9	72	08·9	12·0	17·0	I62; K46 (361)
68	00	59·0	74	27·0	11·9	17·0	I59; K44; 276/184
69	00	59·7	74	15·9	14·9	3·4	I61; K45; 275/67
70	00	59·9	72	48·6	12·3	3·4	I63; K47; 275/69
71	01	00·1	72	36·7	—	79·3	I64; K48; (371)
72	01	00·6	73	21·5	11·8	7·9	I65; K49
73	01	01·1	70	52·9	15·5	4·5	Ib2
74	01	01·2	72	41·9	12·3	5·7	I66; K50; 275/72
75	01	01·9	72	31·7	—	17·0	I67; K51; (395)
76	01	02·1	72	34·5	12·5	6·8	I68; K52; (1624)
77	01	03·1	73	49·5	13·0	5·7	I69; K53; (1626)
78	01	03·7	72	13·4	13·0	11·3	I73; 276/214
79	01	03·7	72	48·3	12·0	5·7	I70; K54; 275/75
80	01	04·3	73	18·0	13·7	9·1	I72; 276/212
81	01	04·6	72	38·8	14·1	5·7	I71; K55; 276/211
82	01	04·7	72	17·8	11·0	12·5	I77; K60; (411)
83	01	05·1	72	52·8	12·0	11·3	I76; K59; (416)
84	01	05·3	72	31·2	—	11·3	I78; 275/79
85	01	05·3	73	24·7	10·2	22·7	I75; K58; (419)
86	01	05·3	73	47·1	14·5	5·7	I74; K57; 276/218
87	01	06·3	72	17·4	12·7	4·5	I79; K62; (422)
88	01	07·8	73	19·0	13·7	3·4	I80; K63; 276/225
89	01	09·5	72	16·7	12·7	9·1	I85; K64; (1660)
90	01	09·8	71	51·2	12·5	10·2	I83; (1655)

TABLE III (*continued*)

No.	R.A. (1900) h m	Dec. (1900) ° ′	m_{pg}	d'	Reference
91	01 09·8	−73 37·7	14·8	5·7	I82; 276/230
92	01 09·8	73 58·3	13·7	4·5	I81; (1662)
93	01 10·0	73 59·5	—	5·7	II28; 276/228
94	01 11·2	73 48·1	—	22·7	I84; K65; (456)
95	01 11·8	71 52·0	14·3	2·3	II30
96	01 11·9	72 04·3	10·5	12·5	I89; K69; (458)
97	01 12·0	72 49·8	—	9·1	I86; K66; (460)
98	01 12·7	73 08·7	14·9	4·5	I88; K68; 276/235
99	01 13·1	73 51·0	—	90·7	I87; K67; (465)
100	01 15·5	72 31·2	14·5	4·5	I90
101	01 21·9	73 40·5	—	68·0	I91
102	01 22·1	71 42·3	14·3	4·5	II31
103	01 22·7	73 45·7	—	34·0	I92
104	01 23·2	73 53·9	—	56·7	Ia4
105	01 27·3	74 04·3	—	34·0	I93 (602)
106	01 28·8	76 34·7	16·4	2·3	Ia5
107	01 28·9	73 55·6	—	45·3	I94
108	01 29·5	72 28·0	14·8	5·7	Ib3
109	01 31·5	74 40·4	15·1	3·4	Ia6
110	01 32·2	73 22·7	14·3	11·3	Ib5
111	01 33·5	76 04·4	13·4	20·4	Ia7 (643)
112	01 34·5	75 58·5	16·2	3·4	Ia8
113	01 47·9	74 13·3	11·9	22·7	Ib6
114	01 48·9	74 50·9	12·1	3·4	Ia9
115	01 55·5	74 42·1	—	3·4	Ib7 (796)
116	01 55·5	78 08·6	—	2·3	Ia10

Apparent photographic magnitudes.—Magnitudes were estimated on ADH plates (scale 68″/mm), one of 60^m exposure and three each of 30^m, 10^m and 5^m exposures, and on four MF plates (scale 167″/mm) of 60^m exposure. Comparison stars were those of Sequence I. For the brighter stars c–h the magnitudes of Cox and Hallam (**7**) have been used; for stars k and fainter, King's magnitudes (**8**). No high degree of accuracy is claimed for the magnitudes and the magnitudes of the sequence stars were taken to the nearest tenth. The ADH plates were first measured by making direct eye estimates. The measurements were repeated using a low-power eyepiece. This latter method was used for the MF plates. The mean differences between the MF results and others are given in Table IV.

TABLE IV

Mean differences between apparent magnitudes of clusters estimated on MF *plates and other sources* (Δm = MF *magnitudes minus magnitudes from sources in column* 1 *of table*)

Source	Δm	Remarks
ADH 60^m and 30^m	+2·9	Direct eye estimates: 73 clusters.
ADH 60^m and 30^m	+1·2	Eye estimates with eyepiece: 45 clusters.
ADH 10^m	+0·5	Eye estimates with eyepiece: 48 clusters.
ADH 5^m	+0·2	Eye estimates with eyepiece.
Shapley-Wilson	+0·6	H.C. 275: 39 clusters: see below.
Kron	−0·2	19 clusters; see below.

The quality of the 60^m plate was not quite as good as that of the 30^m plates and its limiting magnitude would be fainter by perhaps $0^m{\cdot}5$ or less. On all the long-exposure plates star γ of Sequence I ($m = 17{\cdot}3$) is about $1^m{\cdot}5$–2^m above the plate limit so that the latter is around $m_{pg} = 19{\cdot}0$. There is a slight systematic difference, less than $0^m{\cdot}1$, between the 60^m and 30^m cluster magnitudes, the former being the brighter, but all have been combined in Table IV.

The difficulties of estimating magnitudes of clusters by comparison with stars are accentuated with the pin-point stellar images of the ADH Baker–Schmidt. Looking directly at a plate, many of the clusters appeared quite stellar and it was rather surprising that, at least for these types, the differences from the MF plates were so large. The differences might be largely subjective. However, Dr A. R. Hogg, during a brief visit to Armagh, kindly estimated the magnitudes of twenty clusters. The mean difference between his estimates and the writer's was less than $0^m{\cdot}2$, Hogg's magnitudes being the brighter. In making direct eye estimates probably too much emphasis is placed on the size of a cluster. An eyepiece shows more of the structure; with it there is a tendency to concentrate on the nucleus, and attention is paid to density rather than size. By reducing the exposure time many clusters become more stellar-like. This is not so for globular or circular objects; they remain disks with a different texture of the stars. It is much easier on MF plates to compare clusters with stars due to the chromatic aberration of the refractor which gives stellar images like the ADH out of focus.

There are eighty-four objects in Table III common to the two papers of Shapley and Miss Wilson (*ibid*) and thirty-nine of these have magnitudes determined by these authors and the writer. The Harvard magnitudes are given as absolute magnitudes and allowance has been made for the different modulus used. They are based on comparison with stars "in the numerous standard sequences" set up in the Small Cloud. From the situation of the clusters with respect to Sequence I a guess was made as to which were based on this sequence. Due to the revision of the Harvard magnitudes it is likely that an average correction of $-0^m{\cdot}1$ should be added to the Harvard clusters here compared thus reducing the mean difference in the absolute magnitudes from $+0{\cdot}6$ to $+0{\cdot}5$.

Considering the changes in appearance of clusters with exposure time and telescope it is not surprising to find differences between Armagh and Harvard. The latter were obtained from estimates on 8-inch Bache doublet plates (scale 179″/mm) and 1½-inch Cooke plates (scale 600″/mm).

Magnitudes of twenty clusters in the Small Cloud have been published by Kron (**9**). He classified ten of these as globular and ten as non-globular. The magnitudes of the twenty clusters were estimated on ADH plate 640. A sequence of four globular clusters established photoelectrically by Gascoigne and Kron (**10**) was used to find the magnitudes of the remaining six of the ten. It will be seen from Table IV that the mean difference between the writer's MF magnitudes using the stars of Sequence I as standard and Kron's ADH magnitudes using a sequence of globular clusters is $-0{\cdot}2$. That is, Kron's absolute magnitudes are on the average fainter by this than the writer's, whose values are roughly half-way between Kron's and those of Shapley and Miss Wilson. In comparing with Kron, No. 54 (NGC 330) was omitted. The difference in this case amounted to $+3^m{\cdot}1$ but it was considered by the writer (and by Shapley and

Miss Wilson) to be too bright and scattered to measure. It was found extremely difficult to compare the globular clusters with stars, not only on account of the spread of the clusters but the different texture of their images. It was therefore surprising that the mean difference from Kron was the same for globular and non-globular objects. It is presumed that Kron compared the open clusters with stars of Sequence I and not with his globular cluster sequence. With one exception they lie beyond the range of the globular cluster sequence. Presumably, also, he used the magnitude system of Gascoigne and Kron (**11**) for Sequence I. If so, that would account for approximately $0^m{\cdot}1$ in the differences between his open clusters magnitudes and the present ones. Both Hogg and the writer estimated globular cluster magnitudes on a 30^m exposure ADH plate using Kron's globular cluster sequence. The same order of agreement was found as in Table IV.

Considering the uncertainty in estimating integrated magnitudes of clusters, and that Kron's magnitudes were determined from a single ADH plate compared to four MF plates of the writer, the agreement between the two is remarkably good. This may be purely fortuitous. As will be seen from Table IV, different instruments and exposure times yield markedly different results and it is not possible to say what is the critical exposure time that gives correct magnitudes. Indeed what holds for one type of cluster may not hold for another. The behaviour of a cluster image with exposure time is very different from that of a stellar image. For example, on a 30^m exposure ADH plate, it would appear that cluster No. 85 (NGC 419) is very much brighter than the nearby star b of Sequence I ($m = 7{\cdot}0$); on a 5^m exposure ADH plate it is estimated to be over a magnitude fainter. As a matter of interest the behaviour of cluster No. 72 was followed on plates of different exposure until it was too faint to register. The results of the magnitude estimates are given in Table V.

TABLE V

Estimates of m_{pg} of Cluster No. 72 on different exposures

Plate	Exp.	m_{pg}
ADH	60^m	8·0
ADH	30^m	7·9
ADH	10^m	8·4
ADH	5^m	9·0
ADH*	20^s	12·0
ADH**	5^s	13·0
MF***	60^m	11·8

* On this plate the cluster was reduced to three images whose magnitudes measured on the Iris photometer were 13·08, 13·14 and 13·32 giving a total magnitude equivalent to $m = 12{\cdot}0$.

** The cluster was at the limiting magnitude of the plate. So was star *q* of Sequence I ($m = 13{\cdot}0$).

*** Kron's value is $m_{pg} = 12{\cdot}0$.

Diameters. For the diameters of the clusters there is on the average, and individually with one or two exceptions, agreement with Kron. It is uncertain, however, how near to standard diameters they are; if a standard diameter is defined by the relative surface brightness they must certainly, at least for the globular clusters, be lower limits. For a given telescope the diameter depends

strongly on the exposure time. The behaviour of NGC 104 (47 Tucanae) was followed on ADH plates of exposures from 60^m to 5^s. The measured diameters ranged from 60′ to 205″ which, with a modulus of 14·17 (**12**), correspond to 118 and 7 parsecs. On the 5^s exposure plate the image of NGC 104 is similar to cluster images at long exposure in the Small Cloud. Due to the absence of background stars it is easy with this exposure to recognize some of the faint stars of the cluster outside the core and thus to classify it as globular. If this same image were, however, on a long exposure plate necessary to show many of the Cloud clusters the dense background of stars would mask the non-core stars. Only the core would be measured. From appearance it would be classified as a "cluster, probably globular".

On the 5^s exposure plate the core was measured as 68″. The exposure was too short to show any Cloud clusters. On a 60^s exposure the globular cluster NGC 121 (No. 10) showed a measurable disk. Should this be similar to NGC 104, being seven times more distant, since the apparent diameters are inversely proportional to the distances, its core should be one-seventh. The measured cores were 270″ and 35″, or NGC 121 was one-eighth of NGC 104. The crude method indicates little difference between them. On a 30^m exposure the core of NGC 104 was measured as 680″. The mean of Nos. 8 and 15 was 163″ on the same plate; if we include No. 1, which is circular or globular, 177″. In this case the cores are only one-fourth that of NGC 104. Nos. 1 and 8 are the largest circular or globular clusters measured. They are also away from the main body of the Cloud so that possibly more of their cores are recognizable.

On a 30^m exposure plate the core of NGC 362 was measured as 340″. The mean of Nos. 27, 34, 43, 59, 67, 85 and 83 measured on the same plate was 88″. Taking the modulus of NGC 362 to be 15·55 (**11**), if its dimensions are equal to this group its core should be between three and four times as large, which is what is found. The two globular clusters NGC 104 and 362 should be subject to the same amount of space absorption as the clusters of the Small Cloud.

With a realization of the difficulties encountered in comparing galactic with Small Cloud clusters, Kron (**9**) has suggested that the latter may be smaller and less luminous than the former. His alternative is an increase in the modulus of the Cloud. There are so many uncertainties involved, including the estimation of magnitudes, the different methods of arriving at these for galactic and Cloud clusters, the different instruments involved, the difficulties of measuring diameters, and the effects of absorption in our galaxy, that it would seem at present impossible to come to any conclusion. From our present knowledge of the origin of clusters it would also not be possible to say whether one could expect a smaller galaxy would produce larger or smaller clusters than a larger galaxy.

Shapley (**13**) considers that only one group of objects in the Small Cloud can be called a constellation in the sense as used in the Large Cloud. This is the group NGC 456, 460 and 465 (Nos. 94, 97 and 99). The group of Nos. 101, 103 and 104 containing bright stars and nebulosity and with overall dimensions 230×90 parsecs might be in the constellation class. Similar in appearance but less pronounced, also with bright stars and nebulosity, are Nos. 105 and 107 with dimensions 200×90 parsecs. On a 30^m exposure the nebulosity is well defined, measuring 45×30 parsecs. These three groups form the outstanding connecting links with the wing of the Cloud. In Paper I, NGC 371 (No. 71), NGC 395 (No. 75) and NGC 346 (No. 60) were added to these. The name

stellar associations would probably be more appropriate, at least to these smaller groups, than constellations. Kron (*ibid*) lists Nos. 18, 46, 60, 68, 71, 75, 94, 97 and 99 in this category.

In Kron's first paper (**5**) on the Small Cloud clusters he listed twelve clusters as globular, four questioned as globular and two as globular in appearance. In his second paper (**9**), applying a more rigorous test, namely that the brightest stars had to be of photographic magnitude of about 17, eight of the twelve and two of the four were retained as globular. Taking into account Kron's first list and the appearance of clusters as seen by Haffner and the writer, fourteen clusters were listed in Paper I as possibly globular. On the basis of integrated spectra, colours, magnitudes, apparent smooth structure and dimensions, Shapley (**13**) considers that only NGC 121, 416 and 419 can at present be listed as genuine globular clusters. NGC 339, 458 and H.C. 275/3 are classified by him as circular; he points out that M 11 and NGC 2477, non-globular clusters in our own system, would appear circular to a remote external observer.

Red magnitudes.—An attempt was made to get some idea of the redness of some of the clusters by comparison with unpublished red magnitudes of King's of some stars of Sequence I. The plates were 103a.E with Wratten 25A filter; two of 90^m, one of 60^m and two of 30^m exposure. The same effect was found as for the blue plates, namely, decreasing magnitudes with lower limiting magnitude of the plate. The differences between the 90^m and 60^m plates were small and also between one of the 30^m plates which was of exceptionally good quality with a limiting magnitude about the same as the 60^m. The clusters on the other 30^m plate averaged $0^m{\cdot}6$ fainter than on the first and this plate represents a fairly normal 30^m exposure red plate. The red magnitudes are not given in Table II because it is not known what is a "standard" exposure time nor what are corresponding blue and red exposure times for comparison. Some qualitative ideas may, however, be obtained from the red plates. Colour indices were found by comparing the "normal" 30^m exposure red plate with a 5^m exposure blue plate. Due to the plates not being on the same centre and to difficulties of estimating magnitudes on one or the other or both, only twenty-seven clusters could be compared. All gave negative (blue minus red photographic) red indices. They included the ten brightest open clusters listed by Kron but only one, No. 29, of his globular clusters.

Kron's globular cluster sequence consisted of the following objects; his *P* and *V* magnitudes are in brackets: NGC 419 (10·6; 10·1), 121 (11·4; 10·7), 416 (11·9; 11·4) and 339 (12·3; 11·8). It is clear from the red plates that the sequence is also in order of fainter red magnitudes. His other globular clusters were graded on the 103a.E plates with red filter. The results are given in Table VI which also includes Nos. 54, 82 and 96.

TABLE VI

Estimates of red magnitudes ("m_r") according to Pickering's method by comparison with Kron's globular cluster sequence

No.	m_{pg}	"m_r"	No.	m_{pg}	"m_r"	No.	m_{pg}	"m_r"
8	11·5	416·7·339	34	12·0	~339	67	12·0	~339
15	12·0	<50	43	12·0	<50	82	11·8	416·4·339
31	12·3	<50	54	7·4	419·4·121	96	10·5	416·4·339

It will be seen from the Table that Nos. 54 and 96 are blue objects, the former being very blue. Nos. 8, 34, 67 and 82 are all about equal to NGC 339 in the red, Nos. 8 and 82 being somewhat brighter and Nos. 34 and 67 probably somewhat fainter. Since the first two are slightly brighter than NGC 339 in the blue and the last two about equal to it, it is likely that these four are red objects. The remaining clusters, Nos. 15, 31 and 43 are all about equal to NGC 339 in the blue but fainter in the red so it is not possible to say if there is or is not a few tenths of a magnitude of reddening. Little can be added to what has already been written. There are other objects in the Small Cloud which could be considered as possibly globular; e.g. No. 58, a faint object in red, the texture of which resembles that of a globular cluster. For the present, Kron's ten clusters together with Nos. 1, 82 and 113 are considered to be globular or circular.

Distribution.—The clusters in the main part of the Cloud have all been plotted on Fig. 1. As measured from the cluster system the longest diagonal of the Small Cloud is 8040 parsecs; the shortest diagonal 5385 parsecs. The E–W extent is 6445 parsecs; the N–S extent 7130 parsecs. These dimensions are larger than any so far published and probably represent the extreme limits except that star-counts would show a further slight extension in the direction of the wing. Shapley and Virginia Nail (**14**) have expressed some doubt that the wing may not be a part of the Cloud but a structure distinct from it. The clusters extend, however, from the main body of the Cloud to the wing and end in it, leaving

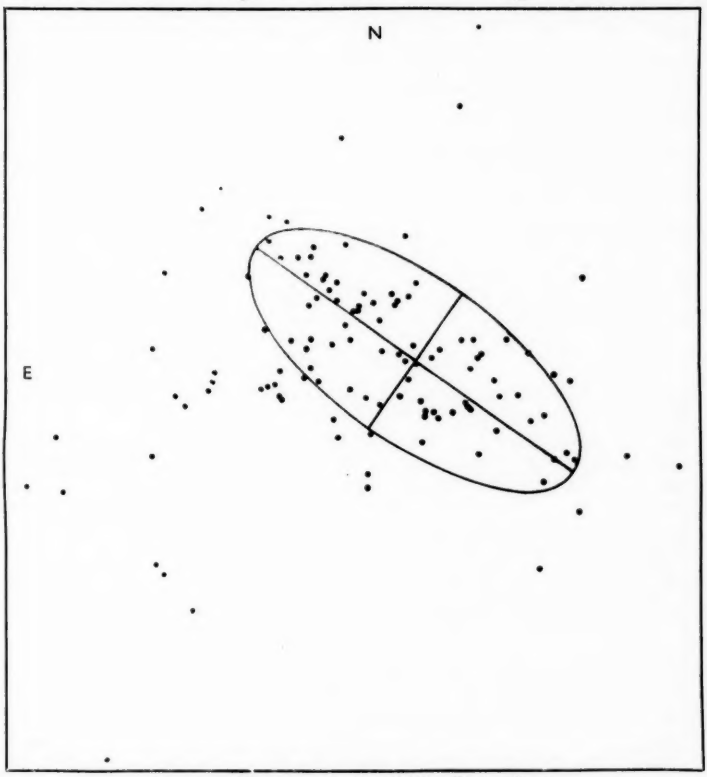

FIG. 1.—*Clusters in the Small Magellanic Cloud.*

a gap between the two Clouds. A preliminary survey of ADH prism plates shows a bridge of emission objects, which follows closely the cluster bridge, from the main body of the Cloud to the wing and in it. There seems little doubt but that the wing is part of the structure of the Small Cloud.

Little can be said about the distribution of the globular or circular clusters; their numbers are too small and their classification too uncertain. While it is easy in the majority of cases to recognize a cluster as open, there are a number of objects on the western side of the Cloud which are questionable. Neglecting the clusters towards the wing and the obviously outlying ones, an ellipse has been drawn to contain the main body of clusters. Within this are 63 per cent of all clusters; not counting twenty-two outlying clusters it contains 78 per cent of the remainder. The number of clusters in the four quadrants of the ellipse are 24, 17, 16 and 16 (see Fig. 1). The excess of clusters on the wing side would, if distributed over the three sparse quadrants, give just an even number in all quadrants.

Kron (**15**) considered that the non-globular clusters lie in a roughly spiral distribution and contained within an elliptic area. Within this are 57 per cent of his sixty-nine clusters. His field did not contain any of the outlying clusters. The ratio of his minor to major axis was 1 : 1·4 which, if interpreted as due to the tilt of a flat circular object, gave him a tilt of the Cloud of 45° and position angle of the major axis of the ellipse 60°. The position angle here of the major axis is also 60° but the ellipse drawn is much more elongated with ratio of minor to major axis 1 : 2·4, almost twice Kron's. On the assumption of a flat circular object this would give a tilt of 65°. There is no sign of any spiral distribution of the non-globular clusters. From the distribution of clusters the Small Cloud could well be an irregular galaxy distorted by the tidal action of the Large Cloud. The tidal arm, culminating in the wing of the Cloud, while in the general direction of the Large Cloud, is not directed towards it but drops southward. This trailing arm might be a result of a past near approach of the two Clouds and the rotation of the Small Cloud.

Armagh Observatory,
Armagh, N. Ireland:
1958 *January* 1.

References

(1) E. M. Lindsay, *Irish Astr. Journal*, **4**, 65, 1956; *Armagh Obs. Contr.* No. 18.
(2) Jenka Mohr, *H.B.* 899, 1936.
(3) G. de Vaucouleurs, *P.A.S.P.*, **67**, 350, 1955.
(4) G. de Vaucouleurs, *P.A.S.P.*, **69**, 252, 1957.
(5) Gerald E. Kron, *P.A.S.P.*, **68**, 125, 1956.
(6) Harlow Shapley and Harvia H. Wilson, *H.C.* 275 and 276, 1925.
(7) A. N. Cox and K. L. Hallam, *Ap. J.*, **118**, 314, 1953.
(8) Ivan King, *A.J.*, **56**, 43, 1951.
(9) Gerald E. Kron, *P.A.S.P.*, **68**, 230, 1956.
(10) S. C. B. Gascoigne and Gerald E. Kron, *P.A.S.P.*, **64**, 196, 1952.
(11) S. C. B. Gascoigne and Gerald E. Kron, *Suppl. of Australian J. of Sc.*, **17**, No. 3, 22, 1955.
(12) Harlow Shapley, Star Clusters, *Harvard Obs. Monograph*, No. 2, 1930, 224.
(13) Harlow Shapley, *American Scientist*, **44**, No. 1, 89, 1956; *H.R.* 431.
(14) Harlow Shapley and Virginia McKibbin Nail, *Proc. Nat. Acad. Sc.*, **41**, No. 11, 835, 1955; *H.R.* 430.
(15) Gerald E. Kron, *P.A.S.P.*, **68**, 326, 1956.

XUM

EVIDENCE ON THE SPATIAL DISTRIBUTION OF RADIO SOURCES DERIVED FROM A SURVEY AT A FREQUENCY OF 159 MC/S

D. O. Edge, P. A. G. Scheuer and J. R. Shakeshaft

(Communicated by M. Ryle)

(Received 1957 December 24)

Summary

Some results from a survey of radio sources at 159 Mc/s are available for limited regions of the sky. These are discussed in relation to the spatial distribution of sources.

A comparison of the individual sources shows that about one quarter of those in the previous survey at 81·5 Mc/s are confirmed, but that for the weaker ones the reliability is worse than was indicated in the list. A comparison between the new positions and those found by Mills and Slee at 85 Mc/s indicates fair agreement for sources with flux densities more than 20×10^{-26} w.m.$^{-2}$ (c/s)$^{-1}$ at 85 Mc/s but poor agreement among the weaker sources.

A simple plot of log N against log S, where N is the number of sources with flux density greater than S, gives a slope of $-2{\cdot}2$ for one region and $-2{\cdot}7$ for another, but these slopes may be affected to an unknown extent by confusion between nearby sources and by sources having finite angular diameters.

A method of analysis depending on the statistical distribution of amplitudes on the records and independent of confusion errors shows that for the fainter sources the observations are consistent with a uniform distribution of sources. Between these and the intense sources a discrepancy in numbers remains. An argument may be devised to show that the 159 Mc/s observations, when taken together with previous results at 81·5 Mc/s, are inconsistent with a uniform distribution. This result is, however, based on data of which the statistical significance is not sufficiently great to be conclusive and further observations are needed.

---

1. *Introduction.*—The most detailed surveys of radio sources which have been published are those of Shakeshaft *et al.* (1955) at 81·5 Mc/s (which will be referred to as the 2C survey), and of Mills and Slee (1957) at 85 Mc/s (referred to as the MS survey). More recently the aerial system used for the 2C survey has been adapted to a frequency of 159 Mc/s and a survey of radio sources (the 3C survey) is approaching completion at this frequency. Some preliminary results from this survey, in particular those relating to the spatial distribution of radio sources, will be presented in this paper.

The 159 Mc/s observations at Cambridge have been carried out, like those at 81·5 Mc/s, with the double interferometer described by Ryle and Hewish (1955). This has four aerials situated at the corners of a rectangle, 308 wave-lengths East–West by 27 wave-lengths North–South (at 159 Mc/s), so that the

overall reception pattern is that due to a single aerial, i.e. 8° by 1° between half-power points, but containing interference fringes in two planes at right angles. A phase-switching receiver (Ryle, 1952) is used so that any sources with angular extent comparable with the fringe separation are observed at reduced intensity. By phase-switching between the East pair and the West pair of aerials, sources with angular diameters greater than about 7′ are eliminated. A survey using such a technique will be called a "small diameter" survey. By phase-switching between the North pair and the South pair, it is possible to record sources with diameters up to about 1° and measure any angular diameters between the limits 2′ to 10′. This procedure gives a "large-diameter" survey.

The 85 Mc/s observations at Sydney were made with the Mills Cross aerial (Mills and Little, 1953), an instrument having a pencil beam reception pattern 50′ by 50′ between half-power points when directed at the zenith. Sources of all angular diameters are detectable if their surface brightness is sufficiently high. Angular diameters can be measured by the increased width of the profile on the record, but the broadening is difficult to detect for sources much smaller than 50′. Thus it is likely that some of the MS "point" sources will appear as extended sources in the 2C and 3C surveys.

The principal purpose of the present paper is to set out the further information on the distribution of radio sources revealed by the 3C survey. Such information may be obtained by investigating the numbers of sources in different intensity ranges. If radio sources, for example, are distributed uniformly in space then $N(S)$, the number with flux densities greater than S, is proportional to $S^{-3/2}$, so that a graph of $\log N$ against $\log S$ has a slope of $-1{\cdot}5$. Counts of 2C sources indicated a slope of nearly -3, implying a marked excess of faint sources, or a deficit of strong ones (Ryle and Scheuer, 1955). Mills and Slee (1957) on the other hand obtained a slope of $-1{\cdot}8$ and suggested that the discrepancy between this and $-1{\cdot}5$ of a uniform distribution could be explained by instrumental effects. They also found poor agreement between the individual sources of the two surveys and suggested that both this and the steep slope of -3 might be due to the effects of confusion between adjacent sources in the 2C survey.

The various factors which may affect the counts of radio sources will first be summarized, and a brief comparison between the different surveys follows. This will indicate the extent to which agreement may be reached at present regarding the existence of individual sources. Finally the law $N = \text{constant} \times S^{-3/2}$ will be tested both by counts of individual sources and by a method (Scheuer, 1957) which avoids the errors which may arise from confusion.

2. *Instrumental limitations and selection effects.*—It is known that there are sources situated inside our Galaxy with a disk-like distribution near the galactic plane, among them being Cassiopeia A, the remnants of the supernovae of AD 1054, AD 1572 and AD 1604, and a number of extended sources of relatively low surface brightness (Cygnus X, Puppis A, IC 443, M 42, etc.). The inclusion of such sources would confuse the present issue since the $\log N - \log S$ plot for a distribution of this type has a slope less steep than $-1{\cdot}5$. The analysis is therefore restricted to regions away from the galactic equator.

The factors affecting the detection of sources are discussed below.

(i) *Sensitivity.*—The random noise on the records is not a serious limitation in either the 2C or 3C surveys; the noise level with a recording time constant of six seconds corresponds to a flux density of about 10^{-26} w.m.$^{-2}$ (c/s)$^{-1}$ in each

case*. Averaged over the time taken for a source to pass through the aerial beam, it becomes negligible.

In the survey of Mills and Slee the r.m.s. noise, smoothed over the time of observation of a source (about three to five minutes) corresponds to a flux of $3{\cdot}5 \times 10^{-26}$ w.m.$^{-2}$ (c/s)$^{-1}$ and is the principal limitation of the survey.

(ii) *Confusion.*—If the reception pattern of an aerial system is wide enough to contain several sources of perceptible intensity, the records from the receiver no longer show the transits of a succession of individual sources but a "confused" record is obtained on which several sources contribute to the deflection at any instant. Only sources whose flux densities are some three or four times greater than that equivalent to the average level of confusion can be distinguished unambiguously, and the measured flux densities of all sources are uncertain.

Confusion is the principal limitation of the 2C and 3C surveys†. The confusion level may conveniently be indicated by a flux density such that half the record shows deflections more, and half shows deflections less, than the deflection corresponding to that flux density. In these terms the confusion level is about 15×10^{-26} w.m.$^{-2}$ (c/s)$^{-1}$ for the 2C survey, and about 2×10^{-26} w.m.$^{-2}$ (c/s)$^{-1}$ for the 3C survey.

In the 2C catalogue the majority of sources having flux densities less than 25×10^{-26} w.m.$^{-2}$ (c/s)$^{-1}$, i.e. about one-third the total number, were bracketed to indicate their unreliability. The more recent analysis suggests that in fact the intensity at which individual sources can be reliably identified should be increased to about 40×10^{-26} w.m.$^{-2}$ (c/s)$^{-1}$. This conclusion is confirmed by a comparison of the individual sources in the 2C and 3C surveys. Of 143 sources in the 2C catalogue between declinations 40° and 50°, 35 coincidences were found (allowing single lobe-shifts in right ascension and declination for the 2C positions); this result corresponds to a flux level of 40×10^{-26} w.m.$^{-2}$(c/s)$^{-1}$ at 81·5 Mc/s.

Since the solid angle of the reception pattern of an aerial of given physical size is proportional to the square of the wave-length, nearly four times as many sources can be distinguished to the same level of confidence in the 3C survey as in the 2C survey. The present analysis suggests that about 150 sources per steradian should be reliable in the 3C survey, a figure which is comparable with the total number of sources in the MS survey, for which the confusion level (as defined above) and noise level are about the same.

(iii) *The effects of angular diameter.*—The equipment used for the MS survey detects all sources which produce a sufficient flux density within the reception pattern of $50' \times 50'$. Thus the limiting flux density is constant for sources smaller than $50' \times 50'$ and increases for sources with larger angular diameters.

As explained above, the interferometer used in the 2C and 3C surveys normally observes sources of small angular diameter preferentially, i.e. in the small diameter surveys sources with diameters greater than 6′ and 3′ respectively (in R.A.) are recorded with appreciably reduced intensity. The corresponding limits for the large diameter surveys are 2° and 1° (in Dec.) respectively at the zenith and larger values at increased zenith angles. Intense sources can, of

* Flux densities refer to the frequency of the relevant survey.

† This limitation by confusion is not peculiar to interferometer systems, but is related in any system to the solid angle over which sources may contribute to the output (cf. the blending of closely adjacent star images on an ordinary astronomical photograph).

course, be observed irrespective of their angular diameters by using one of the four arrays as a pencil beam instrument.

Within any specified class of source, the nearest members will be the most intense and will at the same time have the largest angular diameters; in the 2C and 3C small diameter surveys there must therefore be to some extent a systematic bias against intense sources, and any apparent deficit of such sources must be corrected for this selection effect.

There may be an added complication to statistical analysis, not confined to interferometric surveys, if radio sources occur predominantly in clusters. Such clusters would be resolved into individual sources when close by, but at great distances would appear as intense point sources. At intermediate positions the clusters would behave as sources of large angular diameter. An argument concerning the distribution which avoids these difficulties is presented in Section 4.

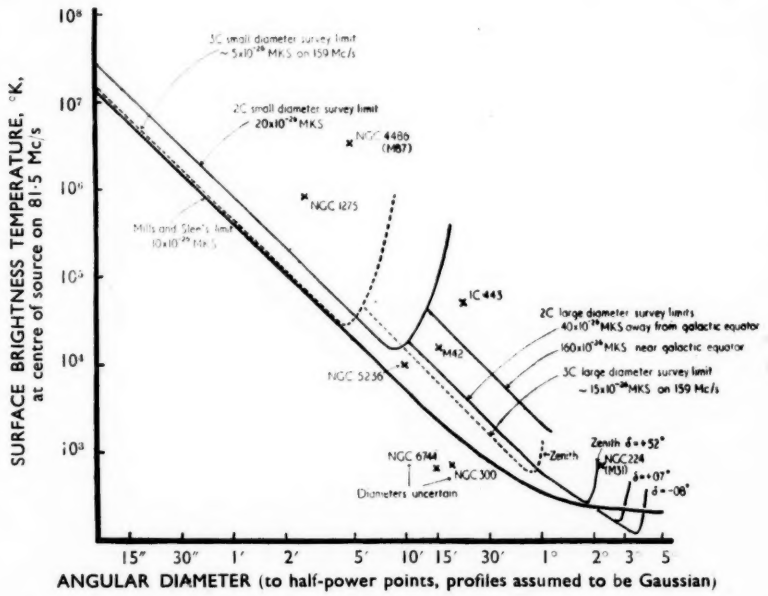
SURFACE BRIGHTNESS TEMPERATURE, °K, at centre of source on 81·5 Mc/s
3C small diameter survey limit ~ 5×10⁻²⁸ MKS on 159 Mc/s
2C small diameter survey limit 20×10⁻²⁸ MKS
NGC 4486 (M87)
NGC 1275
Mills and Slee's limit 10×10⁻²⁸ MKS
IC 443
M42
2C large diameter survey limits 40×10⁻²⁸ MKS away from galactic equator
160×10⁻²⁸ MKS near galactic equator
3C large diameter survey limit ~ 15×10⁻²⁸ MKS on 159 Mc/s
NGC 5236
Zenith δ = +52°
Zenith
NGC 224 (M31)
δ = +07°
δ = −08°
NGC 6744
NGC 300
Diameters uncertain
15″ 30″ 1′ 2′ 5′ 10′ 15′ 30′ 1° 2° 3° 5°
ANGULAR DIAMETER (to half-power points, profiles assumed to be Gaussian)

FIG. 1.—*The ranges of sources visible on the* 2C, 3C *and* MS *surveys. The curves show the lower limits of the surveys. The approximate positions of several sources are shown on the diagram.* [NGC 300 *and* NGC 6744 *were observed by Mills during a special search* (Mills, 1955).]

(iv) *Side-lobes of the reception pattern.*—Since the most intense sources in the sky have flux densities over 1000 times greater than those of the faintest sources listed in the surveys under review, care must be taken to ensure that the passage of intense sources through subsidiary maxima of the reception pattern does not produce responses which are listed as true sources. The danger of spurious responses is particularly high for aerials with "incompletely filled" apertures such as the Mills Cross, because, if the ratio of a subsidiary maximum to the principal maximum is R^2 (say) for a conventional aerial (or an interferometer using two similar arrays) it is only R for an "unfilled" aerial having a similar

resolving power. In order to reduce the spurious responses to an acceptable level it is therefore necessary to maintain a very much more accurate current distribution across the aperture in the latter case.

In connection with the 2C survey a special investigation of the spurious responses was carried out and R^2 was measured accurately for subsidiary maxima down to one-tenthousandth of the main lobe. Mills and Slee were not able to make a similar check, and although they have taken considerable care to eliminate the side-lobe effects of intense sources it may be that some of them have escaped detection. Examples are given in Section 3 of two fairly intense MS sources which have not been found in the 3C survey: possible explanations of this are that the flux density of the sources falls exceptionally rapidly with frequency or that they are spurious responses.

A further check on the reception of intense sources in subsidiary maxima of the 2C and 3C interferometer was made by comparing the apparent declination of the source as revealed by the periodicity of the interference fringes with that derived from the North–South reception pattern.

The instrumental limits of the three surveys are illustrated in Fig. 1, in which the surface brightnesses of sources are plotted against their angular diameters. The regions of the plane accessible to the different instruments are marked. The approximate characteristics of several sources are shown on the diagram. It will be seen that IC 443 is visible both to the 2C large diameter survey and the MS survey, but the Orion nebula (M 42), though observable by Mills and Slee, is outside the 2C limits. Mills and Slee also observe NGC 300 and NGC 6744 which are undetectable on the 2C or 3C surveys.

3. *A comparison of the 3C and MS surveys.*—The reduction of the 3C small diameter survey records has been completed for two regions: $+37^\circ < \text{Dec.} < +52^\circ$, $00^h < \text{R.A.} < 24^h$ and $-10^\circ < \text{Dec.} < +10^\circ$, $00^h < \text{R.A.} < 08^h$, the latter region being common to the 2C, 3C and MS surveys. A comparison of the positions of the 2C and 3C sources shows little better agreement than that already found by Mills and Slee between their survey and the 2C survey*. A comparison of the 3C and MS surveys is more promising, however, and it may be noted that the limit set by confusion in the former is about the same as that set by noise in the latter (see Section 2 (ii) and (iii)). In cases where an MS source does not correspond to a source in the 3C list, the original 3C records have been consulted to check for possible errors.

There appears to be a systematic difference between declinations quoted in the two surveys. If a correction, varying linearly between $-7'$ at Dec. $= +10^\circ$ and $-19'$ at Dec. $= -10^\circ$, is added to the 3C declinations, better agreement is found between the bright sources of the two surveys and in addition agreement to within the limits of error is reached between the 3C positions of Hydra A and Hercules A and those of the peculiar optical objects nearby. Because of the positional errors and the limited evidence this correction is not yet certain and it does not follow that all of the discrepancy lies in the 3C survey.

A "coincidence" has been defined as agreement of the positions within the sum of the quoted errors in right ascension and within twice the sum of the quoted errors in declination. Owing to the possibility of picking the wrong interference lobe as the position of a 3C source, MS sources lying within similar

* The reliability of all the surveys decreases towards the horizon, so that the agreement between the 2C and 3C surveys in the region $-10^\circ < \text{Dec.} < +10^\circ$ is poorer than that for $40^\circ < \text{Dec.} < 50^\circ$.

distances of the alternative positions on each side of the quoted one have been counted as coincidences.

The results are as follows:—

TABLE I (*a*)

MS Flux density (10^{-26}w.m.$^{-2}$(c/s)$^{-1}$)	No. of MS sources	No. of observed coincidences	Mean expected no. of random coincidences
$S > 30$	28	16	1·4
$30 > S > 20$	49	13	3·6
$20 > S > 15$	59	4	4·3
$15 > S$	71	6	5·4
Total	207	39	14·7

When the "coincidence" range was extended to include sources within twice the sum of the right ascension errors and three times the declination errors, and a total of two lobe-shifts were allowed (but only one in declination) on each 3C position, the increases in numbers of "coincidences" were as follows:—

TABLE I (*b*)

MS Flux density	Observed increase	Mean expected increase if random
$S > 30$	4	1·4
$30 > S > 20$	8	3·7
$20 > S > 15$	10	5·7
$15 > S$	6	7·0
Total	28	17·8

In these tables the expected numbers have been calculated from the areas covered by the quoted errors for the sources.

Eight of the MS sources in the highest intensity range are not accounted for in this comparison. One is almost certainly related to a 3C source of equivalent flux density about 1° away; another is near the southern limit of the 3C survey, where there are insufficient data to complete the analysis; and a third cannot be separated in the 3C survey from the side-lobes of Taurus A. Three are quoted in the MS list as being "possibly extended" and one of these has been found in the 3C large diameter survey. There is no 3C evidence for the remaining two.

Assuming that the 67 observed "coincidences" out of 207 in Table I (*a*) and (*b*) are genuine, there are still 140 MS sources to be accounted for. In the case of 63 of these, the 3C evidence is inconclusive, but 77 sources definitely do not appear on the 3C small diameter survey records. This may mean that they have (i) angular diameters greater than 5′ or (ii) peculiar spectra, or (iii) that they are spurious side-lobe responses. In Section 4 evidence is presented to show that such a high proportion (77 out of 207) of extended sources is unlikely.

A search has been conducted in the MS list around the positions of each 3C source to ascertain how many of the 3C sources can be explained in terms of MS sources. Of the 24 with flux densities $> 12 \times 10^{-26}$ w.m.$^{-2}$(c/s)$^{-1}$, 16 can be directly related to MS "point" sources, 2 are presumably the sources referred to in the MS list as possible components of the "extended" source 00−010 (2C 50), 1 occurs close to the extended source 01+02, 3 are close to the source Taurus A and listed as unreliable, 1 is near 3 MS sources and is likely to be related to them, and 1 is not explicable in terms of MS sources.

Of the 138 fainter sources, 50 are confirmed directly by MS sources while a further 30 may originate in the same physical objects as nearby sources in the MS list but the evidence is not conclusive. The remaining 58 3C sources in the area have no corresponding sources in the MS list, but most of them have flux densities near the lower limit of the MS survey.

Search has been made on the 3C large diameter records for MS sources listed as extended. Out of 18 sources, 3 were directly confirmed, in 7 cases the record was confused or there was a nearby source of about the right flux density but a small angular diameter, and in 8 cases no trace of the sources could be found. Two notable sources absent on the 3C records are 06+03 and 06+06. To investigate the discrepancy further, one of the four Cambridge aerials was set at declination +7° and a record made of the total power received. Relevant parts of the resulting trace are shown in Fig. 2. The size of the comparison sources reveals that the sensitivity should be quite adequate for the detection of 06+03 and 06+06, so that their absence (if they are assumed to be genuine sources) can only be explained by very special peculiarities in their spectra.

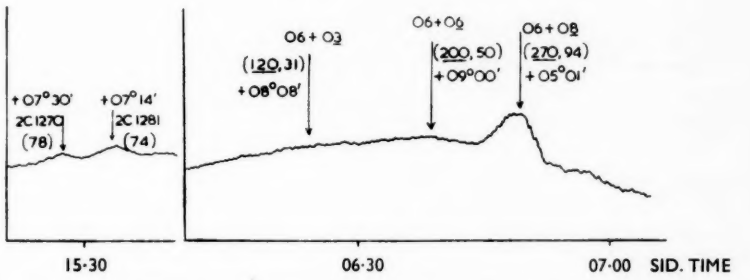

FIG. 2.—*Parts of the record resulting from a total power run using one element of the Cambridge aerial as a pencil beam instrument, centred on declination +7° (as described in the text). On the right, the record in the vicinity of three* MS *sources is shown, together with their expected times of transit. On the left, for comparison is the record obtained from two* 2C *sources* (2C1270 *and* 2C1281). *The source flux densities are quoted in brackets: for* MS *sources, two figures are quoted, representing the integrated (underlined) and peak flux densities: these flux densities are at a frequency of* 85 Mc/s. *The declinations of the sources are also shown.*

Whatever the final conclusions may be concerning the weaker sources, there is fair agreement on the whole about those with flux densities more than 20×10^{-26} w.m.$^{-2}$ (c/s)$^{-1}$ at 85 Mc/s (10×10^{-26} w.m.$^{-2}$ (c/s)$^{-1}$ at 159 Mc/s).

4. ***The relationship between the number of sources and the flux density.***—The analysis of the 2C survey indicated that the numbers $N(S)$ of radio sources above various levels S of flux density did not follow the law $N(S) = \text{constant} \times S^{-3/2}$ which would be expected if the sources were scattered uniformly through (Euclidean) space (Ryle and Scheuer, 1955). There appeared to be an excess of faint sources (or a deficit of intense ones). The data were of two kinds:—

(i) *Counts of sources.*—Owing to the effects of confusion, measured flux densities are subject to an uncertainty which becomes relatively greater for the faint sources (Bolton, 1956), and many of the weak "sources" recorded probably represent the joint effects of a number of sources with no dominant member. For these reasons the counts may be unreliable.

(ii) *Counts of deflections.*—The statistical properties of the deflections on a chart which records the output of the receiving system can be predicted for any assumed number–flux density law (Scheuer, 1957). For the case $N = \text{constant} \times S^{-3/2}$ and a receiving system of the type used in the 2C and 3C surveys the fraction of the record in which the deflections have amplitudes between D and $D + dD$ is $P^*(D)\,dD$, given by

$$P^*(D) = \int_0^\infty \exp(-\alpha\omega^{3/2})\omega D J_0(\omega D)\,d\omega \qquad (1)$$

where α is a scale factor determined by the constant in the number–flux density law and the reception pattern of the aerial, and $J_0(\omega D)$ is the Bessel function of zero order.

Apart from the value of α, the relation (1) is independent of the form of the reception pattern; it is, however, affected if sources have finite angular diameters. By expanding the D axis and compressing the $P^*(D)$ axis by a factor $2\alpha^{2/3}$ in the graph of $P(D)$, the scale factor α may be removed and the resulting graph is a unique one representing the function

$$F(\sigma) = \int_0^\infty \sigma t \exp[-(\tfrac{1}{2}t)^{3/2}] J_0(\sigma t)\,dt. \qquad (2)$$

The parameter $\sigma = D/2\alpha^{2/3}$ is a measure of the deflection as a multiple of the confusion level (which, when defined as in Section 2 (ii) by the median deflection, corresponds to $\sigma = 0{\cdot}83$).

For large deflections, each of which is generally dominated by the presence of a single intense source, the graph of $P(D)$ against D is similar to a graph of $-(dN/dS)$ against S, but for small deflections, where the overlapping of "images" of sources on the record is important it approaches a Rayleigh distribution.

By comparing the probability distribution (1) with the frequency histogram of observed deflections, the relationship $N \propto S^{-3/2}$ may be tested in a manner independent of confusion and uncertainties in flux densities.

Further data of both kinds are discussed below.

(*a*) *Counts of sources.*—The 3C records for the region $+37° < \text{Dec.} < +52°$ provide results free from interference and the spurious responses due to intense sources for an area of 0·25 steradians remote from the galactic equator. The graph of $\log N$ against $\log S$ for the 85 sources in this area has an average slope of $-2{\cdot}2$.

The second area for which the analysis is complete, that common to all the surveys, covers about 0·7 steradians, of which 0·5 steradians are further than 15° from the galactic equator. Fig. 3 shows graphs of $\log N$ against $\log S$ for this region ($|b| > 15°$), both for the 2C and 3C sources. Each of the graphs is linear and the slopes are almost identical, viz. $-2{\cdot}5$ for 2C and $-2{\cdot}7$ for 3C. The effects of confusion should be much larger for the 2C results, so that the agreement between the two slopes would seem to indicate that the systematic effects of confusion have not seriously affected them. There is the possibility, however, that the decreased confusion at 159 Mc/s may be compensated by an increased effect of the angular diameter of sources.

(*b*) *Counts of deflections.*—Counts of deflections expressed in terms of σ from both the 3C and 2C records are shown in Tables II and III. The areas of sky used do not contain any point within 15° of the galactic equator, and those

parts of the records which show man-made interference, solar radiation, or the passage of very intense sources through side-lobes of the reception pattern*

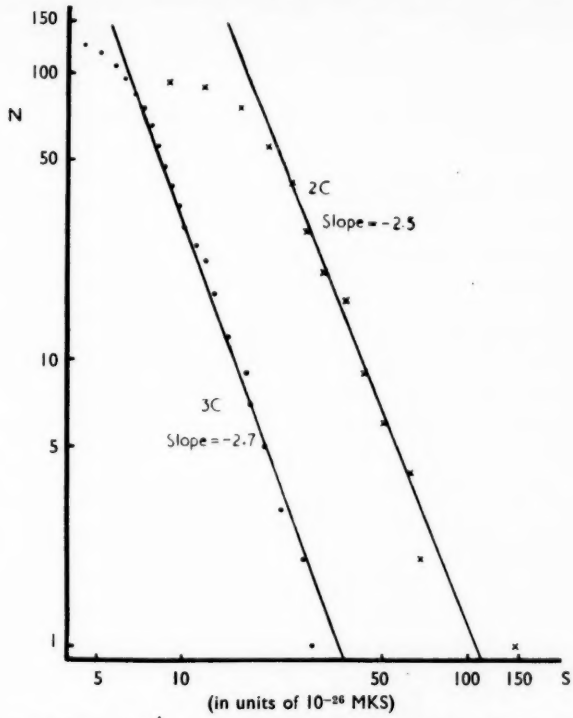

FIG. 3.—*Log N-log S plots for the two Cambridge surveys in the area common to the* MS *survey, excluding regions where* $|b| < 15°$. *The solid angle involved is approximately* 0·5 *steradians, and N here refers to the actual number of sources observed.* $N = 10$ *corresponds to* 1 *source per* 20 *beam-widths.*

TABLE II (159 Mc/s)

σ	0 to 0·869	0·869 to 2·197	2·197 to 4·355	4·355 to 6·505	6·505 to 8·65	8·65 to 10·64	10·64 to 12·67	12·67 to 14·61	14·61 to 20·45	> 20·45	> 8·65	8·65 to 20·45
No. observed	1056	750	153	29	8	2	1	1	0	6	10	4
No. computed	1056	749·5	137·8	29·2	12·3	5·9	3·75	2·3	3·9	5·4	21·2	15·85

$\sigma = 4{\cdot}355$ corresponds approximately to the deflection produced by a source of flux density 10×10^{-26} w.m.$^{-2}$ (c/s)$^{-1}$ at the centre of the reception pattern.

TABLE III (81·5 Mc/s)

σ	0 to 0·79	0·79 to 1·57	1·57 to 2·36	2·36 to 3·15	3·15 to 3·93	3·93 to 4·72	4·72 to 5·51	5·51 to 6·29	6·29 to 7·08	7·08 to 7·87	> 7·87	> 3·15	3·15 to 7·87
No. observed	2443	2040	419	131	46	35	14	7	13	4	57	176	119
No. computed	2443	1816	497	175	85	48	30	21	16	12	64	277	213

* The justification for the elimination of the side-lobe responses of the intense sources in Cassiopeia, Cygnus, Taurus and Virgo rests on the fact that their flux densities are far greater than those expected from any reasonable extrapolation of the log N-log S curve of other sources. In addition, only the source Virgo A lies more than 15° from the galactic plane. Whatever the declination setting of the aerial, most of the large deflections recorded are due to these four sources, and the statistics of large deflection amplitudes would be overwhelmed by their presence if all their side-lobe responses were included.

were omitted from the analysis. The 159 Mc/s data comprise 2006 readings of deflection from an area of about 1·7 steradians in the region $-10° < \text{Dec.} < +56°$, $08^h < \text{R.A.} < 16^h$. The 81·5 Mc/s readings refer to a similar region but the amplitudes were noted at nearly ten points per beamwidth and the statistical errors are therefore about three times larger than the numbers would appear to indicate.

The scale factor in (1) was adjusted by equalizing the observed and computed fractions of deflections in the lowest range of deflections in the table (about half the total number of deflections in each case)*. Table II shows good agreement between the observations and the predictions for a uniform distribution up to σ about 8·65 (the precision of the agreement is fortuitous). Counts of the small deflections at smaller intervals of D also show agreement with the predicted values. For the larger deflections there are fewer data but the observed numbers are consistently less than the predicted numbers except in the highest range ($\sigma > 20{\cdot}45$), which should perhaps be considered separately since the deflections are nearly all due to the intense source Virgo A (observed in the primary lobe of the reception pattern). It will be seen that there are only 10 deflection amplitudes with $\sigma > 8{\cdot}65$ instead of the predicted 21 and in the range $\sigma = 8{\cdot}65$ to 20·45 only 4 instead of 16. A similar effect can be seen in Table III with the 2C results but it sets in much sooner, at about $\sigma = 3{\cdot}15$. The following argument shows that a difference of this kind is to be expected if the discrepancy is due to a true deficit of intense sources. If the aerial, when operating at 81·5 Mc/s, has a reception pattern covering $1/N$th of the sky the confusion level ($\sigma = 0{\cdot}83$) corresponds approximately to the flux density of the Nth source in order of decreasing intensity. The same aerial structure operating at twice this frequency has a reception pattern covering $\frac{1}{4}N$th of the sky, so that $\sigma = 0{\cdot}83$ corresponds to the flux density of the $4N$th source, and the Nth source corresponds to a higher value of σ. Assuming for the sake of the argument that $N \propto S^{-3/2}$, this value would be $\sigma = 0{\cdot}83 \times 4^{2/3} = 0{\cdot}83 \times 2{\cdot}5$. Thus the sources contributing most to the deflections in the neighbourhood of $\sigma = 3{\cdot}2$ at 81·5 Mc/s are the same sources which are important near $\sigma = 3{\cdot}2 \times 2{\cdot}5 = 8{\cdot}0$ at 159 Mc/s.

The method of analysis just described was developed especially to avoid the disturbing effects of confusion between adjacent sources. It does not allow for the effects of angular diameters. Ryle and Scheuer (1955) showed that the source counts on 81·5 Mc/s could not be explained by the effects of angular diameters alone, but since the counts were also very severely affected by confusion, the whole question must be re-examined.

(*c*) *The effects due to extended sources.*—The existence of extended sources at low galactic latitudes is well known but observations away from the plane have shown few extended sources and most of those investigated have had angular diameters less than the limits of measurement. The published data are summarized below together with some new results provided by the 3C large diameter survey. Since the most intense sources in any given class will have the largest angular sizes these data may be used to derive the errors in the flux densities measured with an interferometer of given resolving power.

(i) Morris, Palmer and Thompson (1957) have recently investigated the angular diameters of some sources in the catalogue of Hanbury Brown and

* In an earlier paper by Ryle and Scheuer (1955) the curves were scaled by fitting at large values of D.

Hazard (HBH, 1953). The catalogue covers a region between declinations $+38°$ and $+68°$. They find that "with the exception of the Andromeda nebula all the intense sources in the catalogue of Hanbury Brown and Hazard with galactic latitudes greater than 10° have angular diameters $< 5'$". They quote results for five sources:

HBH 6 (NGC 1275)	$2'{\cdot}4 \pm 0'{\cdot}5$,
HBH 10	$< 12''$,
HBH 11	$< 12''$,
HBH 12	$4'\,20'' \pm 2'$,
HBH 18	$< 12''$.

The Andromeda nebula is the only normal galaxy of which the angular diameter is known. Baldwin (1954) finds it to be larger than the optical and equal to $2°{\cdot}3$ between half-power points.

(ii) The angular diameters of other sources known not to belong to classes concentrated to the galactic plane have been measured:

Cygnus A: Two disks each of about 40″ diameter separated by 90″ (Jennison and Das Gupta 1956).

Virgo A: Central concentration $5' \times 2'{\cdot}5$ (Mills, 1953) with 80 per cent of the flux surrounded by a disk about 50′ in diameter (Baldwin and Smith, 1956).

Centaurus A: Central concentration 3′ in diameter (Mills, 1953), with extended source about $1°{\cdot}5$ in diameter.

Hydra A: $1'{\cdot}6$ (Carter, 1955).

(iii) Baldwin and Archer (private communication) have determined upper limits to the angular diameters of the 27 brightest sources in the region $-10° < \text{Dec.} < +47°$, $|b| > 20°$, and found that 25 have angular diameters less than 5′, 21 less than $3'{\cdot}5$ and 10 less than $2'{\cdot}5$.

The observations show immediately that unless faint sources differ radically from intense ones by having much larger angular diameters (the opposite being expected) then the fraction of sources with angular diameters more than 5′ is considerably less than one-third (see Section 3). They also suggest that for the great majority of the relevant sources the reduction in apparent intensity due to finite angular diameters is small, even with a spacing of 308 wave-lengths. For the 2C observations, in which the interferometer spacing was only 157 wave-lengths, the reduction should be smaller still.

It is clear from an inspection of Fig. 1 that normal galaxies having a surface brightness similar to that of M 31 leave no trace on the 2C or 3C small diameter survey records and therefore cannot affect the counts of individual sources. A calculation shows that the effect of normal galaxies on the $P^*(D)$ histogram is also negligible.

The results of Baldwin and Archer quoted in (iii) above refer to a representative sample of sources and may therefore be used to estimate the effect of angular diameters on the data in Table II. The number of sources per steradian is about the same as the expected number of independent deflections with $\sigma > 8{\cdot}65$, per steradian, at 159 Mc/s, and it is reasonable to assume that the sources which should be responsible for deflections with $\sigma > 8{\cdot}65$ have the same distribution of angular diameters as the sources observed by Baldwin and

Archer. With this assumption, it is found that up to 8 of the 21·2 expected deflections with $\sigma > 8{\cdot}65$ might be reduced below $\sigma = 8{\cdot}65$ owing to the resolution of sources by the interferometer. The remaining discrepancy between 10 observed and 13·2 expected large deflections in Table II would not be significant. The estimate just given is an upper limit to the effect of angular diameters, since the upper limits as quoted by Baldwin and Archer have been taken as actual angular diameters. On 81·5 Mc/s the interference lobes in the reception pattern are more widely spaced and a smaller reduction in the apparent intensity would occur, so it would be very difficult to explain the results in Table III as an effect of angular diameters.

Quite apart from considerations of individual source diameters it is possible to use a general argument, based on the geometrical similarity between the reception patterns of the 2C and 3C surveys, to show that the data in Tables II and III taken as a whole cannot be explained on the hypothesis that the distribution of sources is uniform on a large scale, whatever the angular extent or clustering tendencies of these sources may be. For assume a uniform distribution and consider:

(A) the sources in the spherical shell of thickness δR at a distance R, observed at a frequency of 81·5 Mc/s; and

(B) the sources in the spherical shell of the same thickness δR at a distance $(159/81{\cdot}5)R$, observed at 159 Mc/s.

The two situations are geometrically similar, for the angular dimensions of the reception pattern and the interference lobes, of the sources and the clusters of sources (if any) are all reduced by the same factor (81·5/159) in case (B). The mean number of sources in the reception pattern, however, remains the same and the statistical properties of the receiver response are therefore the same in both cases.

The identity holds if we consider the net effect of all the shells filling space in case (A) and the corresponding shells in case (B). These latter are spread throughout space but only fill a fraction (81·5/159) of it, since the thickness of each shell is the same as in case (A). We see therefore that the 159 Mc/s observations for a uniform distribution should be those which would have been obtained at 81·5 Mc/s from a distribution of sources with a space density increased by a factor (159/81·5). Now, if the density of sources is increased, the flux density which corresponds to any given σ in Tables II and III is also increased, so that the discrepancy between the observed and computed numbers (if due to angular diameters or clustering) should become apparent at a lower value of σ at 159 Mc/s than at 81·5 Mc/s; Tables II and III indicate that the reverse is true.

This reasoning shows that the data in Tables II and III are incompatible with a distribution of sources in space which is uniform even if the sources have finite angular diameters or exist in clusters. The data are compatible with a model in which there are fewer intense sources than expected on the basis of the number of faint ones. An estimate will now be made of the intensity level at which this deficit appears. In Table II the deviation occurs at about $\sigma = 8{\cdot}65$, corresponding to a flux density of 20×10^{-26} w.m.$^{-2}$(c/s)$^{-1}$. The sources responsible for these deflections must, in general, have somewhat greater fluxes, since the point at which a deflection is read on the record rarely coincides exactly with the transit of a source through the peak of the reception pattern. Thus the

deficit of intense sources chiefly concerns those with flux densities greater than about 30×10^{-26} w.m.$^{-2}$(c/s)$^{-1}$ at 159 Mc/s.

If the deficit is isotropic there are in the whole sky some 100 sources brighter than 30×10^{-26} w.m.$^{-2}$(c/s)$^{-1}$ whereas, on the basis of a uniform distribution and the observed numbers of fainter sources, about 200 would be expected.

5. *Summary.*—An attempt has been made in this paper to present the evidence concerning the distribution of radio sources in space which has been obtained from a new survey at a frequency of 159 Mc/s. When the reduction of the records has been completed, more flux densities will be available for plotting number counts, but it is doubtful whether this additional information will alter the situation materially.

The evidence may be summarized as follows:—

(i) Counts of sources in the small diameter survey give a $\log N$–$\log S$ graph of slope $-2{\cdot}7$ for a region of area 0·7 steradians, in good agreement with the slope of $-2{\cdot}5$ obtained from the 81·5 Mc/s observations of the same area. For another region (0·25 steradians) the slope is $-2{\cdot}2$. These counts are, however, subject to two important instrumental effects, namely confusion, and the resolution of sources with appreciable angular diameters, confusion being more severe on the lower frequency, and the effect of angular diameters on the higher.

(ii) By a direct comparison of observed and calculated distributions of the deflection amplitudes on interferometer records, the errors due to confusion can be avoided. A deficit of large deflections is found.

(iii) The deficit of large deflections found on 159 Mc/s could possibly be explained as the effect of angular diameters, but it would be very difficult to account for the 81·5 Mc/s observations in this way.

(iv) A general argument shows that the 159 and 81·5 Mc/s data, taken together, cannot be explained in terms of a uniform distribution in space, whatever the angular diameters or clustering tendencies of the sources may be.

(v) For the smaller deflections, the distribution of deflection amplitudes in Table II agrees well with that expected from a uniform distribution of sources in space.

If complete reliance may be placed on the data, it follows that there are fewer sources with flux densities $> 30 \times 10^{-26}$ w.m.$^{-2}$(c/s)$^{-1}$ at 159 Mc/s than one would expect if the distribution of sources in space were uniform. This conclusion, however, depends on data of which the statistical significance is not very great, and which are subject to errors in reading and calibration. In addition, doubts may be entertained about the procedure of excluding side-lobe responses of the intense sources in Cassiopeia, Cygnus, Taurus and Virgo, when counting deflections.

It has been noted in Section 4, that the departure from a uniform distribution, if real and isotropic, shows up mainly among the brightest hundred or so sources in the sky. Only about half of these sources are situated in regions of the sky remote from the galactic equator and accessible to any one radio telescope. The use of elaborate statistical arguments in connection with a fairly small number such as fifty seems undesirable and should soon become unnecessary. There are now several very powerful radio telescopes in, or about to begin, operation and it should therefore be possible to reach complete agreement concerning the existence and flux densities of the brightest few hundred sources.

XUM

This work forms part of a programme of research supported at the Cavendish Laboratory by the Department of Scientific and Industrial Research to which two of the authors (D. O. E. and J. R. S.) are indebted for maintenance allowances.

The authors wish to thank Professor R. O. Redman for reading the paper, and Mr M. Ryle and Dr J. E. Baldwin for valuable advice and encouragement.

Cavendish Laboratory,
Cambridge:

1957 *December* 23.

References

Baldwin, J. E., *Nature*, **174,** 320, 1954.
Baldwin, J. E. and Smith, F. G., *Observatory*, **76,** 141, 1956.
Bolton, J. G., *Observatory*, **76,** 62, 1956.
Brown, R. Hanbury and Hazard, C., *M.N.*, **113,** 123, 1953.
Carter, A. W. L., *Aust. J. Phys.*, **8,** 564, 1955.
Jennison, R. C. and Das Gupta, M. K., *Phil. Mag.*, Ser. 8, **1,** 55, 1956.
Mills, B. Y. and Little, A. G., *Aust. J. Phys.*, **6,** 272, 1953.
Mills, B. Y., *Aust. J. Phys.*, **6,** 452, 1953.
Mills, B. Y., *Aust. J. Phys.*, **8,** 368, 1955.
Mills, B. Y. and Slee, O. B., *Aust. J. Phys.*, **10,** 162, 1957.
Morris, D., Palmer, H. P. and Thompson, A. R., *Observatory*, **77,** 103, 1957.
Ryle, M., *Proc. Roy. Soc.* A, **211,** 351, 1952.
Ryle, M. and Hewish, A., *Mem. R.A.S.*, **67,** 97, 1955.
Ryle, M. and Scheuer, P. A. G., *Proc. Roy. Soc.* A, **230,** 448, 1955.
Scheuer, P. A. G., *Proc. Cam. Phil. Soc.*, **53,** 764, 1957.
Shakeshaft, J. R., Ryle, M., Baldwin, J. E., Elsmore, B. and Thomson, J. H., *Mem. R.A.S.*, **67,** 106, 1955.

XUM

РЕЗЮМЕ ПОДЛИННЫХ ДОКЛАДОВ, В ПЕРЕВОДЕ НА РУССКИЙ ЯЗЫК

ИНТЕРФЕРОМЕТРИЧЕСКИЕ ИЗМЕРЕНИЯ ДЛИН ВОЛН. IV. ТОЧНОСТЬ ИЗМЕРЕННЫХ ДЛИН ВОЛН

М. Г. Адам и С. Никольс

Характеристика солнечных линий поглощения намного отличается от соответствующих лабораторных линий и точность определения длины волны первых значительно ниже. При этом возможно, что некоторая часть красного смещения и изменение красного смещения с интенсивностью линий, возникают при микрометрическом измерении широких линий поглощения и узких линий эмиссии. Исследованы точность и последовательность результатов полученных при измерении длины дуговых и солнечных волн методом кольцевой диаграммы. По этим исследованиям оказывается, что можно получить достоверные красные смещения с точностью превосходящей 0,001 Å.

ИНТЕРФЕРОМЕТРИЧЕСКИЕ ИЗМЕРЕНИЯ ДЛИН ВОЛН. V. ИСТОЛКОВАНИЕ КРАСНЫХ СОЛНЕЧНЫХ СМЕЩЕНИЙ ПРИ ПОМОЩИ РАДИАЛЬНЫХ ПОТОКОВ

М. Г. Адам

Раньше считалось, что теория влияния относительного эффекта радиальных потоков на красные солнечные смещения приводит к потокам невозможно большой скорости. Однако, благодаря новой модели атмосферы, базированной на гранулах диаметром в 0,4 сек и большого контраста яркостей по отношению к интергрануловым пространствам, Шретер нашел, что смещения можно объяснить при поточных скоростях всего в 2–3 км/сек. Его теоретические предсказания достаточно согласуются с наблюдаемыми изменениями смещения от центра к периферии. Эту теорию можно также проверить при помощи оксфордских измерений длины волн в центре солнечного диска и в вакуумной дуге. Последние дают возможность определить равнодействующую поточной скорости в зависимости от интенсивности линий; но полученные таким образом скорости не согласуются с предсказаниями Шретера. Затем рассмотрена зависимость смещений от длин волн, пользуясь измерениями аллеганской обсерватории и бюро стандартов США; этот опыт также не поддерживает теории радиальных потоков.

ПЕРИОДЫ И КРИВЫЕ СВЕТИМОСТИ НЕСКОЛЬКИХ ПЕРЕМЕННЫХ ЗВЕЗД В СКОПЛЕНИИ NGC 121

А. Д. Тэккерэй

Пользуясь 82 снимками шарового скопления NGC 121 во внешней части Малого Магелланова облака за девятилетний период, хотя большинство их было снято в течение 3^{N} последовательных годов, выведены периоды и кривые светимости пяти переменных звезд, находящихся в пределах дуги в 1′ от центра скопления. Из них три являются переменными короткого периода (их периоды—от 0,50 до 0,64 дня), типа *a* или *b* по Белею, с обычными соотношениями между периодом, амплитудой и формой кривой светимости. Периоды остальных двух, принадлежащих к самым красным и светлым звездам скопления, оказываются 140,2 и 112,4 суток. Изменения светимости характеризуются ступенчатыми оценками по отношению к « основному » порядку последовательности.

На снимках обнаружены еще четыре переменных звезды короткого периода, расположенные слишком далеко от скопления для того, чтобы принадлежать к нему. Эти звезды достаточно слабы, чтобы можно было их рассматривать как первый пример переменных RR Lyrae в общем поле Малого Магелланова облака.

XUM

АНАЛИЗ РАДИАЛЬНЫХ СКОРОСТЕЙ ДАЛЬНИХ ЗВЕЗД ТИПА В

М. В. Фист и А. Д. Тэккерей

Радиальные скорости 314 звезд типа В, раннего подразделения, с вычисленными расстояниями (по фотоэлектрическим цветам и классификации Моргана-Кинана) превышающими 1 кпс, анализируются с целью определения дифференциального галактического вращения. Включение скоростей южных звезд, согласно определениям радклиффской обсерватории, дает гораздо более однородное распределение по долготе, чем при предыдущих анализах. На расстояниях превышающих 2 кпс даже заметно не хватает звезд северного полушария.

Тщательно проанализированы звездные и междузвездные скорости групп различных расстояний (отдел 5, таблица III). Отрицательный термин K (отдел 6) получается для области от 1 до 2 кпс, но согласно более далеким группам нет указания, что это является результатом общего сжатия Галактики. Вкратце обсуждается возможность связи между наблюдаемым явлением и отклонением вершины. Термин K в области от 1 до 2 кпс значительно уменьшается когда принимается в соображение систематическое исправление, что видимо применимо к скоростям Ликка слабых звезд типа В (отдел 3). Под влиянием этого исправления также увеличиваются величины, выведенные в результате применения постоянной A Оорта. Группа звезд удаленных более чем на 3,0 кпс, дает исключительно низкое значение A, но это объясняется, главным образом, как результат отбора, приводящего к несоразмерно большой пропорции в этой группе преувеличенных расстояний.

Рассеяние скоростей во внутренней части Галактики не является несоразмерным (отдел 7).

Применяется приблизительный линейный расчёт Камма (отдел 8) для вывода величины постоянной A Оорта. Принята окончательная величина $A = 17{,}5 \pm 1{,}5$ км/сек.кпс.

Для вывода величины R_0, расстояния до центра Галактики, применяются два частично независимых метода. Наиболее вероятная величина—8,9 кпс (отдел 10, табл. IX). Отношение осей эллипсоида скоростей для дальних звезд типа В видимо следует считать равным 0,5.

Проверяется калибрация шкалы светимости Моргана-Кинана (отдел 11) для звезд в зоне от B5 до O9,5.

Выводится кривая дифференциального вращения $\omega(R)$ (отдел 12). Между этим решением и результатами радио-наблюдений нет существенной разницы и предполагается, что ω'' положительна в области исследуемых R.

ЗВЕЗДНЫЕ ГРУППЫ. II. ГРУППЫ ЗВЕЗД БОЛЬШОЙ СКОРОСТИ ζ ГЕРКУЛЕСА, ε ИНДЕЕЦА И 61 ЛЕБЕДЯ

Олин Я. Эгген

Просмотрен каталог семисот звезд большой скорости, с целью найти звезды с явно определенным движением в пространстве, подобным ζ Геркулеса (23 звезды), ε Индейца (14 звезд) и 61 Лебедя (15 звезд). Движения в пространстве этих групп могут быть обобщены следующим образом (группы Гиад и Сириуса включены для сравнения):

Группа	A	D	V_t	U	V	W
				км/сек		
Сириуса	20ч 44м	−42,7°	18,4	−14	0	−12
Гиад	6ч 18м	+ 7,5°	44,0	+40	−18	− 2
ζ *Her*	5ч 48м	−16,5°	74,5	+54	−45	−26
ε *Ind*	6ч 44м	+ 6,7°	88,5	+79	−39	+ 6
61 *Cyg*	6ч 28м	+ 0,3°	108,0	+92	−53	− 6

где значения (A, D) представляют собой точки сходимости кажущихся движений, а V_t—общую скорость в пространстве каждой группы по отношению к Солнцу (причем направления векториальных скоростей в пространстве: $l = 148°$, $b = 0°$; $l = 58°$, $b = 0°$ и $b = +90°$ соответственно для U, V и W). Поиски в том же каталоге звезд могущих принадлежать к синтетическим группам с точкой сходимости в $\delta = -90°$, а $V_t = 74{,}5$; 88,5 и 108 км/сек, дают указания на то, что всего 2 или 3 случайных звезды могут быть включены в каждую группу.

Диаграмма цвета-светимости звезд всех трех групп большой скорости подобна диаграмме галактического скопления M 67.

ЭЛЛИПСОИД СКОРОСТЕЙ ДЛЯ ЗВЕЗД ТИПА Ao

Дж. Б. Александер

Радиальные скорости звезд спектрового типа Ao, вблизи вершины траектории Солнца, сопоставляются с тангенциальными скоростями звезд того же типа в зоне неба, отклоненной на 90° от вершины, что приводит к кинематической средней абсолютной величине в $+0^m,14$. Предполагая, что каждая звезда типа Ao обладает одной и той же абсолютной величиной, можно найти приблизительные расстояния из наблюдаемых кажущихся величин. Этот метод применяется к 475 звездам типа Ao, ясность которых превосходит $6^m,5$, чтобы получить экваториальные составляющие линейной скорости из собственных движений и радиальных скоростей.

Значения скорости Солнца и параметров эллипсоида скоростей вычисляются и сопоставляются с результатами других исследований.

Галактическая долгота большой оси получается в 354°, а средние квадратичные собственных скоростей в направлении главных осей соответственно 18,9 км/сек., 11,1 км/сек. и 8,4 км/сек.

СИСТЕМА СКОПЛЕНИЙ В МАЛОМ МАГЕЛЛАНОВОМ ОБЛАКЕ

Е. М. Линдсей

Выполнена съемка скоплений в Малом Магеллановом облаке при помощи телескопа ADH (Армах-Дансинк-Харвард) и пластинок 103a.O с выдержкой в 30 мин. В общем 116 тел рассматриваются как скопления в облаке. Система этих скоплений распространяется до крыла облака. Определены кажущиеся размеры на 10 дюймовых (250 мм) пластинках Меткальф. Облачная система простирается на 8000 пс по наибольшей диагонали (включая крыло) и на 5400 пс по наименьшей диагонали. Ничто не свидетельствует о спиральной структуре распределения скоплений.

НАЛИЧИЕ РАСПРЕДЕЛЕНИЯ В ПРОСТРАНСТВЕ РАДИО-ИСТОЧНИКОВ В РЕЗУЛЬТАТЕ СЪЕМОК НА ЧАСТОТЕ В 159 МГГЦ

Д. О. Эдж, П. А. Г. Шейер и Дж. А. Шейкшафт.

Рассмотрены некоторые результаты съёмки радио-источников на частоте в 159 мгцц, для ограниченных участков неба, относительно распределения этих источников в пространстве.

Сопоставление отдельных источников подтверждает реальность около четверти источников, найденных при прежней съёмке на частоте в 81,5 мгцц, но надежность определения слабых источников хуже, чем оно являлось по прежнему списку. Сравнивая новые положения с положениями, определенными Милльсом и Сли на частоте в 85 мгцц, найдено, что положение источников, плотность потока энергии которых на частоте в 85 мгцц превосходит 20.10^{-26} вт.м$^{-2}$. гц$^{-1}$, достаточно согласуются, но согласование неудовлетворительно для более слабых источников.

Построение графика $\log N$ в зависимости от $\log S$ (где N—число источников, плотность потока энергии которых превосходит S) дает наклон в —2,2 для одного участка и —2,7 для другого. Но эти наклоны могут быть искажены до неизвестной степени, благодаря неясности между соседними источниками и благодаря тому, что угловые диаметры источников конечны.

Анализ при помощи метода, зависящего от статистического распределения амплитуд на снимках, но не зависящего от ошибок из-за неясности, указывает, что наблюдения более слабых источников не противоречит гипотезе однородного распределения источников. Остается противоречие между этим однородным распределением и числом сильных источников.

Можно доказать, что наблюдения на частоте в 159 мгцц, сопоставленные с наблюдениями на частоте в 81,5 мгцц, противоречат гипотезе однородного распределения. Этот результат, однако, основан на данных, статистическое значение которых недостаточно, чтобы дать исчерпывающие выводы и необходимы дальнейшие исследования.